Study of carbon nanotubes network modification in polyethylene under temperature variation and deformation

Anatole Collet

N°d'ordre NNT : 2021LYSE1100

THESE de DOCTORAT DE L'UNIVERSITE DE LYON
opérée au sein de
l'Université Claude Bernard Lyon 1

Ecole Doctorale N° 34
Matériaux

Spécialité de doctorat : Polymères et matériaux composites
Discipline : Physique des matériaux

Soutenue publiquement le 15/06/2021, par :
Anatole Collet

Etude des mécanismes de dispersion et de structuration multi-échelle de nanotubes de carbone dans une matrice polyéthylène sous sollicitation thermique et mécanique

---

Devant le jury composé de :

Dr. Edith Peuvrel-Disdier	Mines ParisTech CNRS Nice	Rapporteure
Prof. Thierry Aubry	Université de Bretagne Occidentale	Rapporteur
Dr. Jean-Paul Chapel	CRPP CNRS bordeaux	Examinateur
Prof. Catherine Journet	Université Lyon 1	Examinatrice
Prof. René Fulchiron	Université Lyon 1	Directeur de thèse
Prof. Philippe Cassagnau	Université Lyon 1	Directeur de thèse
Dr. Olivier Lhost	Total Research & Technology Feluy	Invité
M. Yves Trolez	Total Research & Technology Feluy	Invité

Université Claude Bernard – Lyon 1

Président de l'Université	M. Frédéric FLEURY
Président du Conseil Académique	M. Hamda BEN HADID
Vice-Président du Conseil d'Administration	M. Didier REVEL
Vice-Président du Conseil des Etudes et de la Vie Universitaire	M. Philippe CHEVALLIER
Vice-Président de la Commission de Recherche	M. Petru MIRONESCU
Directeur Général des Services	M. Pierre ROLLAND

Composantes Santé

Département de Formation et Centre de Recherche en Biologie Humaine	Directrice : Mme Anne-Marie SCHOTT
Faculté d'Odontologie	Doyenne : Mme Dominique SEUX
Faculté de Médecine et Maïeutique Lyon Sud - Charles Mérieux	Doyenne : Mme Carole BURILLON
Faculté de Médecine Lyon-Est	Doyen : M. Gilles RODE
Institut des Sciences et Techniques de la Réadaptation (ISTR)	Directeur : M. Xavier PERROT
Institut des Sciences Pharmaceutiques et Biologiques (ISBP)	Directrice : Mme Christine VINCIGUERRA

Composantes & Départements de Sciences & Technologie

Département Génie Electrique et des Procédés (GEP)	Directrice : Mme Rosaria FERRIGNO
Département Informatique	Directeur : M. Behzad SHARIAT
Département Mécanique	Directeur M. Marc BUFFAT
Ecole Supérieure de Chimie, Physique, Electronique (CPE Lyon)	Directeur : Gérard PIGNAULT
Institut de Science Financière et d'Assurances (ISFA)	Directeur : M. Nicolas LEBOISNE
Institut National du Professorat et de l'Education	Administrateur Provisoire : M. Pierre CHAREYRON
Institut Universitaire de Technologie de Lyon 1	Directeur : M. Christophe VITON
Observatoire de Lyon	Directrice : Mme Isabelle DANIEL
Polytechnique Lyon	Directeur : Emmanuel PERRIN
UFR Biosciences	Administratrice provisoire : Mme Kathrin GIESELER
UFR des Sciences et Techniques des Activités Physiques et Sportives (STAPS)	Directeur : M. Yannick VANPOULLE
UFR Faculté des Sciences	Directeur : M. Bruno ANDRIOLETTI

"Deborah knew two things. First, that the mountains flow, as everything flows. But, secondly, that they flowed before the Lord, and not before man, for the simple reason that man in his short lifetime cannot see them flowing, while the time of observation of God is infinite."

Reiner, M. The deborah number. *Physics today*, 1964, vol. 17, no 1, p. 62.

Remerciements

Tout d'abord, je remercie Thierry Aubry et Edith Peuvrel-Disdier d'avoir accepté d'être rapporteurs de ce travail et d'avoir pris le temps de juger de la qualité de ce travail. Merci aussi à Catherine Journet et Jean-Paul Chapel pour leur rôle d'examinateurs.

Je voudrais ensuite remercier mes encadrants René et Philippe pour leur disponibilité et toute l'aide qu'ils m'ont apporté au long de ces trois ans. J'ai beaucoup appris grâce à eux, que ce soit durant la thèse, mais aussi avant, tant sur la connaissance scientifique que sur la manière de raisonner. Merci plus particulièrement à René pour son aide précieuse dans la mise en point du modèle, à Philippe pour la découverte de l'acide stéarique et aussi à Anatoli Serghei pour son expertise sur les mesures électriques. J'aimerais aussi les remercier pour leur confiance, me donnant l'autonomie nécessaire pour gérer ce projet comme je le souhaitais. Ils m'ont aussi permis de rencontrer et partager avec différents acteurs de la recherche, même si un certain virus est venu empêcher un dernier congrès à Montréal.

Ce travail n'aurait pas existé sans les financements de la part de l'Association Nationale de la Recherche et de la Technologie ainsi que de la société Total. J'aimerais alors remercier Olivier Lhost et Yves Trollez du Centre de recherche de Total à Feluy qui m'ont accompagné et conseillé pendant ces trois ans. Mais je pense aussi à tous les amis et collègues que j'ai rencontrés à Feluy, dans le cadre des travaux de Marjorie. Je pense notamment à ma covoit' Fanni avec qui j'ai pu apprendre beaucoup sur moi, tandis que de mon côté je lui ai appris quelques étrangetés de la langue française. Merci aussi à Nabil, Christo et Eddi qui se sont toujours rendu disponible. Je dois aussi toute ma reconnaissance à Marjorie pour m'avoir fait confiance et fait découvrir la mise en forme par thermoformage, qui m'a poussé à poinçonner des centaines de feuilles. Merci aussi à Dimitri Rousseaux de m'avoir proposé cette thèse à la suite de cette première expérience. Il m'a aussi montré que la motivation permet de réaliser les choses qui nous tiennent à cœur, et qu'on peut être ingénieur et brasseur.

J'ai eu beaucoup de chance d'effectuer ma thèse au l'IMP et de faire partie intégrante du laboratoire. J'ai pu profiter des expertises variées de tout le personnel (permanent ou non) et j'ai eu accès à de nombreuses techniques d'analyse et mise en forme pour mener à bien ce projet. Merci par exemple à Corinne pour sa bonne humeur, et à Laurent Cavetier d'avoir réparé et soudé à de nombreuses reprises un montage capricieux.

J'aimerai remercier la totalité des doctorants de l'IMP Lyon 1 qui ont rendu cette expérience si particulière. De tous les mots qui me viennent en tête, je retiens surtout le verbe partager : que ce soit une connaissance scientifique, un repas, une bière ou juste un rire. Merci à Matou, Yoanh, Florian, Clémence et Benedetta du bureau 326 de m'avoir supporté moi et mes blagues nulles, même si en contrepartie, j'ai dû subir les vôtres, qui sont encore pires ! Merci aux incroyables copains du Mardinsa : Kilian, Mathieu, Mathilde, Léa, Alexane, Yo et Raflouti. Je suis content de faire partie de ce groupe hétéroclite qui a vraiment contribué à mon bien-être mental à grand renfort de musique et de bières. Merci à Renaud pour son sourire et sa manière de me rendre proactif et merci à Chloé, binôme de thèse qui a toujours été là pour

moi. Enfin, je n'oublie pas Claire qui a été pour moi comme un rayon de soleil pendant ces trois ans. Merci de m'avoir soutenu, conseillé et aussi de me suivre dans mes idées bizarres !

Je remercie finalement ma famille qui m'a beaucoup soutenu tout a long de la thèse. Merci énormément à Théodore de m'avoir sorti la tête du travail à chaque fois que c'était nécessaire et de m'avoir motivé comme personne, par exemple pour le semi-marathon du beaujolais ! J'ai aussi une pensée particulière pour mes grands-parents sans qui je n'aurais pas pu aller à Feluy. Grâce à cette expérience, j'ai pu profiter d'eux et être présent au bon moment.

Merci finalement aux quelques cheveux qui sont restés solidaires et qui ne m'ont pas quitté malgré les moments difficiles. Je doute cependant que cette phrase ne vieillira pas trop mal avec le temps.

Abstract

A study of the electrical conductivity evolution of polyethylene filled with carbon nanotubes during quiescent annealing as well as under shear deformation is proposed in this work. For such nanocomposites, the electrical conductivity can be theoretically obtained at filler content lower than 1 %. This material containing a percolated network can be used in industrial applications as protection from electrostatic discharge. Hence, CNTs filled materials can advantageously replace polymer-carbon black composites which contain usually around 20 wt. % of fillers. However, during forming process, the structure created by CNTs connections is strongly modified by the applied stress, possibly resulting in an insulating final product.

This study investigates the filler network structuring and destructing mechanisms that occurs during processing steps by means of conductivity monitoring. The dynamic percolation was studied in the first instance to evaluate the extent of the CNT network strengthening ability in the melt polymer. In the case of semi-crystalline polymer, the composite morphology is modified during the cooling by the apparition of a crystalline phase. The disruption of the conducting network by the polyethylene crystallization process has then been considered more especially as the CNT present a certain nucleating character. Finally, combined rheological and electrical measurements were performed to study the shear-induced fillers network modification. A kinetic equation is proposed to follow the effective CNT content and therefore predict the conductivity evolution during and after a shear deformation. As a result, this work contributed to deepen the comprehension of the thermo-rheological history influence on the conductivity of polymer-CNT composites.

Key words: Carbon nanotubes, Polyethylene, Electrical conductivity, Shear deformation, Crystallization

Résumé

Les travaux présentent une analyse de l'évolution de la conductivité électrique de composites à matrices polyéthylène chargées en nanotubes de carbone (NTCs) lors de recuits thermiques et durant des déformations par cisaillement. L'ajout d'une quantité suffisante de NTCs dans une matrice polymère permet d'obtenir une conductivité électrique suffisante pour être utilisée dans des applications de protection aux décharges électrostatiques. L'utilisation des NTCs s'avère particulièrement intéressante, du fait de leurs facteurs de forme, car seulement une faible quantité (autour d'un pourcent) est nécessaire à la formation un réseau percolant de charges, responsable de la conduction électrique. Cependant, les étapes de mise en forme peuvent changer l'arrangement des charges, modifiant alors les propriétés électriques du matériau.

Les mécanismes de structuration et de destruction du réseau percolant ont été étudiés par l'intermédiaire de mesure de conductivité. La portée du phénomène d'auto-assemblage du réseau dans le polymère à l'état fondu a été évaluée. Aussi appelée dans la littérature percolation dynamique, cet effet permet d'améliorer la conductivité du composite ainsi que de réduire le seuil de percolation. Lors du refroidissement du composite, la morphologie du matériau est modifiée avec l'apparition d'une phase cristalline. La cristallisation de la matrice conduit à une perte de conductivité rendant compte de la dégradation du réseau de charge. Finalement, un montage couplant une mesure rhéologique avec une mesure électrique a été utilisé dans l'objectif d'analyser les processus structurants s'opérant pendant et après un écoulement en cisaillement. La concurrence des mécanismes de création et de destruction de contacts électriques entre charges a pu être observée. Un modèle permettant de prédire l'évolution de la conductivité des composites à l'état fondu pendant et après la déformation en cisaillement est proposé.

Mots clés : Nanotubes de carbone, Polyéthylène, Conductivité électrique, cisaillement, Cristallisation

Présentation synthétique des travaux de thèse

Les présents travaux de thèse sont le résultat d'une collaboration entre le laboratoire Ingénierie des Matériaux Polymères (IMP) de Lyon et le centre de recherche de Total de Feluy en Belgique (TRTF). L'ajout de particules dans une matrice polymère permet d'augmenter grandement la valeur ajoutée d'un polymère de commodité à la base bon marché, tel que les polyoléfines. Dans le cas présent, un ajout suffisant d'une charge conductrice dans un polymère permet de conférer des propriétés de conductivité électrique au composite. Cette nouvelle fonction peut s'avérer très utile dans plusieurs applications pour éviter tout dommage occasionné par le phénomène de décharge électrostatique (endommagement de composants électronique, incendie, explosion…).

En effet, des charges électriques peuvent se former et s'accumuler à la surface d'un matériau si celui-ci est isolant et ne permet pas alors aux charges de s'écouler à la terre. Cette accumulation de charges peut alors provoquer une décharge électrostatique qui, dans une atmosphère explosive, peut être à l'origine d'une inflammation (par exemple lors de transfert de liquides pétroliers). L'utilisation de composites polymères contenant des charges conductrices apparait comme une solution pertinente de par le faible coût et la facilité de mise en forme des matrices polymères thermoplastiques. Pour bénéficier des propriétés électriques de la charge, cette dernière doit être ajoutée dans des proportions suffisantes pour créer un réseau électriquement interconnecté dans la matrice.

Quant au choix de la charge, la première option est d'utiliser une charge conductrice et d'ajouter la quantité nécessaire pour obtenir la conductivité ciblée : par exemple, le noir de carbone est un bon candidat. Cependant, la forme sphérique (le facteur de forme défini par le rapport du diamètre sur la longueur apparente vaut environ 1) de cette particule implique qu'une quantité importante (au-delà de 10 % en masse) soit ajoutée dans la matrice pour obtenir une conductivité satisfaisante. Bien que le coût soit faible, un ajout important de charge dans la matrice peut induire des phénomènes néfastes de relargage, de difficultés de mise en œuvre ou encore de fragilisations mécaniques. Une seconde option est alors d'utiliser une charge carbonée présentant un facteur de forme beaucoup plus important comme par exemple les nanotubes de carbone (NTC). Avec une longueur jusqu'à 1000 fois supérieure à son diamètre, cette charge permet l'obtention de propriétés électriques à des concentrations beaucoup plus faibles (autour d'un pourcent). Cependant, du fait de leur forme, le réseau interconnecté responsable de la conductivité est en général facilement endommagé lors des étapes de mise en forme, ce qui a pour effet de rendre difficile l'obtention d'un matériau conducteur ayant des propriétés homogènes et reproductibles.

Les présents travaux de thèse font suite à une première thèse en collaboration entre les deux entités portant sur le comportement de polystyrène amorphe chargé en nanotubes de carbone. Ces travaux ont permis notamment d'étudier les mécanismes de modification de la

structure des composites lors de leur mise en forme par thermoformage. Dans le cas présent, on s'est intéressé au comportement de composites polyéthylène (PE) chargé en NTC. Lors de la mise en forme par extrusion, la qualité du réseau conducteur est modifiée et la conductivité résultante est dégradée. Les effets de différents mécanismes intervenant lors de la mise en forme ont alors été étudiés, pour tenter d'améliorer les propriétés électriques d'un système PE-NTC.

Le contexte de recherche autour des matériaux composites chargés en nanotubes de carbone et leur mise en forme est tout d'abord développé dans l'état de l'art. Cette partie permet d'introduire les problématiques ciblées dans les chapitres expérimentaux, tel que l'importance de l'histoire thermique et rhéologique du matériau sur sa conductivité. Les techniques utilisées pour caractériser la qualité du réseau et son évolution sont ensuite présentées. Le suivi de la conductivité dans le composite fondu avec le temps est en particulier présenté, ce dernier donnant des informations cruciales sur l'état du réseau conducteur à l'équilibre.

Le premier chapitre expérimental est dédié à la caractérisation du comportement électrique d'un système PE-NTC fixé. Le potentiel de percolation du composite a été en premier lieu déterminé. Celui-ci est largement dépendant des matériaux utilisés (type de polymère et nanotubes, viscosité…). Lorsque le matériau est chauffé et maintenu à une température supérieure à la température de fusion du polymère, un mécanisme d'autoassemblage de la charge conductrice est déclenché. Appelé « percolation dynamique » dans la littérature, ce mécanisme permet aux nanotubes de carbones de former de nouvelles connections entre eux, renforçant alors la conductivité globale du composite. La portée de ce traitement thermique sur l'augmentation de la conductivité du matériau a été évaluée en comparant le comportement du matériau avec celui de polyéthylènes de structure et de viscosités différentes. A l'aide d'un recuit de deux heures à 200°C, le seuil de percolation du système polyéthylène-NTC a ainsi pu être réduit de 1,4 % volumique de charge à moins de 1 %. Cependant cette valeur reste supérieure aux seuils de percolation pour les polyéthylènes plus fluides étudiés.

Dans un second temps, et toujours dans l'objectif de réduire la quantité de nanotubes dans le composite pour une même conductivité, une autre voie a été considérée avec l'ajout d'acide stéarique. Cet acide gras, déjà utilisé dans d'autres systèmes pour améliorer la dispersion des charges a permis ici de réduire le seuil de percolation vers des taux de nanotubes encore plus bas durant le recuit.

Le deuxième chapitre expérimental se concentre sur l'impact de la cristallisation du polymère sur la conductivité du matériau. L'utilisation de polymères semi-cristallins est susceptible de modifier la structure du réseau conducteur. Dans la littérature, deux effets opposés ont été mis en évidence. Dans le premier cas, l'apparition de la phase cristalline peut augmenter la conductivité du matériau en réduisant le volume disponible au NTC. Les NTCs n'étant présents que dans la phase amorphe de la matrice, une diminution du volume avec l'apparition de cristaux peut alors favoriser une densification des charges dans la phase amorphe et donc une augmentation de la conductivité. A l'inverse, une réduction de la conductivité peut être observée durant l'apparition de la phase cristalline. Pour notre système

PE-CNT, c'est ce deuxième cas de figure qui a été observé comme souligné sur la **Figure 1** par les flèches bleues.

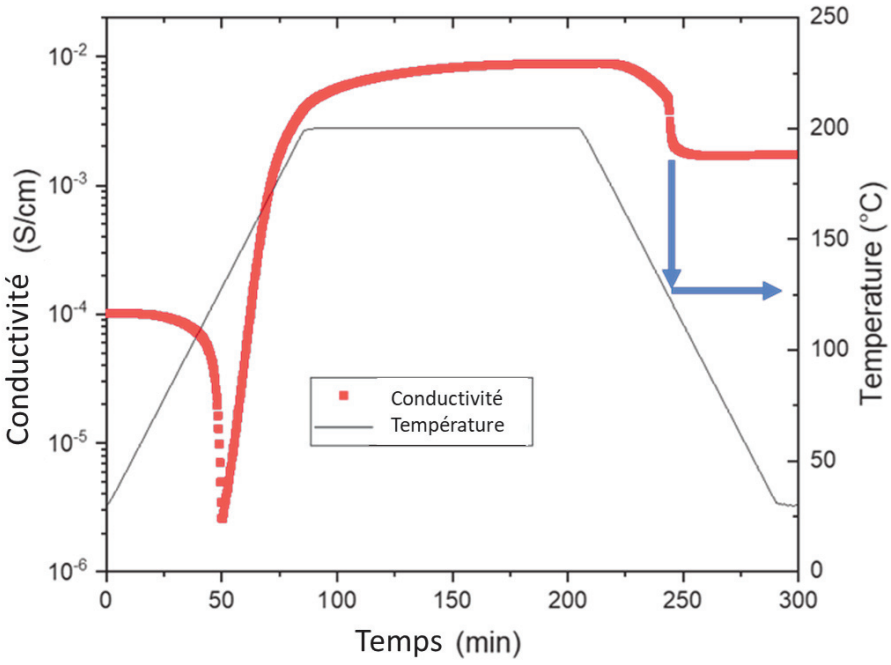

Figure 1: évolution de la conductivité d'un composite PE-CNT (1.45 vol%) au cours d'un recuit à 200 °C pendant deux heures et son refroidissement à 30°C. Les flèches bleues soulignent la cristallisation du PE.

Durant la cristallisation, une transition d'un comportement conducteur à isolant peut même être observée pour les plus faibles concentrations. Ce comportement suggère que les nanotubes sont séparés les uns des autres par les cristaux grandissant à leur proche voisinage. On observe alors une dépercolation du réseau ou en tout cas, une réduction de la conductivité du composite. On remarque cependant que la perturbation induite par la cristallisation du PE semble limitée à une modification équivalente à une réduction d'au maximum 35% de la quantité effective de charge.

Le dernier chapitre est dédié à l'étude du comportement du réseau conducteur lors de déformations du composite à l'état fondu par cisaillement (rencontré notamment lors de l'extrusion). Un montage expérimental couplant une mesure électrique et rhéologique a été utilisé dans l'objectif d'analyser l'influence des conditions de cisaillement sur les propriétés électriques. Lors d'un cisaillement, une modification de la conductivité est observée comme présenté sur la **Figure 2**, attestant ici aussi de la modification de la structure du réseau. La conductivité d'un composite au cours d'un cisaillement atteint un niveau stable de conductivité pour les cisaillements prolongés, suggérant un état d'équilibre dynamique entre connexion et déconnexion entre les charges. Ce niveau d'équilibre se trouve être sensible aux conditions expérimentales (température, vitesse de cisaillement, polymère, taux de charges…).

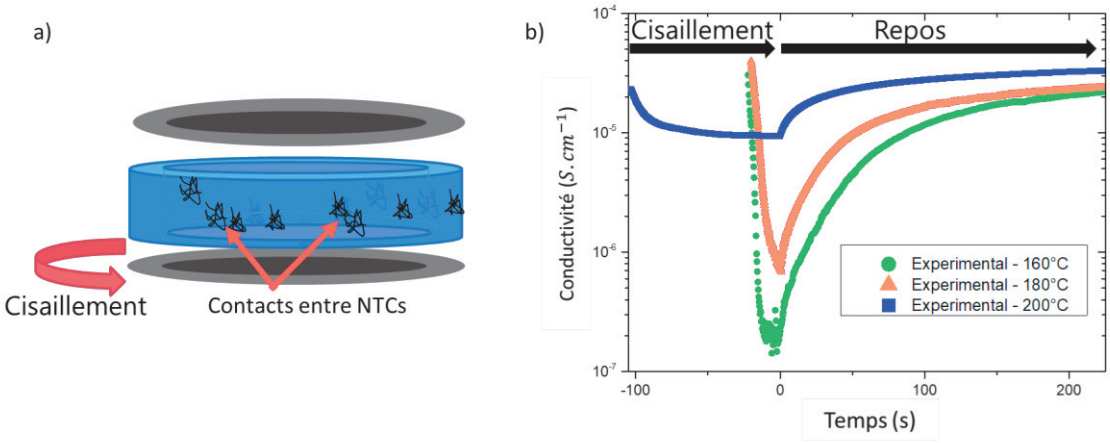

Figure 2: schéma explicatif du montage rhéo-électrique utilisé (a). Courbes d'évolution de la conductivité pendant et après le cisaillement de PE-NTC (1,75 vol%) sous différentes conditions (b).

L'étude de l'influence de différents paramètres a permis de proposer un modèle permettant de relier l'évolution de la structure du réseau de charge à la conductivité du matériau. Une équation cinétique est utilisée pour décrire la variation de la quantité de nanotubes participant au réseau conducteur au cours de la déformation du matériau fondu. Elle se base d'une part sur l'effet structurant décrit au premier chapitre, qui permet une consolidation du réseau conducteur, par la reconnection des nanotubes isolés et d'autre part sur le mécanisme de destruction partielle du réseau à cause du cisaillement jusqu'à l'obtention eventuelle d'un nouvel équilibre dynamique. A partir de l'étude approfondie des paramètres, la structuration se trouve être uniquement dépendante de la température alors que l'effet de la déformation est lui sensible à la vitesse de cisaillement et à la quantité de charge. Ce modèle a été validé pour prédire l'évolution de la conductivité d'un matériau lors de déformation par cisaillement, indépendamment de l'état initial du réseau.

Table of contents

General introduction

Polymer based composites are nowadays used for many purposes and are found in numerous applications such as pipes for liquid transport, skis or even bags of chips. The addition of specific particles at a sufficient quantity can improve the polymer intrinsic properties but also reveal new physical features. Composite material can in this way present low density and ease of processability thanks to the polymer along with interesting mechanical properties, thermal or electrical conductivity provided by the filler chosen. In the end polymer-based composites may appear as an alternative to more extensive or heavier materials, such as metals.

The incorporation of carbon nanotubes (CNTs) in a polymer matrix is particularly appealing for electric discharge applications as they are characterized by a high aspect ratio and, thanks to the atomic structure and bonds, can present remarkable electrical conductivity. As a result, a low filler content (around 1 %) can be sufficient to create a percolating path, allowing the electron charge transport. The amount required is thus by far lower than using traditional filler, such as carbon black (around 20 wt. %). Issues encountered with carbon black filled polymers, for instance filler release and mechanical weakening, can therefore be avoided with CNTs. In practice the CNT quantity needed is however often greater than in theory to reach a conductivity sufficient to allow electric dissipation ($> 10^{-7}$ S.cm^{-1}) so that it may not be industrially viable. The composite conductivity relies on a filler continuous network, but this microstructure is disturbed during processing steps inducing filler-filler disconnection, reducing the global conductivity. The network modification mechanisms occurring during the melt forming steps of polymer-CNT composites are not clearly defined yet. This could help to predict and optimize the conductivity of the final product.

The first chapter of this work is a literature review of the understanding in the field of polymer filled carbon nanotubes, especially for electrical application. The current obstacles faced during the processing steps and the existing solutions to obtain adequate conductivities. The characterization methods used in this work are then presented in the second chapter along with the materials and the sample preparation. The polyethylene-CNT composite used in this study is firstly characterized and the extent of the dynamic percolation process in the melt polymer is evaluated in the third chapter. Another way to enhance the conductivity of the system is proposed by the incorporation of stearic acid, acting as a surfactant, during the melt mixing of the composite. The chapter four is focused on the conductivity modification by the crystallization of the polyethylene matrix. A nucleating effect of the filler on the polymer is observed, and consequently the crystal growth damages the filler network inducing a conductivity decrease during the cooling of the composite. Finally, a set up allowing combined conductivity and rheological measurement is used to study the shear induced network modification. A simple model, based on a kinetic equation, is proposed to predict the conductivity evolution of molten composite during shear deformation.

Chapter I.
State of the art

I. Materials

1- Carbon nanotubes

a) Description of carbon nanotubes

Helical microtubules of graphitic carbon, also known as Carbon Nanotubes (CNT), were first observed by Iijima in 1991 and described as needle-like carbon tubes [1]. The simplest form is called Single Walled Carbon Nanotube (SWCNT) and consists in a cylindrically rolled sheet of hybrid carbon sp^2 [2, 3]. The structure can also be found with several concentric graphitic layers as observed in **Figure 3** and is then referred as Multiwalled carbon nanotubes (MWCNT) [4].

Figure 3: First TEM picture of carbon nanotubes. Cross section of nanotubes with dark lines representing the (002) lattice images of graphite. a), b) and c) are Carbon nanotubes containing respectively 5, 2 and 7 graphitic sheets [1]

Three most commons methods are used to obtain carbon nanotubes: arc-discharge [1], laser ablation [5] and chemical vapor deposition [6, 7]. The latter is the most interesting method for industrials as it offers high efficiency production (in the range of hundreds of kg per day) with reduced impurities.

The popularity of CNTs in research is due to their remarkable physical properties. Carbon-carbon covalent bonds are one of the strongest observed [7]. As a result, the tensile strength of defect free MWCNT was evaluated to 150 GPa, well above other known materials (e.g.; of steel with a tensile strength of 1-2 GPa) [8]. Regarding thermal properties, CNTs thermal conductivity was measured at 600 $W.(m.K)^{-1}$ to compare with silver with a conductivity of 430 $W.(m.K)^{-1}$ [9]. However, this value is well below the theory that predicts a thermal conductivity more than five times higher [10].

Presented value must be taken with a pinch of salt as a lot of variation can appear when characterizing nanoscale structure [7]. It must also be remembered that CNT own an important anisotropy inducing stronger physical properties along the tube axis compared with perpendicularly to the tube axis. Moreover, the atomic arrangement and the presence of defects can drastically modify physical properties of CNTs [11-14].

b) Electrical Properties

Concerning electrical properties (which are in question in this work), the synthesis is crucial as the CNT structure determines the final conductivity. Along the tube axis, CNTs can either be metallic or semiconducting. In 2004, Ormsby and King applied the Clar Valence Bond model to describe the electrical conductivity of SWCNT along the axis [15].

CNTs can be seen as a strip of a graphite sheet rolled into a tube as explained in **Figure 4**. The atomic structure is described by the chirality (or helicity) of the tube. The chiral vector ($\overrightarrow{C_h}$) is given by the following **Equation 1**:

$$\overrightarrow{C_h} = \mathrm{n} \times \vec{a}_1 + m \times \vec{a}_2 \qquad \textbf{Equation 1}$$

Where $\vec{a}_1$ and $\vec{a}_2$ are unit vectors and integers (*n*,*m*) are the number of steps along the hexagonal mesh as described in **Figure 4**. Chiral angle (θ) varies between limit values of 0 and 30°. The configuration where θ = 0° (*n*=0 or *m*=0) is called "zig zag", the opposite configuration is "armchair" when θ=30° (*n*=*m*) and for 0<θ<30° the configuration is referred as chiral [16, 17].

Figure 4: Schematic diagram showing how a hexagonal sheet of graphite is 'rolled' to form a carbon nanotube [7]

If *n*=*m* the nanotube is metallic, thus armchair nanotubes are conductor. Other (*n*,*m*) configurations conducts to semi-conductor nanotubes and the band gap is usually inversely proportional to the tube diameter [18, 19]. When n – m is a multiple of 3, $n \neq m$ and $n \cdot m \neq 0$ the material is semi-conductor with a small band gap [20]. However, the curvature of the nanotube can modify electrical properties predicted by the structure, especially for tubes of small diameters. [20, 21]. In the case of MWCNT conduction mechanism is quite similar,

electrical charge transport is mostly operated by the external wall [16]. Some modification in electrical properties can appear due to interactions between internal walls though [21].

Regarding the electronic charge transport efficiency, carbon nanotubes stand out once again from the crowd. Carbon nanotubes are usually considered as one-dimensional conductors as electrons propagate along the nanoscale tube axis. This feature enables a ballistic transport of charges responsible for astonishing electrical properties. Metallic nanotubes can carry an electric current density in the order of 10^9 A.cm^{-2}, well higher than any other material [22]. To give a comparison with metals, the measured current density of copper is around 10^6 A.cm^{-2}.

But while it is possible to manufacture macroscopic components with metals, outstanding properties of nanotubes remains at the nanoscopic scale. However, CNTs were found to be a competitive choice as fillers in composites for many applications. The following section is focused on this use of carbon nanotubes.

2- Polymer composites filled with CNTs

Thanks to intensive research on this groundbreaking material, carbon nanotubes are now used for various applications [23]. The uniqueness of CNTs relies on the combination of nanoscopic size with high aspect ratio and spectacular physical properties. These specificities solved problems with former traditional fillers and eased the development of polymer filled composites.

A certain electrical conductivity σ can be obtained in polymer composites by the addition of conductive fillers in a commonly insulator matrix. Depending on the application, the aimed conductivity of the material can vary substantially (from $\sigma > 10^{-7}\ S.cm^{-1}$ to $> 10^{-2}\ S.cm^{-1}$) [24]. Polymer composites filled with conductive materials are now widely used in various applications as they offer a convenient way to tune the electrical properties of the material while preserving a light weight and the processability of the polymer [25, 26]. A non-exhaustive wide range of applications for polymer composites depending on their electrical conductivity is illustrated in **Figure 5**.

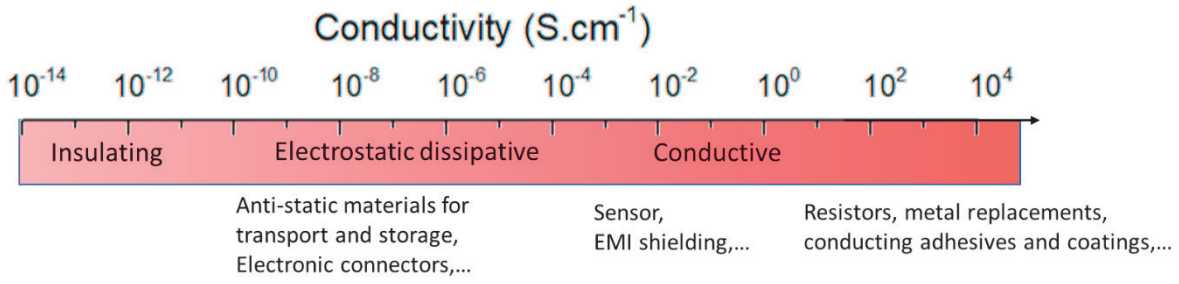

Figure 5: classification of polymer composites as a function of the electrical conductivity and their relative applications. Plotted from [24]

In this section, after an introduction to the electrical properties of polymer composites filled with CNTs, various elaboration techniques will be presented, and remaining challenges for their use will be exhibited.

a) Benefit from the electrical properties of nanotubes at the macro scale

Even though most polymers are insulator, the addition of a conductive filler in a matrix can result in a decrease of the initially high resistivity (i.e inverse of conductivity) of the material [24, 27]. **Figure 6** illustrates the evolution of the electrical conductivity with increasing filler's concentration (MWCNTs in this case) in a High-Density Polyethylene (HDPE) matrix.

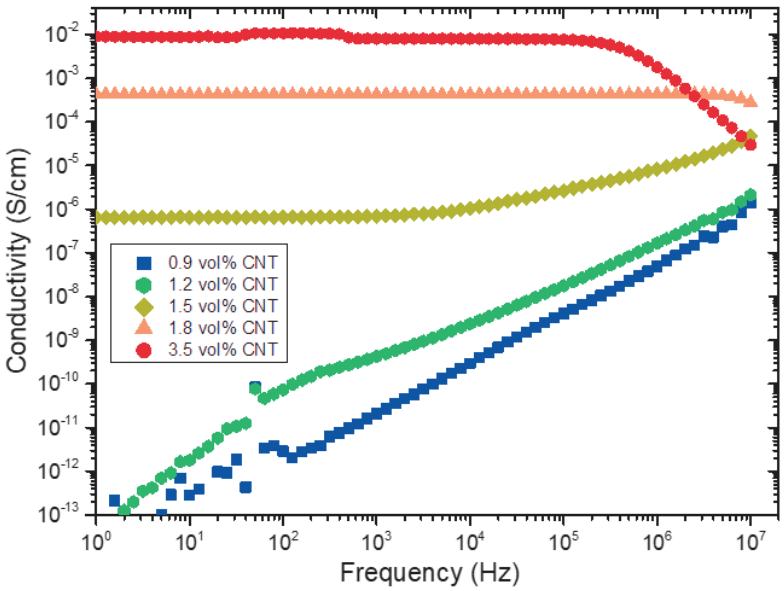

Figure 6: AC conductivity as a function of frequency for polyethylene with different MWCNT content.

For lowest concentrations (0.9 and 1.2 vol%), the composite shows similar behavior as the neat matrix with a conductivity around 10^{-13} S.cm^{-1} at low frequencies. However, a tremendous increase is observed from a certain fraction and the conductivity becomes independent to the frequency, characteristic of a conductive material. Consequently, a material composed of 96.5 vol% of an insulating polymeric matrix can be considered as electrically conductive with a measured conductivity of around 10^{-2} S.cm. The electrical conductivity of CNTs filled polymer composites has been extensively studied during last decades. Electrical properties of composites are sensitive to many parameters as pointed out by several reviews [28-30].

b) Percolation threshold

In polymer composites, the electron transport is handled by the conductive filler organization. A sufficient amount of filler is needed to observe an increase of the electrical conductivity by many orders of magnitude. As presented in **Figure 6**, the composite remains an insulator up to 1.5 vol% of CNT. Starting from this volume fraction, the conductivity increases nonlinearly with the filler content. The percolation theory is nowadays widely used to describe the evolution of the conductivity of polymer filled composites at the macroscale based on the filler network in the nanoscale [27, 31]. The same way the water goes through a sufficiently connected porous system of finely ground compacted coffee, electrons in polymer composites are transported through the material by the network of filler connections.

In our case and according to this mathematical theory, a critical value of the filler connections concentration is necessary to create an infinite network through the material. In the percolation theory, this critical value is referred as the percolation threshold. Starting from this amount, the percolating network governs the material conductivity. Below the percolation threshold, CNTs connections form, at best, clusters isolated from each other. The composite conductivity then remains governed by the polymer matrix conductivity.

Figure 7 illustrates schematically the formation of a percolated network. For insufficiently connected fillers (**Figure 7 left**), the network does not allow electrons to go through the material as the polymer is insulator. Once there are enough connections, the electron is transported from one electrode to the other by the conductive pathway (**Figure 7 right**).

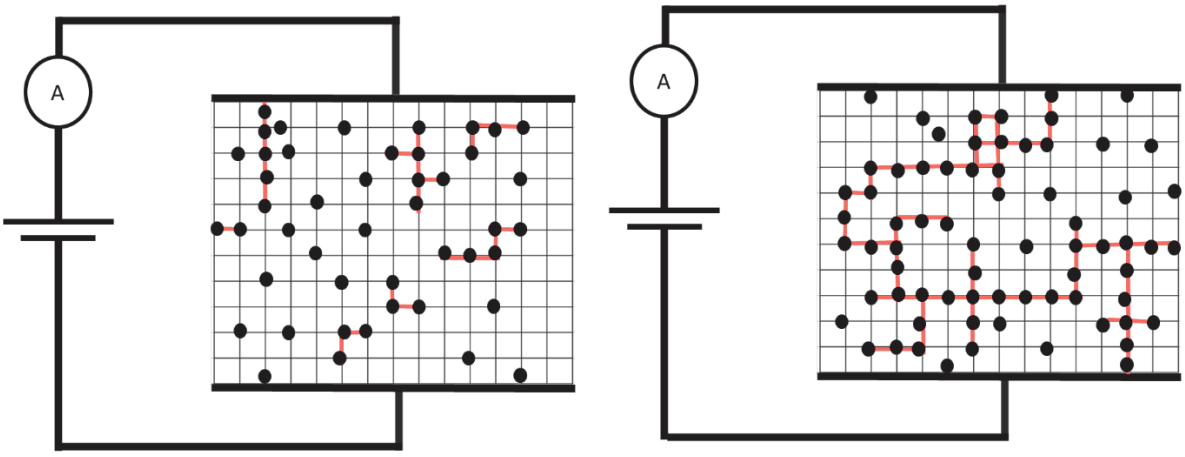

Figure 7: schematic view of electron path for an insufficiently connected fillers network (left) and percolated network (right)

In the case of polymer composites, the percolation theory is used to describe the evolution of electrical conductivity with filler fraction. When the filler volume fraction φ is below the percolation threshold φ_c, the conductivity is close to the polymer conductivity. Once the filler volume fraction exceeds the critical value φ_c the evolution of the conductivity is well described by the following Kirkpatrick's power law [32]:

$$\sigma = \sigma_0(\varphi - \varphi_c)^n \text{ for } \varphi > \varphi_c \qquad \text{Equation 2}$$

With σ_0 the theoretical macroscopic conductivity of the filler, *n* a critical exponent dependent on the dimension of the percolated system (rather than the fillers geometry). For a three-dimensional network, the value of *n* is around 2, even though values ranging from 1 to 4 are commonly reported in the literature [28]. An example of conductivity evolution as function of the CNT content is given in **Figure 8** for polystyrene-CNT composites.

Figure 8: Evolution of the electrical conductivity of PS filled with CNT as a function of the filler concentration. As inset, is plotted linearized expression of the conductivity. plotted from [33]

c) Assets and challenges of electrically conductive polymer-CNT composites

Concerning the percolation threshold value, this parameter is inherent to the filler geometry and the filler-matrix interactions. A filler geometry is generally described by the ratio of its length to the diameter, called the aspect ratio. In 1984, Balberg et al. reported a simple dependence of the percolation threshold on the aspect ratio [34]. For randomly oriented filler in a three dimensions space and for equivalent filler-filler and filler-matrix interactions, the percolation threshold φ_c is proportional to the inverse of the aspect ratio:

$$\varphi_c \propto \frac{1}{\frac{L}{D}} \qquad \text{Equation 3}$$

With *D* and *L* respectively diameter and length of the filler. With such a relation, the advantage of carbon nanotubes for conductive composites is clearly exposed as they offer a competitively high aspect ratio while presenting outstanding intrinsic electrical conductivity. To compare with another type of carbon nanofiller, carbon black presents an aspect ratio around 1 whereas

carbon nanotube can reach an aspect ratio of 1000. It follows that the filler concentration needed to create a percolated network is theoretically up to 1000 times lower with CNT.

Plenty of works reported in the literature investigated the electrical conductivity of polymer-carbon nanotubes composites. To present a survey, Bauhofer gathered 147 experimental results from various polymer-carbon nanotube systems. They showed the relatively good validity of the percolation theory for homogeneously distributed fillers. However, a non-negligible variation between theoretical and experimental parameters of the percolation law was pointed out [28]. In the case of some thermoplastics (Polyethylene for instance), the experimentally determined percolation threshold was often found above the predicted value whereas for other matrix (such as epoxy) the critical concentration was obtained at significantly lower values [35].

The deviation observed illustrates well the difference between a statistical model with an assumed perfect system and the experimental reality. In practice, carbon nanotubes are not straight but rather flexible, inducing a reduction of their length. In addition, because of strong interactions between CNTs, they can be found aggregated rather than being homogeneously distributed within the matrix.

Conclusion

With outstanding physical properties and a large aspect ratio, carbon nanotubes have been placed by researchers among the best candidates for many applications, especially for reinforced polymers.

For now, a perfect system was considered to explain the origin of conductivity whereas in fact, a lot of parameters in the composite preparation govern the electrical properties of the final polymer-carbon nanotubes composite. To present the experimental reality, the next section will be focused on challenges emerging during the preparation of CNT-Polymer composites and their final structure and properties.

II. Parameters influencing the conductivity of processed polymer-carbon nanotube composites

1- Composite processing

a) Carbon nanotube in a polymer matrix

A major problem encountered during polymer filled carbon nanotubes is the high disposition of carbon nanotubes to agglomerates. To benefit the best of the intrinsic mechanical and electrical properties of the filler for the final composite, CNTs have to be well dispersed in the matrix. Yet, commercially available carbon nanotubes are provided in highly agglomerated state due to the synthesis process and strong interaction between CNTs. An image of commercially CNT bundles can be seen in **Figure 9**.

Figure 9: SEM of commercially available carbon nanotube NC 7000 (Nanocyl). A) Primary agglomerate and B) at higher magnification [36]

Carbon nanotubes are characterized by a remarkably large surface area as they present a high aspect ratio (>100) with a diameter in the nanometer scale inducing strong Van der Walls and electrostatic forces. To facilitate the formation of a percolated network (i.e. to obtain the highest conductivity), the conductive filler must be homogeneously distributed and widely dispersed in the matrix. Therefore, initial bundles, large agglomerates, and clusters have to be untangled as much as possible by mechanical forces.

b) Steps of agglomerates dispersion

Dispersion routes of carbon nanotubes in a polymer matrix are diverse but the main dispersion mechanisms are the same. In the case of polymer processing, the fragmentation of aggregates by hydrodynamic forces is predominant. Dispersion steps can be summarized as follows: initial CNTs agglomerates are firstly wetted by the polymer. Polymer chains will infiltrate into fillers bundles to weaken them. Agglomerates will then be dispersed by encountering rupture and erosion phenomena to initiate a distribution of individualized CNTs and small aggregates in the matrix.

Interfacial energy between the filler and the liquid used are important as the initial wetting mainly depends on this property. CNTs are reported as polar. Then, when non-polar polymer melts (such as polyolefin) are used, problems can occur as early as the wetting should begin [37]. Once the agglomerate surface is covered, the polymer infiltration can arise. For a fully wettable capillary, the time dependent infiltration length $h(t)^2$ is expressed by the following Lucas-Washburn equation:

$$h(t)^2 = \frac{r \cdot \gamma \cdot \cos\theta \cdot t}{2 \cdot \eta} \qquad \text{Equation 4}$$

In this this equation r is the pore radius, γ the interfacial tension between capillary and liquid, θ the contact angle and η the viscosity. From this equation, it appears evident that a lower liquid viscosity helps agglomerates infiltration as it was observed by Yamada et al. on carbon black agglomerate infiltration by polymer melts [38, 39]. The infiltration was found to rely on liquid characteristics. To infiltrate agglomerates in the best possible way, it can therefore be useful to modify, when it is possible, the polymer type or the molar mass.

The agglomerates break-down under hydrodynamic forces has been widely studied [40, 41]. To disperse the agglomerates, hydrodynamic forces F_h must be stronger than the agglomerate cohesive forces F_c. The dispersion mechanism can be characterized by the ratio between the two latter forces as the fragmentation number F_a :

$$F_a = \frac{F_h}{F_c} = \frac{\eta \cdot \dot{\gamma} \cdot R^2}{F_c} \qquad \text{Equation 5}$$

With η the medium viscosity, $\dot{\gamma}$ the applied shear rate, R the radius of the agglomerate and F_c the cohesive force of the agglomerate [42]. Depending on the fragmentation number, two specific cases emerge. For $F_a \gg 1$, agglomerates will mainly encounter rupture or shutter mechanisms, breaking the initial agglomerate into two parts (rupture) or more (shutter) of similar size. For $F_a \ll 1$ a slower dispersion process takes place, small fragments (<10% of the volume of the primary particle) or individual particles eroded from agglomerates [40]. This mechanism has been described kinetically in the literature [43, 44]. In both cases, smaller entities can then be dispersed and homogeneously distributed in the polymer matrix.

c) Method for composite processing

A wide choice of routes is available to disperse CNTs homogeneously in a polymer matrix but there are mainly three methods commercially viable.

c.i) Solution mixing

A simple method for CNT incorporation in low viscous polymer composite is the solution mixing. CNTs and polymer are mixed separately in the same suitable solvent. First, the de-agglomeration of CNT cluster takes place in this low viscosity media and therefore requires external forces to be adequate. For this reason, researchers proposed many techniques such as ultrasonic agitation [45, 46], mechanical mixing, surface modification of CNT [47] or the addition of surfactants [48, 49]. Dispersed CNTs solution and polymer are then mixed together in the solvent. To obtain a CNT-polymer composite, the solvent is then removed using generally one of the following methods. A slow mechanism of evaporation can be employed, giving the possibility to directly produce composite films or fibers. It is also possible to add an excess of a liquid solely miscible with the solvent quickly excluding CNTs and the polymer. This technique in principally used for gel spinning and electrospinning [50].

c.ii) Dispersion reaction route

The dispersion reaction route is not so different from the solution mixing and regroups thermosets composite generation and in-situ polymerization. Here again CNT are first dispersed in a liquid system, but then inserted in the monomers. Controlled polymerization of the desired polymer is subsequently triggered by the addition of an initiator or another monomer. Polystyrene and polyacrylates filled with CNT can namely be produced by this route as they have liquid monomer [51, 52]. The presence of CNT can interfere with known polymerization techniques. Indeed, CNTs are absorbing ultraviolet, preventing this kind of initiation. But microwaves can trigger polymerization by the local temperature increase induced by the CNTs absorption of such radiation [53].

In the case of thermosets, CNT-epoxy can for instance be obtained by a first dispersion in the resin followed by the cure of the resin with hardener [54, 55], polyimide [56, 57] ,… This route is currently used in the industry for thermosets and rubber-based composites whereas another method is preferred for industrial application of thermoplastics polymer composites.

c.iii) Melt processing

The third presented mixing technique consists in the incorporation of the filler in the molten matrix. This approach is attractive for composite preparation as it can be used for a wide range of polymer. In addition, no solvents are used, and less steps and time are required compared to the mixing techniques presented previously. It is commonly used for the fabrication of thermoplastic polymer composites, for instance polypropylene [58] or polystyrene [59]. Industrially, this route allows continuous and large production of composite as they can be processed directly after the incorporation of the filler using extrusion, injection molding, blow molding, calendaring…. The melt mixing strategy can be composed of a unique step of incorporation and mixing in the melt matrix (direct mixing) or comprise two or more

stages (masterbatch dilution). In the second case, the filler is firstly incorporated at high loading (typically between 10 to 20 wt%) in a matrix, this blend is called masterbatch. The masterbatch is then diluted by addition of pure polymer matrix by melt mixing to decrease the filler concentration to the desired value. For sake of easier processing and dispersion, the polymer used in the masterbatch does not necessarily have the same molar mass as the one used for the final dilution.

While fillers are dispersed in a low viscous liquid during solution mixing by sonication, this task is here achieved owing to high mechanical mixing energies in higher viscosities melts [60, 61]. Not only the energies used for the dispersion are lower but also a high number of input parameters can lower its efficiency. Factors influencing the final electrical properties and the structure of composites have been well studied and will now be presented as this was the process used in the experimental sections of this work.

2- Dispersion characterization and improvement methods

a) Characterization

Polymer-CNT composites are employed in specific applications with precise properties (mechanical reinforcement, thermal or electrical conductivity). These composites characteristics depend significantly on the state of dispersion and distribution of CNTs in the polymer matrix and this dispersion can vary with the characteristics of the polymer material as well as processing conditions. It remains difficult to quantify the impact of these parameters.

Morphological characterization is commonly based on microscopy. The state of dispersion can be observed by scanning electron microscopy (SEM), transmission electron microscopy (TEM), atomic force microscopy (AFM) as well as Optical microscopy (OM). Qualitative observations can be made to investigate the influence of processing conditions on the quality of the filler dispersion. A dispersion index is often introduced to compare samples. The CNT length distribution can also be evaluated using AFM or TEM. Concretely, the morphological characterization provides useful and visual information about the state of dispersion but presents some limitations. The quantitative deduction of the 3D structure of the composite by microscopy is complex when possible. It may be noted that those measurements are principally carried out on solid sample and may require time consuming preparations to be analyzed.

For instance, charge contrast SEM (by means of an in-lens detector) allows the obtention of a 2D picture of the CNT dispersion in a matrix as observed by Marcourt et al. for polystyrene-CNT composites in **Figure 10** [33]. This technique enhances the contrast between the electrically conductor filler and the insulating matrix and allows the observation of the filler in the volume (as compared as typical topographic observation by SEM). However, a special attention must be paid to the surface preparation to promote the electrical contrast over the topographic contrast.

Figure 10: SEM observation with in-Lens detector of a PS filled with 0.79 vol. % CNT (compression molded). Reproduced from [33]

Indirect methods of characterization are also often used to determine the CNT dispersion quality. The characterization of physical properties can also turn out useful to interpret the state of dispersion of CNT in the polymer matrix. In that sense, rheological as well as electrical measurements can be used to characterize the state of dispersion. Electrical percolation thresholds and achieved conductivity are important characteristics to evaluate the state of the conductive network. For a given CNT content, an increase of the electrical conductivity can be linked for instance, to an improvement of the dispersion. Interestingly, time resolved electrical characterization can be implemented to monitor important information on the dynamics of the CNTs dispersion of in the melt polymer.

In conclusion, morphological characterization and physical properties are useful tools to analyze the impact of various parameters on the dispersion state. The following sections will present current understandings of the impact of the polymer material characteristics and processing conditions on composites properties.

b) Composition

b.i) Filler

As previously observed in **Figure 9**, CNTs are generally supplied as highly entangled agglomerates of high cohesive strength. The cohesive strength of SWCNT agglomerates is often too strong to be well dispersed during melt processing. The solvent mixing method is then preferred for such fillers. Therefore, the majority of CNTs used on an industrial scale for melt processing of polymer-CNT composites are multi-walled carbon nanotubes as they are offer a good compromise between price and final properties.

However, the properties of polymer-MWCNTs composites can significantly vary depending on the filler manufacturer. Hence, the filler characteristics can vary mainly in terms of purity, length and diameter distribution of tubes and the structure of agglomerates [36, 62]. As explained previously, the dispersion of primary agglomerates is eased for smaller and lower densities aggregates. This can be explained by a higher cohesion strength in agglomerates that makes the wetting and melt infiltration harder. The structure of nanotubes is also important as thinner or longer tubes form agglomerates that are much more entangled hence stronger. However, it should be recalled that spectacular intrinsic properties are also related to the very high aspect ratio of the filler. As a matter of fact, shortening the CNT length improves the dispersion and distribution of CNT in the melt, but to the cost of their properties [63].

The same trend is observed with purity: while the purity of tubes enhances the intrinsic electrical and mechanical properties, the presence of defect will reduce cohesive forces (e.g. lower van des Waals forces) and most likely facilitate the wetting and infiltration by the melt polymer. As expected, studies showed that the choice of nanotubes influence the dispersion state [64, 65].

Due to different manufacturing methods, nanotubes are sold with various characteristics: different purity, tube length and diameter, bulk density, agglomerate size and so on that it remains difficult to clearly determine the impact of each parameter. The preparation of CNT with controlled properties is achievable on a laboratory scale but the same mission is hardly feasible in large production scale.

b.ii) Polymer

As it was presented earlier with the Lucas-Washburn **Equation 4**, interaction between the filler and the matrix play an important role for the dispersion of nanotubes. A strong affinity between two components will favor the wetting and dispersion of one into the other. The affinity of two species is determined by measuring the interfacial energy between them. Studies were performed to determine the impact of different polymer types on the CNTs dispersion. To do so, composites with various thermoplastic polymer matrices were prepared and the state of dispersion (here described by the area ratio of undispersed agglomerates A_A corresponding to the observed area of agglomerates related to the image area) was plotted as a function of the interfacial energy between the polymer and the filler as drawn in **Figure 11** [66].

Figure 11 : Area ratio of undispersed CNT agglomerates A_A versus interfacial energy (dotted line is only a guide). Plotted from ref [66]

The conclusion made from **Figure** 11 is that there is no clear correlation. Yet, the authors underlined in this study that, taken PMMA and PS apart, a tendency can be observed: a higher interfacial energy between the two components tends to hinder the CNT dispersion (dotted line in the figure). This deduction would be in accordance with the Lucas-Washburn equation. To explain the variation from the theory, it could be noted that other parameters such as steric aspects of molecular structure could not be fixed and might play a role in the dispersion mechanism.

Another way to influence the dispersion of agglomerates during melt processing is to increase hydrodynamic forces. For given processing conditions, increasing the melt viscosity will result in higher shear stresses applied on agglomerates which in principle, speed up the size reduction of the agglomerate. Nevertheless, the infiltration of the agglomerates is improved when lower molar mass polymer melts are used. This specific effect was studied by Yamada et al. for carbon black agglomerates infiltration with PDMS of different viscosities [38, 39]. Kasaliwal et al. confirmed this observation by studying the dispersion state of CNTs for different three polycarbonates (PC) of various molar mass [67, 68]. The state of dispersion (characterized by its Area ratio) was compared for every sample as function of the mixing speed and the applied shear stress (plotted in **Figure 12**). It was observed that, for a given mixing speed a higher viscosity of the melt leads to the best dispersion. However, the difference of dispersion state is reduced and vanishes for increasing mixing time. In that respect, when the same state of dispersion was plotted as function of the applied shear stress, it was noted that lower viscosities required lower shear stress to reduce agglomerate size. Two main conclusions were drawn from this study: a lower molar mass does indeed facilitate the infiltration of primary CNT agglomerates, but the applied stress still must be sufficient to overcome the cohesive strength of this porous structure [67].

Figure 12: Area ratio as function of mixing speed (a) and applied shear stress (b) for composites of PCs with different viscosity and 1wt% MWCNT plotted from [67]

It can be observed that the type of material has a logical influence on the state of dispersion and on the properties of the final product. One can therefore choose specific nanotubes (purity, aspect ratio, conductivity…), and matrix (viscosity, type of polymer…) that fulfill the requirements. However, the choice of the matrix and filler can also be restricted depending on the application or other industrial obligation. In that case, there exist other ways to tune the quality of the dispersion and/or the final properties of the composites.

c) Processing conditions

As it was already introduced by the modification of polymer melt viscosity, many parameters can be tailored for the melt mixing method. For instance, the screw profile, the mixing speed and time as well as the melt temperature can be easily modified to adapt the melt viscosity, the shear rate, and the residence time. These latter directly influence the shear stress and mixing energy provided to the composite hence influencing the dispersion and dispersion kinetics of CNTs in the melt polymer.

It is comprehensible that the influence of some processing parameters on the filler dispersion will be linked to previously presented conclusion. Nevertheless, the modification of processing parameters is useful as it may overcome the underlying material limitations imposed by the application. In this way, Kasaliwal et al. varied the melt temperature and mixing speed at a constant mixing time on a micro compounder and compared the dispersion state of CNTs in a polycarbonate matrix [69]. The conclusion was analogous to the one about melt viscosity: for small mixing speed (<100 rpm), lower temperature induces a better dispersion as more energy is provided to disperse agglomerates. For higher mixing speed, for any mixing temperature the mixing energy is sufficient to disperse to a similar state in all the composites [69].

The team directed by Petra Pötschke from the Leibniz Institute of Polymer Research Dresden conducted various studies to understand the impact of various process conditions on the state of CNTs dispersion and final properties from small scale melt mixing to the use of industrial scale extruders [62, 70, 71]. To a certain extent, the observation at a small scale of the

melt mixing is relevant to extrapolate to the industrial scale. Their work particularly highlighted the impact of CNT content, the residence time, and the screw profile on CNT dispersion but also on the electrical properties of the final product. It was concluded that processing conditions must be adapted to optimize the conjugate action of two main parameters: The polymer melt infiltration and the applied shear stress.

The infiltration process mostly relies on characteristics of polymer, using lower melt viscosities polymer facilitates this process but the shear stress applied to the agglomerate will also be reduced. A solution to increase the viscosity of the mix is to insert higher loadings of filler into the melt matrix. It may look counter-intuitive that adding higher content of filler helps the dispersion of primary agglomerate in the polymer but the use of the masterbatch dilution allows the obtention of well dispersed composites with low percolation threshold. In fact, masterbatch preparation and then dilution allows the filler to be mixed twice in a polymer matrix, hence providing more energy and residence time to disperse the primary agglomerates. This route is especially attractive for industrial applications as extrusion allows a good adaptability of processing conditions even with possible materials restrictions. However, mixing conditions must be well controlled as too high shear forces may induce irreversible damages to the filler [71]. The shear stress can lead to a breaking of nanotubes, reducing their aspect ratio, hence deteriorating their intrinsic properties.

d) Filler/matrix interactions

Other techniques might be used to optimize the state of dispersion and/or the final properties of the composite. They will be briefly exposed here.

d.i) Surface modification

Carbon nanotubes chemical bonds are aromatic inducing a chemically stable and inert structure. As a result, nanotubes and nanotubes agglomerates interacts with the matrix mainly by Van der Waals interactions. A strong coupling between CNTs and non-polar polymers (such as Polyethylene) is then particularly difficult to achieve. Modifying the surface properties of CNTs is a solution to improve the dispersion of the filler in the matrix and has been widely studied in the literature [72-75]. Various methods can be employed to modify these surface properties; they are commonly split between chemical and physical approach [76, 77].

A chemical functionalization of CNTs consists in the covalent linkage of functional entities onto the nanotube structure, either on the sidewalls or the extremities [75]. To do so, existing defects in the aromatic structure can be used or created to allow further covalent linkage. Grafted groups then induce enhanced interactions between the nanotube and the polymer; therefore, a better dispersion is obtained. The grafting of a polymer onto the filler surface can enable a good dispersion of CNTs in the matrix [78, 79]. However, the modification of this initially perfect structure results usually in the weakening of intrinsic properties of CNTs [74, 75]. Moreover, chemical treatments may require additional steps and the use of solvent and acid treatment that may be inconvenient and expensive for industrial applications.

To promote the CNTs dispersion while maintaining the integrity of the filler, it is possible to choose the route of non-covalent functionalization [75]. For instance, the wrapping of polymer around the CNTs is possible thanks to strong van der Waals interaction and $\pi - \pi$ stacking when using polymer containing aromatic structure (such as polystyrene) [80]. This wrapping enhances the interaction between the filler and the matrix, facilitating the dispersion.

Some studies also report the use of surfactants to enhance the dispersion of CNT but also the electrical and mechanical behaviors with various matrix [81]. The surface tension of CNTs is lowered by the physical adsorption of surfactant on the filler surface. The effectiveness of the CNTs dispersion using this method strongly depends on the properties of the surfactant and the polymer. As a matter of fact, for water-soluble polymers the use of cationic surfactant is recommended whereas for polymers like polyolefin (polyethylene or polypropylene) the CNTs dispersion is eased in presence of a non-ionic surfactant [81, 82]. The use of additives as compatibilizer happens to be attractive as it can be easily applicable in the melt mixing method to enhance the dispersion and reduce the percolation threshold [83, 84]. However, even if a wide choice of additives is available and efficient, the mechanisms responsible for these positive effects are not always explained and controlled [83].

d.ii) Third component and phase exclusion

The simplest polymer-CNT composite is composed of polymer and carbon nanotube, but the use of other materials can be helpful for some reasons. The addition of a second filler was found beneficial for the CNT dispersion in the matrix in various studies [85-87]. Liu showed that the addition of only 2 wt % of clay in a SWCNT-epoxy composite led to a distinct reduction of the percolation threshold. The increase of applied shear stress to the filler might have caused a better dispersion of the conductive filler [87].

This mechanism can be assisted by another phenomenon when the second filler content is sufficient. The total volume of the composite is composed by the volume of its components, hence the addition of a non-negligible quantity of a second filler will reduce available space for nanotube and therefore increase CNT contact probability [86, 88]. For instance, Marcourt et al. compared the percolation threshold in a pure polystyrene matrix and a rubber-modified polystyrene. The presence of 40 vol % polybutadiene in the latter reduced the percolation threshold by a factor of two as the CNT distribution is modified (CNTs are only found in the polystyrene phasis) [88]. Electrical conductivity can therefore be improved by the segregation in a fraction of the total volume as the conductivity is related to the network created by CNT connections. The expression of effective concentration was introduced as the volume of CNT divided by the sum of the volume of CNT and the polymer to explain and quantify the effect of this phenomenon on the percolation threshold. The conductive filler exclusion from a part of the composite by a second filler is an interesting method to reduce the total quantity of such expansive filler as long as the second filler is cheap and does not induce mechanical or processing problems.

An extreme case of volume exclusion to drastically reduce the total CNT content while obtaining electrical conductivity is the use of polymer blends [89]. Observed as early as 1991 on polymer blends filled with carbon black this method is referred as the double percolation as a percolation is obtained by CNTs and by the co-continuous morphology of polymers [90]. The continuity of the polymer phasis containing the filler allows the reduction of the total CNT content to obtain electrical percolation. In that respect, while a CNT content of 1.4 vol% are required to obtain the percolation threshold in a polycarbonate matrix, the blend of this PC-MWCNT composite with a polyethylene matrix reduces the total concentration of CNT to 0.41 vol% [89].

Conclusion

In this part we introduced the crucial importance of the dispersion of CNTs in a polymer matrix to obtain appropriate physical properties. Mechanisms of carbon nanotubes dispersion and the primordial role of infiltration, rupture and erosion of initial agglomerates were presented. Among some mixing methods introduced, a focus was made on melt processing as this route offers adaptability by the presence of various processing parameters and a certain ease of use. This flexible technique allows the tuning of the dispersion to reach aimed properties (mechanical reinforcement, electrical conductivity). Numerous studies were made to understand the impact of processing parameters as well as the impact of materials used. Thanks to that, the multiple parameters of melt processing can now be seen as an opportunity to tune final properties of the composite. The masterbatch dilution was found useful for the industrial manufacturing of polymer-CNT composites as it makes it easier to disperse primary agglomerate as shear forces are stronger and mixing time are extended. When this method is not applicable or not sufficient, other techniques may be used.

The importance of the dispersion of CNT primary agglomerates was developed to disperse and distribute homogenously the filler in the matrix but the final electrical property of the composite also depends on the connection of these well dispersed fillers to allow electrical charge transport. An inhomogeneous distribution is, in that sense, preferred to increase the number of connections. During composite processing, the applied deformation modifies the state of the filler network responsible for the electrical conductivity.

III. Modifying the conductivity of a polymer-CNT nanocomposite

The electrical conductivity of the composite depends on the state of dispersion of carbon nanotubes, but electrical properties also rely on the existence of electrical contacts between these well dispersed conductive fillers (see **Figure 7**). During compounding and processing, the composite undergoes mechanical deformation that modifies the filler network. The primordial influence of thermal and rheological history on the conductivity of the composite will be exposed in this last part of this state of the art.

1- Dynamic of CNTs in quiescent melt polymer

In the previous section, the effort to disperse the filler homogeneously with as low agglomeration as possible was exposed. To obtain the best isotropic mechanical reinforcement, this random distribution is indeed the best option. However, when CNT are used for an electrical purpose, it turned out that the optimal filler organization relies on small aggregates and individuals CNTs close enough from each other to enables charge transport.

a) Conductivity of composites with well dispersed and homogenously distributed CNT in a polymer matrix

It was shown previously that the destruction of primary agglomerates by means of chemical and physical methods led to better physical properties. However, Pegel et al. observed an interesting behavior when they compared the dispersion state of two specimens with different conductivities [91]. Polycarbonate filled with 0.6 vol% of MWCNT composites were prepared using the masterbatch dilution technique and pressed at various temperatures to be characterized. In terms of conductivity, the composite processed at the higher temperatures (300°C) presented the best properties with a conductivity in the range of $10^{-4}\ S.cm^{-1}$ while a conductivity comparable to the polymer conductivity ($< 10^{-16}\ S.cm^{-1}$) was obtained for lower temperature (260°C). The dispersion state in both samples was then compared using transmission electron micrographs. The specimen characterized by a good dispersion of nanotubes in the polymer was found to be the one presenting the lowest conductivity as observed in **Figure 13**. The sample prepared at higher temperature presented a structure of agglomerates and individual CNTs more closely packed, showing of an interconnected network as it was previously described in **Figure 7**.

Figure 13: transmission electron micrographs from PC-MWCNT plates with 0.6 vol% MWCNT: (a) non-conductive state ($\sigma_{DC} < 10^{-16}\ S.cm^{-1}$) with well dispersed nanotubes, pressed at 265°C and (b,c) conductive state ($\sigma_{DC} = 5 \cdot 10^{-4}\ S.cm^{-1}$) with nanotubes agglomerates pressed at 300°C. reproduced from [92]

At first sight, it can be expected that agglomerates are remaining from primary agglomerates. As the mixing temperature was higher, the viscosity was reduced hence applied shear stress might not have been sufficient to disperse CNTs in the melt matrix. In fact, the origin of agglomerates was explained by another phenomenon: the secondary agglomeration of CNTs. This mechanism was observed by the preparation of samples in two steps: first, samples are mixed to obtain well dispersed nanotubes (**Figure 13 a**), then the samples are heated up to 300°C. The as-prepared specimens show an agglomerated structure close to the one observed in **Figure 13 b and c**. Therefore, the observed agglomerates have been created during the heating step [91]. The secondary agglomeration was also pointed out in other studies either by optical microscopy [93] or by the observation of a conductivity increase during isothermal annealing of PC-MWCNT composite [94].

To explain the increase in conductivity of composites, it must be remembered that it relies on the intrinsic properties of the filler, but small inter-particles is necessary for efficient electron transport. For well dispersed systems, filler is surrounded by polymer chains resulting in a high contact resistance. On the contrary CNTs agglomerates induce small inter-particles distances hence low contact resistance. The presence of secondary agglomerates taking part in a percolated network is therefore related to higher conductivities. The mechanism of the secondary agglomeration will now be presented.

b) Insulator to conductor transition also known as Dynamic percolation

An insulator to conductor transition was observed by Sumita as early as 1995 for polyethylene filled with carbon black [95]. In the same way, with nanotubes, the annealing of thermoplastic polymer-CNT composites above the melting temperature (or glass transition for amorphous polymers) allows the modification of the filler network structure inducing a conductivity increase. Due to processing steps, primary agglomerates were dispersed into small agglomerates and individual CNTs in the matrix. As these fillers are isolated from each other, there is no conductive pathway: the composite is an insulator (see **Figure 7 a**). Above the melting temperature (or glass transition), a mechanism of auto-assembly of these isolated

fillers occurs as soon as a sufficient mobility is provided in the melt polymer. Increasing the temperature was found to increase the kinetics of conductivity recovery [96]. This phenomenon can be simply described as a clustering process where two isolated nanotubes draw near due to diffusion and the attractive interaction between them leads to an interparticle connection: secondary agglomerates are created inside the matrix. The sample then switches from a well dispersed state to an aggregated state. It must be remembered that the interfacial energy between nanotubes and polymer can be strong, hence the filler will likely agglomerate to tend to a thermodynamic equilibrium.

Combessis et al. presented the continuous transition from an insulator to a conductive EVA-CNT composite in an interesting way [96]. The AC conductivity of composite with initially low conductivity ($\sim 10^{-12}\ S.cm^{-1}$) was measured as a function of annealing time at 150°C. With increasing annealing time, the measured conductivity gradually improves as it can be observed in **Figure 14**. Results from this figure are remarkable as an analogy can directly be made between the annealing time and increasing CNT content that were presented in **Figure 6**. In other words, during annealing above the melt temperature, the conductivity evolves as if the filler concentration was increased. For this exact reason, this mechanism is referred as the dynamic percolation. More practically, it can be considered that a large part of the dispersed CNTs do not contribute to the percolated network in the initial material but these CNTs join and reinforce the conductive network over time.

Figure 14: Change in frequency dependence of the conductivity of a composite sample filled with a steady content of 2.2wt. % of MWCNT and annealed at 150°C (inset is conductivity as a function of time for f=10⁴ Hz). reproduced from [96].

In this paper, the difference between the theoretical percolation threshold (depending on the aspect ratio of the filler) and most of the measured percolation threshold was pointed out. Depending on the composite processing way (i.e the obtained dispersion), a non-negligible part of introduced CNTs may be isolated from the conductive network. Annealing was found to reduce the discrepancy between theoretical and practical percolation thresholds as the conductive network is reinforced by the reconnection of isolated CNTs.

As a conclusion, the total filler content introduced in the composite must be distinguished with the effective filler concentration that plays a part in the electrical conductivity of the material. In other words, the percolation law of **Equation 2** may be changed to:

$$\sigma = \sigma_0(\varphi_{eff} - \varphi_c)^t \qquad \text{Equation 6}$$

where φ_{eff} is the effective filler volume fraction, defined as the filler concentration contributing to the conductivity of the sample, necessarily lower or equal to the total filler fraction φ.

c) Modeling the dynamic percolation

The dynamic percolation allows tremendous enhancing of electrical conductivity, hence the control of the network modification by this mechanism appears important and could find a place in industrial process. Indeed, as the filler aggregation is thermally activated, a short annealing time at elevated temperature can for instance be implemented in the industrial process to make possible a conductivity recovery after processing steps. Considering **Equation 6**, the conductivity may be enhanced either by increasing the amount of filler φ or by improving the effective filler concentration. Various origins for this thermally activated mechanism of structuration have been proposed whether they are entropic (Brownian motion, chain relaxation) or thermodynamic (flocculation) [96].

For Cipriano, the relaxation of macromolecules in annealed melt induces a change in the isotropy of filler oriented by processing conditions that then favors filler-filler contacts [97]. The same year, Zhang proposed for polymer filled with carbon black composites that the dynamic percolation kinetics and ability was related to the filler-matrix interfacial energy which in turn depends on annealing time [98].

A comprehensive study of driving forces for the dynamic percolation was conducted by Combessis. From their observation, they proposed a phenomenological model in which both dispersion and distribution of the fillers are modified during dynamic percolation. During annealing, first, the clusters formation modifies the local dispersion by entropic relaxation of polymer chains. For longer times, the macroscopic distribution is changed by diffusion [96]. In 2010, the filler distribution modification over time and the aggregation mechanism was already monitored in PDMS-CNT composite by optical microscopy [93]. A phase separation was also observed to the naked eye in diluted samples for a 24 h annealing at 200°C of an EVA-CNT composite (0.1 wt % MWCNT). The dynamic percolation of CNTs in silicone oil was recently investigated by this team, and an exhaustive model was proposed to describe the evolution of the percolation law with annealing time. They observed a variation of both the percolation threshold and the critical exponent with time, which may be correlated to the change in the distribution state of the filler. The implementation of a time dependent (i.e., dependent on the distribution of the filler) value of critical exponent could enhance the resolution in the determination of the percolation threshold. The used methodology allowed the presentation

of a rigorous model but required a large amount of experimental data close to the percolation threshold [99].

Alig et al. proposed to model the network recovery after shear deformation by combining the classical percolation theory and a model for cluster aggregation in more viscous polymer [94]. A time dependent parameter replaces the filler volume fraction in the percolation theory to introduce the cluster aggregation mechanism:

$$\sigma = \sigma_0(\varphi_{eff}(t) - \varphi_c)^s \qquad \text{Equation 7}$$

where φ_{eff} is the time dependent parameter of effective volume concentration of the nanotube clusters contributing to the percolated network, σ_0 is the conductivity of clusters formed by CNTs, φ_c is the percolation threshold, and s is a critical exponent. φ_{eff} is obtained by the evaluation of the number density of clusters as a function of time using a second order kinetic equation.

More recently, Marcourt et al. proposed a simple kinetic equation, close to the one described by Alig, to express the evolution of the effective fraction of CNTs used in **Equation 7**:

$$\left.\frac{d\varphi_{eff}}{dt}\right|_{structuring} = k_{build}(\varphi - \varphi_{eff}) \qquad \text{Equation 8}$$

With φ the total filler fraction; φ_{eff} is the filler fraction connected in the conductive network, necessarily limited to φ. For a given matrix, the parameter k_{build} was found to be solely dependent on the annealing temperature and more specifically linked to the relaxation time of the polymer matrix [33]. A direct correspondence between the effective concentration and the annealing time could then be proposed as:

$$\varphi_{eff} = \varphi + (\varphi_0 - \varphi)e^{-k_{build}.t} \qquad \text{Equation 9}$$

Where φ_0 corresponds to the initial effective filler fraction. It is easily understandable that modeling the conductivity recovery is a promising support to predict and tune the final properties of manufactured nanocomposites with reduced filler content.

Quiescent annealing treatment could be a method to trigger the conductive nanotube network strengthening. To obtain a final composite with sufficient electrical conductivity, this cure might be necessary after processing steps that modify the network structure.

2- Deformation influence on the electrical properties

Depending on the processing of polymer-CNT composite, the material may be submitted to a wide range of deformation that either modifies the nanotubes conductive network and/or the state of dispersion. As the network quality is accountable for the electrical conductivity, the analysis of the impact of deformation to the system seems crucial. The rheology then appears mandatory to deepen the comprehension of the modification mechanism occurring in the melt.

Conductivity measurements allow an easy monitoring of the nanotubes network. The development of rheological analyses coupled with conductivity measurements were found useful to study the mechanisms responsible for the network modification in the melt polymer.

a) Rheology of polymer-CNT composites

The viscoelastic properties of melt polymer-CNT composites were studied in literature for various systems. With increasing the CNTs content, the material behavior changes from an initially viscous liquid to a solid. For low CNT content, the rheological behavior is controlled by the polymer matrix, but once the percolation is achieved, a noticeable change appears. One can therefore detect the rheological percolation threshold by the increase in the complex shear modulus $G^*(\omega)$ and the apparition of an equilibrium modulus G_e for the storage modulus G' at low frequencies as observed in **Figure 15** by Valentino et al. [100]. This is the common behavior for fillers percolation and was observed for various polymers and fillers [100-102].

Figure 15: (a) complex viscosity (η^*) and (b) storage modulus (G') as function of frequency (ω) for MWCNT/HDPE composites and pure HDPE (T=200°C). plotted from ref [100]

Rheological measurements therefore allow obtaining structural information on the quality of the filler network. However, the percolation threshold observed by rheological measurements can differ from the electrical percolation threshold presented previously. To obtain an electrical percolation, the nanotubes do not necessarily geometrically overlap, as

electron transport mechanisms (electron hopping or tunneling) can occur for nanotubes distanced by between 5 and 10 nm. In contrast, the rheological percolation threshold is determined by a solid-like behavior requiring permanent contacts between fillers and different filler-filler distances are therefore required. In that respect Pötschke et al. and Du et al. reported different CNT content required to achieve the electrical and the rheological percolation threshold [101, 103]. The direct use of rheological measurements to study the electrically conductive network modification during deformation therefore appears less appropriate. Moreover, it must be pointed out that, by nature and contrary to electrical measurements, a rheological measurement requires a deformation of the material which may be enough to partially break the network, especially when it is weak, which is the case for very low percolation thresholds. Thus, the percolation threshold may appear higher from a rheological measurement.

b) Combined rheological and electrical measurements

The development of rheological analysis combined with conductivity measurement allowed to deepen the knowledge on the CNT network modification in melt polymer. The CNT network state is monitored by a conductivity measurement while a well-defined shear rate and deformation is applied to the sample. Simultaneous characterization is enabled using a ring-plate geometry electrode. Obzrut first used this rheoelectric set-up and monitored the destruction of a conductive network for PP/CNT composite under steady shear [104]. They observed that the conductivity evolution induced by a shear deformation was dependent on the shear rate. For sufficient shear rates, the deformation could then induce a transition from an initially conducting behavior to an insulating one [104]. A similar equipment was then used to observe the network modification for various polymer-CNT systems either during deformation or in the quiescent melt [93,105-107].

Figure 16 shows two different evolutions observed during steady shear deformation and the following annealing. For a well-formed network (**Figure 16 a**), the shear stress applied to the sample induces filler connections break-up observed by the conductivity decrease. Once the deformation is stopped, the electrical conductivity increases thanks to the dynamic percolation mechanism and clusters formation. In the case of initially low conductivity (in the order of polymers conductivity), they observed that a transition from insulator to conductor could be observed during a steady shear deformation (**Figure 16 b**). They proposed that shear deformation stimulates the agglomeration between isolated CNT or small aggregates thanks to a "picking-up" mechanism under steady shear [108]. For sufficient duration of the steady shear flow, a dynamic equilibrium state of conductive fillers network is observed by a constant conductivity. Interestingly, this equilibrium state does not depend on the initial state of the conducting nanotubes network [107,108].

Figure 16: Time-dependent conductivity for initially agglomerated (a) and well dispersed (b) composites of MWCNT (0.6 vol%) in PC under steady shear deformation ($\dot{\gamma}$ =0.02 s^{-1} for 1 h) and during quiescent annealing after shear at 230 C. The inserts schematically show the state of nanotube dispersion and the measuring cell with the sample. Plotted from [108]

Rheological analyses combined with electrical measurements showed the influence of deformation on the network structure. The thermo-rheological history therefore appears crucial for the final electrical properties of manufactured polymer-carbon nanotubes composites. As high shear rates are often used in large scale production, the tuning of the final properties is an industrial challenge in conductive polymer-CNT composite.

A few teams analyzed by in-line measurements the conductive network structure modification induced by the extrusion and the injection process. Alig monitored the tremendous impact of an extrusion at a screw speed of 175 rpm on the state of the conductive network and the conductivity recovery after cessation of extrusion [109]. The same team managed to implement in-line conductivity measurements during injection molding of polycarbonate and polyamide filled with carbon nanotubes under various conditions [110]. From these works, they once again observed that the destruction of the conducting network is facilitated using stronger mechanical deformation.

c) Modeling the conductivity loss induced by a deformation

The establishment of a model attracted researchers and industrials as it could help to control the final properties of a processed material. A model was proposed by Skipa following the results from rheo-electrical measurements to describe the conductive network modification during shear deformation [107]. Using the equation of dynamic percolation (**Equation 7**), they propose that the agglomerate fraction contributing to the electrical conductivity φ_{eff} can be expressed by a kinetic equation:

$$\frac{d\varphi_{eff}}{dt} = k_0\left(\varphi - \varphi_{eff}\right)^n + k_1\left(\varphi - \varphi_{eff}\right) - k_2\varphi_{eff} \qquad \text{Equation 10}$$

Where φ represent the filler volume fraction of agglomerates at the equilibrium ($t \to \infty$) and the kinetic parameters k_0, k_1 and k_2 are related respectively to the process of quiescent agglomeration, to the shear induced agglomeration and to shear induced destruction. A first order kinetics (n=1) was chosen for the quiescent agglomeration phenomenon. k_1 and $k_2$are described as dependent on the shear rate and on the CNT species in the sample (CNT are either in large or small agglomerates or separated nanotubes). They proposed that each CNT species proportions are governed by their own kinetic law, corresponding in the introduction of many fitting parameters hardly separable [107].

Marcourt et al. developed a model concerning the description of the conductivity evolution of polymer-CNT composites under extensional deformation [111]. Based on different postulates from Skipa, they simply distinguished isolated CNTs and CNTs connected to the conductive infinite network. A different kinetic equation was then proposed to describe the effective filler volume fraction φ_{eff}:

$$\frac{d\varphi_{eff}}{dt} = k_{build}(\varphi - \varphi_{eff}) - 2k_{break}\dot{\varepsilon}^2\varphi_{eff}t \qquad \text{Equation 11}$$

where φ is the total filler fraction, $\dot{\varepsilon}$ the extensional rate and k_{build} and k_{break} the kinetic parameters corresponding respectively to the structuring and break-up mechanisms. They observed that the network breaking parameter was relative to the deformation, while the structuring mechanism was attributed to molecular mobility around CNTs. An example of the network modification during extensional deformation is given in **Figure 17** with the proposed model that describes the conductivity evolution. They observed, in contrast with shearing deformation, that elongation contributes only to the network destruction inducing a complete conductivity loss at moderate and high elongation rates [111].

Figure 17: Conductivity variation as a function of the Hencky deformation of PS/MWCNT (0.79 vol%) for large W_i . Symbols are the experimental data, and the solid lines are the calculated curves. replotted from [111]

3- Cooling process

Following composite manufacturing steps, after the deformation imposed by the melt mixing and shaping process, the melt composite will be cooled down to room temperature. A focus on the cooling process impact on electrical properties of semi-crystalline polymer filled with CNTs composites will be discussed in this final part.

a) Morphology of semi-crystalline polymer – CNT composites

The use of semicrystalline polymers represents a non-negligible part of studied and manufactured CNTs filled composites. Polyolefins (polyethylene and polypropylene) are in fact, among the most used polymer-CNT composites and have been widely studied in literature [112- 118]. Various observations were made from these studies: Grady reported that, in presence of CNT, the β form isotactic polypropylene (iPP) content increased [112] whereas Assouline showed the role of MWCNT as α nucleation agent [119]. With the numerous heterogeneous nucleation sites offered by CNTs, this filler acts efficiently as a nucleating agent [120]. The crystallization kinetics [112,121,122] and the crystalline morphology [122-124] can be heavily modified.

It is widely accepted to use the Avrami equation to indirectly characterize the dimensionality of growth in CNTs-induced polymer crystallization. The Avrami exponent, *n*, separates the one-, two-, and three-dimensional crystal growth for exponent values range of 1 to 2, 2 to 3 and 3 to 4, respectively. Various observations were made about PE and iPP crystals in presence of CNT. Haggenmueller observed a change from spherulitic to disk-shaped HPDE crystals with 1 wt % SWCNTs [122]. A disk-like growth was observed by Kaminsky et al. for iPP/CNTs [125] while other studies did not observe any noticeable modification by the addition of CNT in iPP matrix [112, 121]. It could be remembered that many polymer-CNT composite preparations exist and CNTs are available with different characteristics (dispersion state, aspect ratio, purity) resulting in different experimental conditions. Therefore, comparison of CNT effects on polymer crystallization should be taken with caution

In addition, shear flows existing during industrial processing may also influence the crystallization kinetics and the crystalline morphology [126-130]. Interaction between CNT induced, and flow induced crystallization was also pointed out in literature [118]. Unusual morphologies could be observed, such as “nano-hybrid shish-kebabs” structure, where disk-shaped polymer single crystals grow periodically epitaxially perpendicular to the surface of CNTs [118, 123].

As a result, the semi-crystalline polymer-CNT composites present another specificity and the impact of crystallization on the state of dispersion and on the final electrical properties must be considered.

b) Impact of crystallization on electrical properties

Despite the large number of scientific papers concerning the morphology of CNT filled semi-crystalline polymer, only a few works studied the effect of crystallization on the conductivity for those materials. It is understandable that the apparition of crystals is likely to modify the filler network structure. Two opposite behaviors have however been observed: crystallization can induce either conductivity increase or decrease.

Concerning the latter, Alig and Deng explained the conductivity decrease by the reduction of the amorphous phase, presenting ionic conductivity, in favor of the crystalline phase [131, 132]. A graphical description of the conductive network modification was proposed by Alig (see **Figure 18**) by comparing the network "freezing" of a composite with an amorphous polymer cooled below glass transition (**Figure 18 a**) and with a semi-crystalline polymer below the crystallization temperature (**Figure 18 b**) [108].

Figure 18: Electrical conductivity of (a) an amorphous and (b) a semi-crystalline polymer-MWCNT composite during heating-annealing-cooling cycles. Drawn from [108]

Another interpretation of the effect of crystallization inducing a reduction in the global conductivity is shared by Peng and Li. They consider that crystallites growth disturbs the conductive network by breaking conductive pathways [133, 134].

However, the crystalline growth was also seen as a mechanism promoting the densification of the conductive network, hence increasing the conductivity [134, 135]. Indeed, the available volume for nanotube is reduced as crystals grow; the network density in the amorphous phase therefore increases. This mechanism is analogous of the one that was evoked to explain the percolation threshold decrease for polymer blends (see 2.c.ii). This new distribution favors the constitution of a conductive paths. The volume reduction effect can be especially observed by experiments monitoring the conductivity during heating treatments above the melt temperature. A conductivity decrease is observed designed as the negative temperature coefficient (NTC) when the conductive network density is diluted by additional melted polymer [132, 136]. Fernandez also proposed that the effect of crystallization rather caused a transition from a less effective conductive network in melt polymer to a more performing three-dimensional network in solid state [137].

From all presented results, the crystallization impact on the conductive network is equivocal. However, the plurality of behaviors is not surprising given the tremendous number of experimental conditions that were modified either by using different materials (nanotubes or polymer), processing conditions, and characterization techniques.

Conclusion

The importance of the rheological and thermal histories of polymer-CNTs composite was exhibited. The modification of the network by structuration and break-up mechanisms were presented and showed the ability of the structure to change. The understanding of such capability allows tuning, to some extent, the final physical properties of the processed composite. However, it was observed that the variety of results may not always be compared due to different experimental conditions. This diversity of observations is, in part, explained by interactions in structuring mechanisms occurring throughout composite processing.

General conclusion

Since the discovery from Iijima, the popularity of this material did not dry up but rather grown. The remarkable physical properties of carbon nanotubes motivated researchers to conduct various studies, whether for the resolution of industrial issues or for the comprehension of complex mechanisms. For instance, the use of CNTs as filler in polymer matrix to obtain an electrically conducting composite raised some questions and challenges.

The mixing of two components may not always be evident. It is generally accepted that to take the best from nanofillers, a good dispersion and homogeneous distribution in the matrix in needed. In the case of electrical reinforcement, it turns out that higher electrical conductivity requires the creation of a specific filler arrangement. The monitoring of this complex network by conductivity measurements allowed analyzing and deepening understandings of structuring and breaking mechanisms taking part in the different processing steps. Depending on the material, the processing steps involved in the composite preparation were presented. However, the difference in starting position (material) and in paths taken (processing methods) may lead researchers to observe different behaviors.

The crucial role of the rheological and thermal histories on the conductivity was pointed out. The management of processing steps could help industrials to tune the properties of their composites depending on the application. The aim of this work is to study breaking and structuring mechanisms that occurs during the processing steps of industrial melt mixing of carbon nanotubes filled polyethylene composites.

References

[1] S. Iijima, "Helical microtubules of graphitic carbon.," *Nature,* vol. 354, no. 6348, pp. 56-58, 1991.

[2] D. S. Bethune, C. H. Kiang, M. S. De Vries, G. Gorman, R. Savoy, J. Vazquez and R. Beyers, "Cobalt-catalysed growth of carbon nanotubes with single-atomic-layer walls.," *Nature,* vol. 363, no. 6430, pp. 605-607, 1993.

[3] S. &. I. T. (. Iijima, "Single-shell carbon nanotubes of 1-nm diameter.," *nature,* vol. 363, no. 6430, pp. 603-605, 1993.

[4] K. Awasthi, A. Srivastava and O. N. Srivastava, "Synthesis of carbon nanotubes," *Journal of nanoscience and nanotechnology,* vol. 5, no. 10, pp. 1616-1636, 2005.

[5] A. G. Rinzler, J. Liu, H. Dai and e. al., "Large-scale purification of single-wall carbon nanotubes: process, product, and characterization.," *Applied Physics A: Materials Science & Processing,* vol. 67, no. 1, pp. 29-37, 1998.

[6] Z. F. Ren, Z. P. Huang, D. Z. Wang and e. al., "Growth of a single freestanding multiwall carbon nanotube on each nanonickel dot.," *Applied physics letters,* vol. 75, no. 8, pp. 1086-1088, 1999.

[7] E. T. Thostenson, Z. Ren and T. W. Chou, "Advances in the science and technology of carbon nanotubes and their composites: a review.," *Composites science and technology,* vol. 61, no. 13, pp. 1899-1912, 2001.

[8] B. G. Demczyk, Y. M. Wang, J. Cumings, M. Hetman, W. Han, A. Zettl and R. O. Ritchie, "Direct mechanical measurement of the tensile strength and elastic modulus of multiwalled carbon nanotubes," *Materials Science and Engineering: A,* vol. 334, no. 1, pp. 173-178, 2002.

[9] S. Berber, Y. K. Kwon and D. Tománek, "Unusually high thermal conductivity of carbon nanotubes," *Physical review letters,* vol. 84, no. 20, p. 4613, 2000.

[10] P. Kim, L. Shi, A. Majumdar and P. L. McEuen, "Thermal transport measurements of individual multiwalled nanotubes," *Physical review letters,* vol. 87, no. 21, p. 215502, 2001.

[11] B. I. Yakobson, C. J. Brabec and J. Bernholc, "Nanomechanics of carbon tubes: instabilities beyond linear response.," *Physical review letters,* vol. 76, no. 14, p. 2511, 1996.

[12] B. I. Yakobson, G. Samsonidze and G. G. Samsonidze, "Atomistic theory of mechanical relaxation in fullerene nanotubes," *Carbon,* vol. 38, no. 11, pp. 1675-1680, 2000.

[13] M. S. Dresselhaus, G. Dresselhaus and P. C. Eklund, Science of fullerenes and carbon nanotubes: their properties and applications, Elsevier, 1996.

[14] D. D. T. K. Kulathunga, K. K. Ang and J. N. Reddy, "Molecular dynamics analysis on buckling of defective carbon nanotubes," *Journal of Physics: Condensed Matter,* vol. 22, no. 34, p. 345301, 2010.

[15] J. L. Ormsby and B. T. King, "Clar valence bond representation of π-bonding in carbon nanotubes," *The Journal of organic chemistry,* vol. 69, no. 13, pp. 4287-4291, 2004.

[16] G. Dresselhaus, M. S. Dresselhaus and R. Saito, Physical properties of carbon nanotubes, London: Imperial College Press, 1998.

[17] S. Iijima, C. Brabec, A. Maiti and J. Bernholc, "Structural flexibility of carbon nanotubes," *The Journal of chemical physics,* vol. 104, no. 5, pp. 2089-2092, 1996.

[18] M. J. O'connell, S. M. Bachilo and e. al., "Band gap fluorescence from individual single-walled carbon nanotubes.," *Science,* vol. 297, no. 5581, pp. 593-596, 2002.

[19] R. B. Weisman, S. M. Bachilo and D. & Tsyboulski, "Fluorescence spectroscopy of single-walled carbon nanotubes in aqueous suspension," *Applied Physics A,* vol. 78, no. 8, pp. 1111-1116, 2004.

[20] X. &. C. Z. Lu, "Curved pi-conjugation, aromaticity, and the related chemistry of small fullerenes (< C60) and single-walled carbon nanotubes.," *Chemical reviews,* vol. 105, no. 10, pp. 3643-3696, 2005.

[21] J. C. Charlier, X. Blase and S. Roche, "Electronic and transport properties of nanotubes," *Reviews of modern physics,* vol. 79, no. 2, p. 677, 2007.

[22] S. Hong and S. Myung, "A flexible approach to mobility," *Nature nanotechnology,* vol. 2, no. 4, pp. 207-208, 2007.

[23] M. S. Dresselhaus, G. Dresselhaus and P. Avouris, Carbon nanotubes: synthesis, structure, properties, and applications, Springer Science & Business Media, 2003.

[24] H. Pang, L. Xu, D. X. Yan and Z. M. Li, "Conductive polymer composites with segregated structures," *Progress in Polymer Science,* vol. 39, no. 11, pp. 1908-1933, 2014.

[25] R. H. Baughman, A. A. Zakhidov and W. A. De Heer, "Carbon nanotubes--the route toward applications," *science,* vol. 297, no. 5582, pp. 787-792, 2002.

[26] G. Mittal, V. Dhand, K. Y. Rhee, S. J. Park and W. R. Lee, "A review on carbon nanotubes and graphene as fillers in reinforced polymer nanocomposites," *Journal of Industrial and Engineering Chemistry,* vol. 21, pp. 11-25, 2015.

[27] D. Stauffer and A. Aharony, Introduction to percolation theory, CRC press, 2018.

[28] W. Bauhofer and J. Z. Kovacs, "A review and analysis of electrical percolation in carbon nanotube polymer composites," *Composites Science and Technology,* vol. 69, no. 10, pp. 1486-1498, 2009.

[29] S. Bose, R. A. Khare and P. Moldenaers, "Assessing the strengths and weaknesses of various types of pre-treatments of carbon nanotubes on the properties of polymer/carbon nanotubes composites: A critical review," *Polymer,* vol. 51, no. 5, pp. 975-993, 2010.

[30] C. Min, X. Shen, Z. Shi, L. Chen and Z. Xu, "The electrical properties and conducting mechanisms of carbon nanotube/polymer nanocomposites: A review.," *Polymer-Plastics Technology and Engineering,* vol. 49, no. 12, pp. 1172-1181, 2010.

[31] D. Stauffer, "Scaling theory of percolation clusters.," *Physics reports,* vol. 54, no. 1, pp. 1-74, 1979.

[32] S. Kirkpatrick, "Percolation and conduction," *Reviews of modern physics,* vol. 45, no. 4, pp. 574-588, 1973.

[33] M. Marcourt, P. Cassagnau, R. Fulchiron, D. Rousseaux, O. Lhost and S. Karam, " An original combined method for electrical conductivity measurement of polymer composites under extensional deformation.," *Journal of Rheology,* vol. 61, no. 5, pp. 845-857, 2017.

[34] I. Balberg, N. Binenbaum and N. Wagner, "Percolation thresholds in the three-dimensional sticks system.," *Physical Review Letters,* vol. 52, no. 17, p. 1465, 1984.

[35] J. Sandler, J. E. Kirk, I. A. Kinloch, M. S. P. Shaffer and A. H. Windle, "Ultra-low electrical percolation threshold in carbon-nanotube-epoxy composites.," *Polymer,* vol. 44, no. 19, pp. 5893-5899, 2003.

[36] B. Krause, M. Mende, P. Pötschke and P. G. , "Dispersability and particle size distribution of CNTs in an aqueous surfactant dispersion as a function of ultrasonic treatment time," *carbon,* vol. 48, no. 10, pp. 2746-2754, 2010.

[37] A. H. Barber, S. R. Cohen and H. D. Wagner, "Static and dynamic wetting measurements of single carbon nanotubes.," *Physical review letters,* vol. 92, no. 18, p. 186103, 2004.

[38] H. Yamada, I. Manas-Zloczower and D. L. Feke, "The influence of matrix viscosity and interfacial properties on the dispersion kinetics of carbon black agglomerates," *Rubber chemistry and technology,* vol. 71, no. 1, pp. 1-16, 1998.

[39] H. Yamada, I. Manas-Zloczower and D. L. Feke, "Influence of matrix infiltration on the dispersion kinetics of carbon black agglomerates," *Powder technology,* vol. 92, no. 2, pp. 163-169, 1997.

[40] H. Rumpf, "The strength of granules and agglomerates.," in *Agglomeration-Proceedings of the First International Symposium on Agglomeration*, Philadelphia, 1962.

[41] J. M. Ottino and D. V. Khakhar, "Mixing and segregation of granular materials," *Annual Review of Fluid Mechanics,* vol. 32, no. 1, pp. 55-91, 2000.

[42] J. M. Ottino, P. DeRoussel, S. Hansen and D. V. Khakhar, "Mixing and dispersion of viscous liquids and powdered solids.," *Advances in chemical engineering,* vol. 25, no. Academic press, pp. 105-204, 1999.

[43] I. Manas-Zloczower, "Model and analysis of kinetics erosion in simple shear flows.," in *Rubber Division Meeting*, Savannah, Georgia, 2002.

[44] S. P. Rwei, I. Manas-Zloczower and D. L. Feke, "Observation of carbon black agglomerate dispersion in simple shear flows.," *Polymer Engineering & Science,* vol. 30, no. 12, pp. 701-706, 1990.

[45] B. Safadi, R. Andrews and E. A. Grulke, "Multiwalled carbon nanotube polymer composites: synthesis and characterization of thin films.," *Journal of applied polymer science,* vol. 84, no. 14, pp. 2660-2669, 2002.

[46] J. Jang, J. Bae and S. H. Yoon, "A study on the effect of surface treatment of carbon nanotubes for liquid crystalline epoxide–carbon nanotube composites.," *Journal of Materials Chemistry,* vol. 13, no. 4, pp. 676-681, 2003.

[47] X. Gong, J. Liu, S. Baskaran, R. D. Voise and J. S. Young, "Surfactant-assisted processing of carbon nanotube/polymer composites.," *Chemistry of materials,* vol. 12, no. 4, pp. 1049-1052, 2000.

[48] S. Cui, R. Canet, A. Derre, M. Couzi and P. Delhaes, "Characterization of multiwall carbon nanotubes and influence of surfactant in the nanocomposite processing," *Carbon,* vol. 41, no. 4, pp. 797-809, 2003.

[49] R. SEN, B. ZHAO, D. PEREA and e. al., "Preparation of single-walled carbon nanotube reinforced polystyrene and polyurethane nanofibers and membranes by electrospinning.," *Nano letters,* vol. 4, no. 3, pp. 459-464, 2004.

[50] Y. Dror, W. Salalha, R. L. Khalfin, Y. Cohen, A. L. Yarin and E. Zussman, "Carbon nanotubes embedded in oriented polymer nanofibers by electrospinning," *Langmuir,* vol. 19, no. 17, pp. 7012-7020, 2003.

[51] H. J. Choi, K. Zhang and J. Y. Lim, "Multi-Walled Carbon Nanotube/Polystyrene Composites Prepared by in-situ BulkSonochemical Polymerization," *Journal of nanoscience and nanotechnology,* vol. 7, no. 10, pp. 3400-3403, 2007.

[52] D. Blond, V. Barron, M. Ruether, K. P. Ryan, V. Nicolosi, W. J. Blau and J. N. Coleman, "Enhancement of modulus, strength, and toughness in poly (methyl methacrylate)-based composites by the incorporation of

poly (methyl methacrylate)-functionalized nanotubes," *Advanced Functional Materials,* vol. 16, no. 12, pp. 1608-1614, 2006.

[53] A. L. Higginbotham, P. G. Moloney, M. C. Waid, J. G. Duque, C. Kittrell, H. K. Schmidt and J. M. Tour, "Carbon nanotube composite curing through absorption of microwave radiation.," *Composites Science and Technology,* vol. 68, no. 15-16, pp. 3087-3092, 2008.

[54] F. H. Gojny, M. H. Wichmann, B. Fiedler, I. A. Kinloch, W. Bauhofer, A. H. Windle and K. Schulte, "Evaluation and identification of electrical and thermal conduction mechanisms in carbon nanotube/epoxy composites.," *Polymer,* vol. 47, no. 6, pp. 2036-2045, 2006.

[55] M. Pumera, A. Merkoçi and S. Alegret, "Carbon nanotube-epoxy composites for electrochemical sensing.," *Sensors and Actuators B: Chemical,* vol. 113, no. 2, pp. 617-622, 2006.

[56] C. Park, Z. Ounaies, K. A. Watson, R. E. Crooks, J. Smith Jr, S. E. Lowther and T. L. St Clair, "Dispersion of single wall carbon nanotubes by in situ polymerization under sonication.," *Chemical physics letters,* vol. 364, no. 3-4, pp. 303-308, 2002.

[57] B. K. Zhu, S. H. Xie, Z. K. Xu and Y. Y. Xu, "Preparation and properties of the polyimide/multi-walled carbon nanotubes (MWNTs) nanocomposites.," *Composites Science and Technology,* vol. 66, no. 3-4, pp. 548-554, 2006.

[58] Q. H. Zhang and D. J. Chen, "Percolation threshold and morphology of composites of conducting carbon black/polypropylene/EVA.," *Journal of materials science,* vol. 39, no. 5, pp. 1751-1757, 2004.

[59] D. E. Hill, Y. Lin, A. M. Rao, L. F. Allard and Y. P. Sun, "Functionalization of carbon nanotubes with polystyrene," *Macromolecules,* vol. 35, no. 25, pp. 9466-9471, 2002.

[60] K. L. Lu, R. M. Lago, Y. K. Chen, M. H. Green and P. F. Harris, "Mechanical damage of carbon nanotubes by ultrasound.," *Carbon,* vol. 34, no. 6, pp. 814-816, 1996.

[61] T. Q. Nguyen, Q. Z. Liang and H. H. Kausch, "Kinetics of ultrasonic and transient elongational flow degradation: a comparative study.," *Polymer,* vol. 38, no. 15, pp. 3783-3793, 1997.

[62] T. Villmow, B. Kretzschmar and P. Pötschke, "Influence of screw configuration, residence time, and specific mechanical energy in twin-screw extrusion of polycaprolactone/multi-walled carbon nanotube composites.," *Composites Science and Technology,* vol. 70, no. 14, pp. 2045-2055, 2010.

[63] C. J. Kerr, Y. Y. Huang, J. E. Marshall and E. M. Terentjev, "Effect of filament aspect ratio on the dielectric response of multiwalled carbon nanotube composites.," *Journal of Applied Physics,* vol. 109, no. 9, p. 094109, 2011.

[64] A. E. Eken, E. J. Tozzi, D. J. Klingenberg and W. Bauhofer, "A simulation study on the combined effects of nanotube shape and shear flow on the electrical percolation thresholds of carbon nanotube/polymer composites.," *Journal of Applied Physics,* vol. 109, no. 8, p. 084342, 2011.

[65] A. E. Eken, E. J. Tozzi, D. J. Klingenberg and W. Bauhofer, "Combined effects of nanotube aspect ratio and shear rate on the carbon nanotube/polymer composites.," *Polymer,* vol. 53, no. 20, pp. 4493-4500, 2012.

[66] T. McNally and P. Pötschke, Polymer-carbon nanotube composites: Preparation, properties and applications., Elsevier, 2011.

[67] G. R. Kasaliwal, A. Göldel, P. Pötschke and G. Heinrich, "Influences of polymer matrix melt viscosity and molecular weight on MWCNT agglomerate dispersion.," *Polymer,* vol. 52, no. 4, pp. 1027-1036, 2011.

[68] G. R. Kasaliwal, S. Pegel, A. Göldel, P. Pötschke and G. Heinrich, "Analysis of agglomerate dispersion mechanisms of multiwalled carbon nanotubes during melt mixing in polycarbonate.," *Polymer,* vol. 51, no. 12, pp. 2708-2720, 2010.

[69] G. Kasaliwal, A. Göldel and P. Pötschke, "Influence of processing conditions in small-scale melt mixing and compression molding on the resistivity and morphology of polycarbonate–MWNT composites.," *Journal of Applied Polymer Science,* vol. 112, no. 6, pp. 3494-3509, 2009.

[70] T. Villmow, P. Pötschke, S. Pegel, L. Häussler and B. Kretzschmar, "Influence of twin-screw extrusion conditions on the dispersion of multi-walled carbon nanotubes in a poly (lactic acid) matrix.," *Polymer,* vol. 49, no. 16, pp. 3500-3509, 2008.

[71] B. Krause, P. Pötschke and L. Häußler, "Influence of small scale melt mixing conditions on electrical resistivity of carbon nanotube-polyamide composites.," *Composites Science and Technology,* vol. 69, no. 10, pp. 1505-1515, 2009.

[72] J. E. Fischer, "Chemical doping of single-wall carbon nanotubes.," *Accounts of chemical research,* vol. 35, no. 12, pp. 1079-1086, 2002.

[73] Q. MU, W. LIU, Y. XING and e. al., "Protein binding by functionalized multiwalled carbon nanotubes is governed by the surface chemistry of both parties and the nanotube diameter.," *The journal of physical chemistry C,* vol. 112, no. 9, pp. 3300-3307, 2008.

[74] L. Meng, C. Fu and Q. Lu, "Advanced technology for functionalization of carbon nanotubes.," *Progress in Natural Science,* vol. 19, no. 7, pp. 801-810, 2009.

[75] P. C. Ma, N. A. Siddiqui, G. Marom and J. K. Kim, "Dispersion and functionalization of carbon nanotubes for polymer-based nanocomposites: a review.," *Composites Part A: Applied Science and Manufacturing,* vol. 41, no. 10, pp. 1345-1367, 2010.

[76] A. Hirsch, "Functionalization of single-walled carbon nanotubes.," *Angewandte Chemie International Edition,* vol. 41, no. 11, pp. 1853-1859, 2002.

[77] D. Tasis, N. Tagmatarchis, A. Bianco and M. Prato, "Chemistry of carbon nanotubes.," *Chemical reviews,* vol. 106, no. 3, pp. 1105-1136, 2006.

[78] B. X. Yang, K. P. Pramoda, G. Q. Xu and S. H. Goh, "Mechanical reinforcement of polyethylene using polyethylene-grafted multiwalled carbon nanotubes.," *Advanced Functional Materials,* vol. 17, no. 13, pp. 2062-2069, 2007.

[79] A. A. Koval'chuk, V. G. Shevchenko, A. N. Shchegolikhin, P. M. Nedorezova, A. N. Klyamkina and A. M. Aladyshev, "Effect of carbon nanotube functionalization on the structural and mechanical properties of polypropylene/MWCNT composites.," *Macromolecules,* vol. 41, no. 20, pp. 7536-7542, 2008.

[80] D. E. Hill, Y. Lin, A. M. Rao, L. F. Allard and Y. P. Sun, "Functionalization of carbon nanotubes with polystyrene.," *Macromolecules,* vol. 35, no. 25, pp. 9466-9471, 2002.

[81] L. Vaisman, H. D. Wagner and G. Marom, "The role of surfactants in dispersion of carbon nanotubes.," *Advances in colloid and interface science,* vol. 128, no. 1, pp. 37-46, 2006.

[82] N. Grossiord, J. Loos, O. Regev and C. E. Koning, "Toolbox for dispersing carbon nanotubes into polymers to get conductive nanocomposites.," *Chemistry of materials,* vol. 18, no. 5, pp. 1089-1099, 2006.

[83] M. T. Müller, B. Krause and P. Pötschke, "A successful approach to disperse MWCNTs in polyethylene by melt mixing using polyethylene glycol as additive.," *Polymer,* vol. 53, no. 15, pp. 3079-3083, 2012.

[84] M. T. Mueller, P. Poetschke and B. Voit, "Dispersion of carbon nanotubes into polyethylene by an additive assisted one-step melt mixing approach.," *Polymer,* vol. 66, pp. 210-221, 2015.

[85] M. T. Müller, J. Dreyße, L. Häußler, B. Krause and P. Pötschke, "Influence of talc with different particle sizes in melt-mixed LLDPE/MWCNT composites.," *Journal of Polymer Science Part B: Polymer Physics,* vol. 51, no. 23, pp. 1680-1691, 2013.

[86] H. D. Bao, Z. X. Guo and J. Yu, "Effect of electrically inert particulate filler on electrical resistivity of polymer/multi-walled carbon nanotube composites.," *Polymer,* vol. 49, no. 17, pp. 3826-3831, 2008.

[87] L. Liu and J. C. Grunlan, "Clay assisted dispersion of carbon nanotubes in conductive epoxy nanocomposites.," *Advanced Functional Materials,* vol. 17, no. 14, pp. 2343-2348, 2007.

[88] M. Marcourt, P. Cassagnau, R. Fulchiron, D. Rousseaux, O. Lhost and S. Karam, "High Impact Polystyrene/CNT nanocomposites: Application of volume segregation strategy and behavior under extensional deformation.," *Polymer,* vol. 157, pp. 156-165, 2018.

[89] P. Pötschke, A. R. Bhattacharyya and A. Janke, "Morphology and electrical resistivity of melt mixed blends of polyethylene and carbon nanotube filled polycarbonate.," *Polymer,* vol. 44, no. 26, pp. 8061-8069, 2003.

[90] M. Sumita, K. Sakata, S. Asai, K. Miyasaka and H. Nakagawa, "Heterogeneous distribution of conductive particles in polymer blends studied by electron microscopy.," *Sen'i Gakkaishi,* vol. 47, no. 8, pp. 384-387, 1991.

[91] S. Pegel, P. Pötschke, G. Petzold, I. Alig, S. M. Dudkin and D. Lellinger, "Dispersion, agglomeration, and network formation of multiwalled carbon nanotubes in polycarbonate melts.," *Polymer,* vol. 49, no. 4, pp. 974-984, 2008.

[92] I. Alig, T. Skipa, D. Lellinger and P. Pötschke, "Destruction and formation of a carbon nanotube network in polymer melts: Rheology and conductivity spectroscopy.," *Polymer,* vol. 49, no. 16, pp. 3524-3532, 2008.

[93] L. Moreira, R. Fulchiron, G. Seytre, P. Dubois and P. Cassagnau, "Aggregation of carbon nanotubes in semidilute suspension.," *Macromolecules,* vol. 43, no. 3, pp. 1467-1472, 2010.

[94] I. Alig, T. Skipa, M. Engel, D. Lellinger, S. Pegel and P. Pötschke, "Electrical conductivity recovery in carbon nanotube–polymer composites after transient shear.," *physica status solidi (b),* vol. 244, no. 11, pp. 4223-4226, 2007.

[95] M. Sumita, K. Takenaka and S. Asai, "Characterization of dispersion and percolation of filled polymers: molding time and temperature dependence of percolation time in carbon black filled low density polyethylene.," *Composite Interfaces,* vol. 3, no. 3, pp. 253-262, 1995.

[96] A. Combessis, N. Charvin, A. Allais, J. Fournier and L. Flandin, "Understanding dynamic percolation mechanisms in carbonaceous polymer nanocomposites through impedance spectroscopy: Experiments and modeling.," *Journal of Applied Physics,* vol. 116, no. 3, p. 034103, 2014.

[97] C. B. H., A. K. Kota, A. L. Gershon, C. J. Laskowski, K. T. B. H. A. and S. R. Raghavan, "Conductivity enhancement of carbon nanotube and nanofiber-based polymer nanocomposites by melt annealing.," *Polymer,* vol. 49, no. 22, pp. 4846-4851, 2008.

[98] C. Zhang, L. Wang, J. Wang and C. A. Ma, "Self-assembly and conductive network formation of vapor-grown carbon fiber in a poly (vinylidene fluoride) melt.," *Carbon,* vol. 46, no. 15, pp. 2053-2058, 2008.

[99] M. Badard, A. Combessis, A. Allais and L. Flandin, "Modeling the dynamic percolation of carbon nanotubes and revisiting critical exponents.," *Materials Chemistry and Physics,* vol. 191, pp. 89-95, 2017.

[100] O. Valentino, M. Sarno, N. G. Rainone, M. R. Nobile, P. Ciambelli, H. C. Neitzert and G. P. Simon, "Influence of the polymer structure and nanotube concentration on the conductivity and rheological properties of polyethylene/CNT composites.," *Physica E: Low-dimensional systems and nanostructures,* vol. 40, no. 7, pp. 2440-2445, 2008.

[101] P. Pötschke, M. Abdel-Goad, I. Alig, S. Dudkin and D. Lellinger, "Rheological and dielectrical characterization of melt mixed polycarbonate-multiwalled carbon nanotube composites," *Polymer,* vol. 45, no. 26, pp. 8863-8870, 2004.

[102] J. Y. Kim and S. H. Kim, "Influence of multiwall carbon nanotube on physical properties of poly (ethylene 2, 6-naphthalate) nanocomposites.," *Journal of Polymer Science Part B: Polymer Physics,* vol. 44, no. 7, pp. 1062-1071, 2006.

[103] F. Du, R. C. Scogna, W. Zhou, S. Brand, J. E. Fischer and K. I. Winey, "Nanotube networks in polymer nanocomposites: rheology and electrical conductivity.," *Macromolecules,* vol. 37, no. 24, pp. 9048-9055, 2004.

[104] J. Obrzut, J. F. Douglas, S. B. Kharchenko and K. B. Migler, "Shear-induced conductor-insulator transition in melt-mixed polypropylene-carbon nanotube dispersions.," *Physical Review B,* vol. 76, no. 19, p. 195420, 2007.

[105] W. Bauhofer, S. Schulz, A. Eken, T. Skipa, D. Lellinger, I. Alig, E. Tozzi and D. Klingenberg, "Shear-controlled electrical conductivity of carbon nanotubes networks suspended in low and high molecular weight liquids," *Polymer,* vol. 51, no. 22, pp. 5024-5027, 2010.

[106] B. Lin, U. Sundararaj and P. Pötschke, "Melt mixing of polycarbonate with multi-walled carbon nanotubes in miniature mixers.," *Macromolecular Materials and Engineering,* vol. 291, no. 3, pp. 227-238, 2006.

[107] T. Skipa, D. Lellinger, W. Böhm, M. Saphiannikova and I. Alig, "Influence of shear deformation on carbon nanotube networks in polycarbonate melts: Interplay between build-up and destruction of agglomerates.," *Polymer,* vol. 51, no. 1, pp. 201-210, 2010.

[108] I. Alig, P. Pötschke, D. Lellinger, T. Skipa, S. Pegel, G. R. Kasaliwal and T. Villmow, "Establishment, morphology and properties of carbon nanotube networks in polymer melts.," *Polymer,* vol. 53, no. 1, pp. 4-28, 2012.

[109] I. Alig, D. Lellinger, M. Engel, T. Skipa and P. Pötschke, "Destruction and formation of a conductive carbon nanotube network in polymer melts: In-line experiments.," *Polymer,* vol. 49, no. 7, pp. 1902-1909, 2008.

[110] D. Lellinger, D. Xu, A. Ohneiser, T. Skipa and I. Alig, "Influence of the injection moulding conditions on the in-line measured electrical conductivity of polymer–carbon nanotube composites.," *physica status solidi (b),* vol. 245, no. 10, pp. 2268-2271, 2008.

[111] M. Marcourt, P. Cassagnau, R. Fulchiron, D. Rousseaux, O. Lhost and S. Karam, "A model for the electrical conductivity variation of molten polymer filled with carbon nanotubes under extensional deformation.," *Composites Science and Technology,* vol. 168, pp. 111-117, 2018.

[112] B. P. Grady, F. Pompeo, R. L. Shambaugh and D. E. Resasco, "Nucleation of polypropylene crystallization by single-walled carbon nanotubes.," *The Journal of Physical Chemistry B,* vol. 106, no. 23, pp. 5852-5858, 2002.

[113] A. Kelarakis, K. Yoon, R. H. Somani, X. Chen, B. S. Hsiao and B. Chu, "Rheological study of carbon nanofiber induced physical gelation in polyolefin nanocomposite melt.," *Polymer,* vol. 46, no. 25, pp. 11591-11599, 2005.

[114] S. Bose, A. R. Bhattacharyya, L. Häußler and P. Pötschke, " Influence of multiwall carbon nanotubes on the mechanical properties and unusual crystallization behavior in melt-mixed co-continuous blends of polyamide6 and acrylonitrile butadiene styrene.," *Polymer Engineering & Science,* vol. 49, no. 8, pp. 1533-1543, 2009.

[115] R. Haggenmueller, W. Zhou, J. E. Fischer and K. I. Winey, "Production and characterization of polymer nanocomposites with highly aligned single-walled carbon nanotubes.," *Journal of nanoscience and nanotechnology,* vol. 3, no. 1-2, pp. 105-110, 2003.

[116] R. Haggenmueller, C. Guthy, J. R. Lukes, J. E. Fischer and K. I. Winey, "Single wall carbon nanotube/polyethylene nanocomposites: thermal and electrical conductivity.," *Macromolecules,* vol. 40, no. 7, pp. 2417-2421, 2007.

[117] T. McNally, P. Pötschke, P. Halley, M. Murphy, D. Martin, S. E. Bell, G. Brennan, D. Bein, P. Lemoine and J. P. Quinn, "Polyethylene multiwalled carbon nanotube composites," *Polymer,* vol. 46, no. 19, pp. 8222-8232, 2005.

[118] Y. H. Chen, G. J. Zhong, J. Lei, Z. M. Li and B. S. Hsiao, "In situ synchrotron X-ray scattering study on isotactic polypropylene crystallization under the coexistence of shear flow and carbon nanotubes.," *Macromolecules,* vol. 44, no. 2, pp. 8080-8092, 2011.

[119] E. Assouline, A. Lustiger, A. H. Barber, C. A. Cooper, E. Klein, E. Wachtel and H. D. Wagner, "Nucleation ability of multiwall carbon nanotubes in polypropylene composites.," *Journal of Polymer Science Part B: Polymer Physics,* vol. 41, no. 5, pp. 520-527, 2003.

[120] C. Marco, M. Naffakh, M. A. Gómez, G. Santoro and G. Ellis, "The crystallization of polypropylene in multiwall carbon nanotube-based composites.," *Polymer composites,* vol. 32, no. 2, pp. 324-333, 2011.

[121] A. R. Bhattacharyya, T. V. Sreekumar, T. Liu, S. Kumar, L. M. Ericson, R. H. Hauge and R. E. Smalley, "Crystallization and orientation studies in polypropylene/single wall carbon nanotube composite.," *Polymer,* vol. 44, no. 8, pp. 2373-2377, 2003.

[122] R. Haggenmueller, J. E. Fischer and K. I. Winey, "Single wall carbon nanotube/polyethylene nanocomposites: nucleating and templating polyethylene crystallites.," *Macromolecules,* vol. 39, no. 8, pp. 2964-2971, 2006.

[123] L. Li, C. Y. Li and C. Ni, "Polymer crystallization-driven, periodic patterning on carbon nanotubes.," *Journal of the American Chemical Society,* vol. 128, no. 5, pp. 1692-1699, 2006.

[124] J. Yang, C. Wang, K. Wang, Q. Zhang, F. Chen, R. Du and Q. Fu, "Direct formation of nanohybrid shish-kebab in the injection molded bar of polyethylene/multiwalled carbon nanotubes composite.," *Macromolecules,* vol. 42, no. 18, pp. 7016-7023, 2009.

[125] A. Funck and W. Kaminsky, "Polypropylene carbon nanotube composites by in situ polymerization.," *Composites Science and Technology,* vol. 67, no. 5, pp. 907-915, 2007.

[126] G. Kumaraswamy, R. Verma, A. Issaian, P. Wang, J. Kornfield, F. Yeh, B. Hsiao and R. Olley, "Shear-enhanced crystallization in isotactic polypropylenePart 2. Analysis of the formation of the oriented "skin"," *Polymer,* vol. 41, no. 25, pp. 8931-8940, 2000.

[127] R. Pantani, I. Coccorullo, V. Volpe and G. Titomanlio, "Shear-induced nucleation and growth in isotactic polypropylene.," *Macromolecules,* vol. 43, no. 21, pp. 9030-9038, 2010.

[128] P. W. Zhu and G. Edward, "Morphological distribution of injection-moulded isotactic polypropylene: a study of synchrotron small angle X-ray scattering.," *Polymer,* vol. 45, no. 8, pp. 2603-2613, 2004.

[129] E. Koscher and R. Fulchiron, "Influence of shear on polypropylene crystallization: morphology development and kinetics.," *Polymer,* vol. 43, no. 25, pp. 6931-6942, 2002.

[130] F. Bustos, P. Cassagnau and R. Fulchiron, "Effect of molecular architecture on quiescent and shear-induced crystallization of polyethylene.," *Journal of Polymer Science Part B: Polymer Physics,* vol. 44, no. 11, pp. 1597-1607, 2006.

[131] I. Alig, D. Lellinger, S. M. Dudkin and P. Pötschke, "Conductivity spectroscopy on melt processed polypropylene–multiwalled carbon nanotube composites: recovery after shear and crystallization.," *Polymer,* vol. 48, no. 4, pp. 1020-1029, 2007.

[132] H. Deng, T. Skipa, R. Zhang, D. Lellinger, E. Bilotti, I. Alig and T. Peijs, "Effect of melting and crystallization on the conductive network in conductive polymer composites.," *Polymer,* vol. 50, no. 15, pp. 3747-3754, 2009.

[133] H. Pang, Y. C. Zhang, T. Chen, B. Q. Zeng and Z. M. Li, "Tunable positive temperature coefficient of resistivity in an electrically conducting polymer/graphene composite.," *Applied Physics Letters,* vol. 96, no. 25, p. 251907, 2010.

[134] B. Li, Y. C. Zhang, Z. M. Li, S. N. Li and X. N. Zhang, "Easy fabrication and resistivity-temperature behavior of an anisotropically conductive carbon nanotube− polymer composite.," *The Journal of Physical Chemistry B,* vol. 114, no. 2, pp. 689-696, 2010.

[135] G. O. Lim, K. T. Min and G. H. Kim, "Effect of cooling rate on the surface resistivity of polymer/multi-walled carbon nanotube nanocomposites.," *Polymer Engineering & Science,* vol. 50, no. 2, pp. 290-294, 2010.

[136] C. Zhang, C. A. Ma, P. Wang and M. Sumita, "Temperature dependence of electrical resistivity for carbon black filled ultra-high molecular weight polyethylene composites prepared by hot compaction.," *Carbon,* vol. 43, no. 12, pp. 2544-2553, 2005.

[137] M. Fernández, M. Landa, M. E. Muñoz and A. Santamaría, "Electrical conductivity of PUR/MWCNT nanocomposites in the molten state, during crystallization and in the solid state.," *European polymer journal,* vol. 47, no. 11, pp. 2078-2086, 2011.

Chapter 2.
Materials and methods

I. Materials

1- Polymer filled composite

a) Polymers

Various polyethylenes were used in this work. Their characteristics are summarized in the following **Table 1**.

Table 1: characteristics of used polyethylenes.

Name	Type	Density g.cm^{-3}	Melt Flow Index (MFI)	Melting temperature (°C)	Zero shear viscosity η_0 at 200°C (Pa.s) *
PE(A) XRT 70 (Total)	HDPE	0.947	0.7 g/10 min (190°C/5.0kg)	133	$1 \cdot 10^5$
PE(B) Hostalen GF 7750 M2 (Lyondellbasel)	HDPE	0.957	3.3 g/10 min (190°C/5.0kg)	135	$1 \cdot 10^4$
PE(C) M4040 (Total)	LLDPE	0.940	4 g/10 min (190°C - 2.16 kg)	130	$3 \cdot 10^3$
M35160 (Total)	LLDPE	0.935	16 g/10 min (190°C - 2.16 kg)	122	$4 \cdot 10^2$

*Zero shear viscosity was taken from following complex viscosity measurements.

The polymer M35160 is the matrix used in the masterbatch while the three others are used for the dilution. The complex viscosities (200°C with an oscillation strain of 1 %) of the three resins used for the dilution are displayed in **Figure 1**.

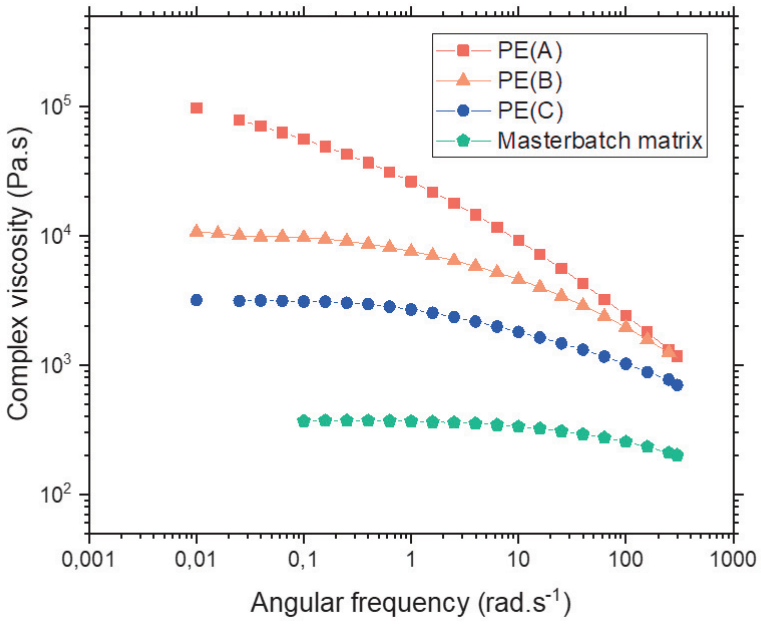

Figure 19: Complex viscosity for various polyethylenes as function of angular frequency (200°C)

b) Carbon nanotubes

Multiwalled Carbon Nanotubes (MWCNTs) NC7000 from the Belgian company Nanocyl® were used as filler in this study. They are produced by catalytic chemical vapor deposition and are characterized by an average diameter *d* of 10 nm, a surface area of 250-300 m^2/g and a volume conductivity of 10^6 S/m.

CNTs were provided in a polyethylene matrix, constituting a highly filled masterbatch (MB). The length average is in the order of 1 µm after mixing with the polymer matrix therefore the aspect ratio corresponding to the length over the diameter of these Carbon Nanotubes (CNTs) is estimated at 100.

2- Composite preparation

a) Masterbatch dilution

Polyethylene - carbon nanotubes (PE-CNT) composites samples were prepared using the melt blending method in a dynamic mixer HAAKE™ Rheomix QC. by diluting a masterbatch (MB) with a polyethylene matrix up to the desired CNT content.

MB and matrix were dried overnight at 60°C under vacuum and mixed at 200°C for 15min at 50 rpm in the internal mixer. The desired CNT content value is obtained by varying the ratio of MB introduced over the pristine polymer and range from 0.15 to 6 vol.%.

b) Sample

To perform this study, samples were prepared by compression molding in a hydraulic press (Servitec Polystat 200 T) to obtain a form of a disk with a diameter of 25mm of various thicknesses. The composite is first heated to a temperature of 200°C, above the melt temperature, then a pressure is applied to conform to the desired shape for 15 minutes. The compound is cooled down at room temperature pressed down by weights.

II. characterization

1- Conductivity measurement

The electrical conductivity of the composite was measured on the sample after different thermal histories. The polyethylene matrix is an insulator, but CNTs used as filler are good conducting paths for electric charges. Conducting electrical measurements therefore allow direct information of the CNT network quality in the composite.

a) Volume conductivity measurement

The volume conductivity was measured at ambient temperature with a Novocontrol® Alpha Broadband Dielectric/Impedance Spectrometer (BDS) as well as a Keysight B2987 Electrometer. As a response to a tension of 1V applied by a generator, the resistive behavior of the sample is measured. The volume conductivity σ of the sample is the calculated using the evaluated resistance R by a simple equation:

$$\sigma = \frac{h}{S.R} \qquad \text{Equation 12}$$

with h the thickness and S the surface of the sample.

To reduce the contact resistance induced by the surface roughness, the samples were gold metalized by plasma deposition. To optimize the reproducibility of the experiment, the samples were always pressed in the same way as shown in **Figure 20**.

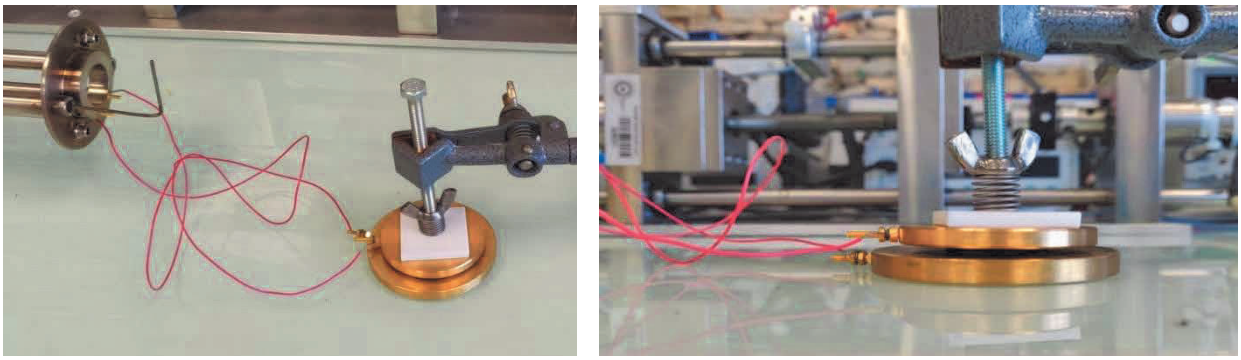

Figure 20 : experimental set up for conductivity spectroscopy

b) Conductivity measurement under temperature variation

In order to study the behavior of the composite when the matrix is in the melt state, the volume conductivity measurement can also be executed under controlled temperature and inert atmosphere (Nitrogen). In this study, a Novocontrol® Alpha BDS coupled with a Quatro Cryosystem was used to measure the electrical conductivity of polymer-CNT composites above the melting temperature of the polymer.

2- Structural information

a) Differential scanning calorimetry

To determine the melting temperature and the crystallinity of the polymer used in this study, thermal analyses have been carried out by differential scanning calorimetry tests (DSC) (Pyris DSC Diamond from Perkin Elmer). Heating and cooling cycles between 25 and 230°C at rates of 5 and 20°C/min were carried out to analyze the crystallization process and determine melting and crystallization temperatures.

b) Microscopy

Optical microscopy was conducted on studied polyethylenes by means of an optical microscope LEICA DM27000 M. Crossed polarizers were employed to observe the spherulitic structure during the cooling at 5 °C/min. thin films were placed between glass slides and the temperature of the sample was controlled by a hot stage FP82HT (METTLER TOLEDO). The structure evolution was recorded by a digital camera QICAM Fast1394 (QIMAGING). **Figure 21** present the spherulitic structure of the PE(A) polymer at a 20 times magnification

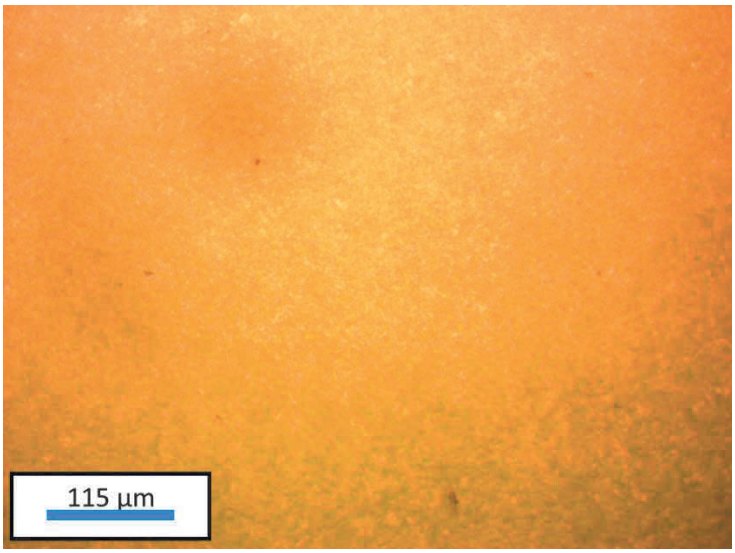

Figure 21: Cross polarized micrograph of PE(A) after a cooling at 5 °C/min. Magnification: 20.

Scanning electron microscopy was carried out on LSM800 (Zeiss) to characterize the state of dispersion of the filler in polymer-CNT composites. An in-lens detector was used to promote the electrical contrast between the insulating matrix and the conducting filler of cryo-fractured samples. Accelerating voltage was chosen between 15 and 20 kV and the working distance was lower than 10 mm.

c) Dynamic rheometry

Rheological measurements were conducted using and ARES G2 (TA instruments). The viscoelastic properties of the materials were evaluated by dynamic frequency sweep tests with parallel plates on disks of diameter *d* of 25 mm and around 2 mm of thickness.

Initially, a strain amplitude sweep allowed determining the linear viscoelastic domain of the material to perform frequency sweep tests. Every experiment was preceded by a 10-minute quiescent treatment at the temperature of the experiment to allow the possible filler aggregation and the polymer relaxation caused by sample preparation.

3- Rheometry coupled with the conductivity measurement

a) Presentation of the setup

A specific geometry-electrode was used to allow combined rheological and electrical measurements. Isolated ring-plate geometry electrodes were used on the rheometer and connected to a B2987A electrometer (Keysight technologies) to measure the samples resistance. Electric wires and welds were chosen to resist to temperature higher than 220 °C. A schema of the experimental set-up is proposed in **Figure 22**.

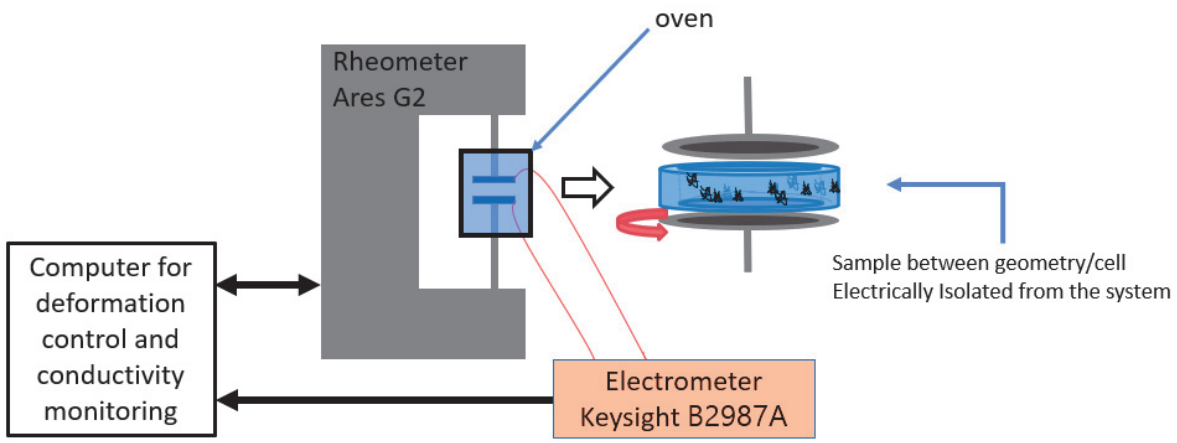

Figure 22: schema of the experimental rheoelectric set-up.

This set-up allows electrical measurements thanks to the sample constant thickness while applying a quasi-homogeneous shear rate throughout the sheared material. The higher and smaller diameters of the cell are respectively 25 and 22 mm, thus the strain difference is only of 14% from extremities of the analyzed sample. The sample resistance is measured perpendicularly to the shear plane every 0.1 s as a response to an applied 1 V direct current. A picture of the experimental set-up is displayed in **Figure 23.**

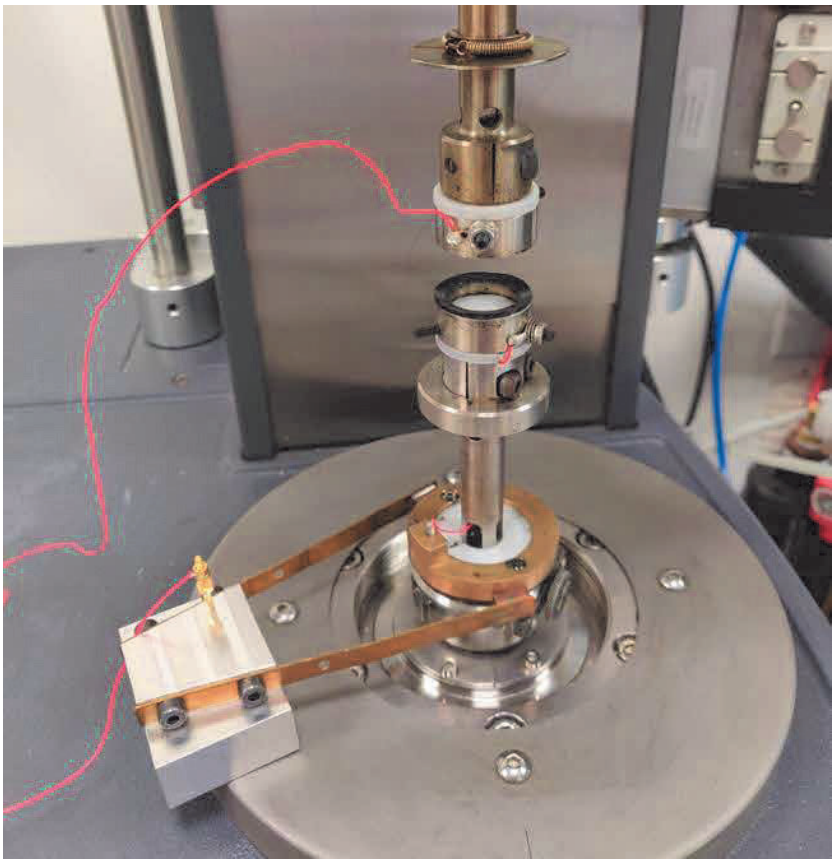

Figure 23: picture of the rheological cell used for simultaneous conductivity measurement

As the lower electrode is rotating, the electrical signal is collected owing to friction conductive tongs whereas the stationary upper electrode is directly connected to the electrometer. The resistance of the short-circuited set-up was first measured, and the obtained value was around 1 Ω, which is negligible compared to the measured resistance of the studied materials.

The samples were cut from pressed disks and placed between the ring cells. To ensure a good contact with both electrodes, temperature was set at 200°C to melt the polyethylene and the upper ring was brought in contact with the sample. The edge was removed to eliminate squeezed out material.

b) Rheological measurement using the ring geometry

In the Trios software used with the Ares G2 rheometer, the ring geometry cell is not implemented so that the rheological parameters (viscosity, modulus…) have to be calculated using the measured rough data (measured torque and angular velocity). The ring geometry can be seen as described in **Figure 24**.

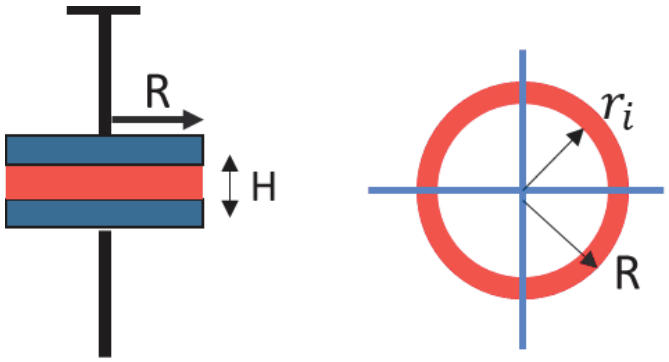

Figure 24: schematic view of the ring geometry

With this geometry using the measured torque, the complex viscosity is obtained by the following equations:

$$\eta'(\omega) = \frac{2HC_O \sin(\delta)}{\pi\omega\theta_0(R^4 - r_i{}^4)} \qquad \textbf{Equation 13}$$

$$\eta'(\omega) = \frac{2HC_O \cos(\delta)}{\pi\omega\theta_0(R^4 - r_i{}^4)} \qquad \textbf{Equation 14}$$

With C_O the torque, θ_0 the imposed rotation, and H, r_i and R respectively the thickness, the internal and external radius of the sample.

In order to validate the home-made ring cell, a comparison with the complex viscosity measured using a classical plate-plate cell is displayed in **Figure 25**. the variation between the complex viscosity measured using plate-plate geometry (blue circles), ring geometry (red triangles). The complex viscosity curves measured using both cells superimpose well, at least in the uncertainty range.

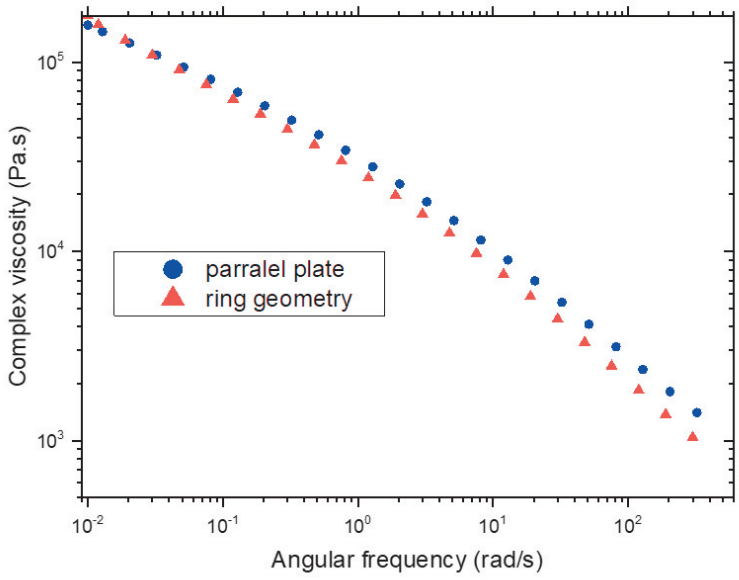

Figure 25: complex viscosity of a composite of PE with 2.5wt% of CNT as a function of the angular frequency measured using parallel plates and using the ring geometry

c) Conductivity monitoring of the sample under shear stress

As described by **Equation 12**, the conductivity is determined by the measured resistance of the sample. The height of the sample is of around 2 mm and precisely known thanks to the gap controlled by the rheometer. The surface of the ring equals to 2 cm^2.

The applied shear rates were ranged between 0.025 s^{-1} to 10 s^{-1} and the duration of the shear was varied according to the desired total strain. **Figure 26** displays a typical conductivity variation under shear stress. The PE/CNT sample is first annealed until the conductivity reaches a quasi-constant level (t<-120 s in **Figure 26**). Then, a shear strain (here of 0.05 s^{-1} for 120 s) is applied followed by a quiescent annealing step (t>0s in **Figure 26**).

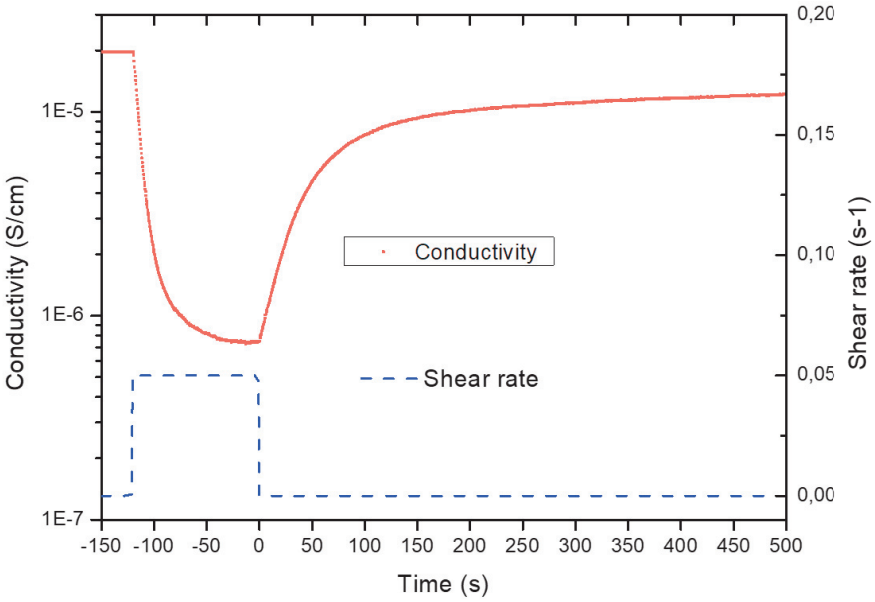

Figure 26: standard time resolved conductivity measurement using the rheoelectrical set up. PE-CNT composite (1.75 vol% MWCNT) is first annealed then deformed at a fixed shear rate for 120 s and finally annealed again. Experience carried out at 200°C

Chapter 3.
Tuning the conductivity of viscous polyethylene-CNT composites through thermal annealing

I. Introduction

The use of conductive filler in polymer composites was found interesting for many applications [1]. The presence of an electrically conductive network (conductivity $\geq 10^{-6}$ S.cm^{-1}) in the polymer matrix can, for instance, prevent damages caused by electrostatic discharge (such as failure of solid-state electronics or even gas explosion) [2, 3]. In this application, the use of such polymer composites is attracting as they present light weight, easy processability and a sufficient conductivity can be reached to allow charge dissipation [4, 5].

The use of carbon nanotubes (CNT) as filler is especially appealing as low content are required to obtain suitable electrical conductivity compared to other conductive fillers (e.g. carbon black) [1]. Thanks to their high aspect ratio, the theoretical percolation threshold, symbolizing the transition from an insulator to a conductor material, is reached at a concentration lower than one percent [6]. With increasing filler content, the conductivity evolution was successfully described by a power law by Kirkpatrick [7]:

$$\sigma = \sigma_0(\varphi - \varphi_c)^{\beta} \qquad \text{Equation 15}$$

where σ is the conductivity, σ_0 the theoretical macroscopic conductivity of the filler, β a critical exponent, φ_c the percolation threshold (the critical filler volume content) and φ the filler content. However, practice was often found quite different and greater CNT quantities are needed to reach φ_c as many parameters can modify the state of filler dispersion and distribution responsible for the electrical conductivity [8]. For instance, the required CNT content might vary significantly depending on the polymer used [9]. As a matter of fact, interactions between filler and polymer must also be considered as CNTs dimension is in the range of polymer chain size.

The masterbatch dilution is an industrially viable processing method that generally leads to suitable filler dispersion into the matrix [10]. This technique facilitates the infiltration and the breakup of primary CNTs agglomerates, essential to obtain appropriate electrical properties. But processing steps are also responsible for reducing the electrical conductivity due to the modification of the filler organization caused by the applied mixing shear forces [9]. As a result, processing conditions such as shear forces, mixing time, temperature or viscosity affects the final properties of the material [11]. For different reasons (price, processing ease, end use mechanical properties…), obtaining sufficient electrical properties of a manufactured composite with the lowest possible CNT content is an obvious industrial interest.

A mechanism of filler auto-assembly was observed during the annealing above the glass transition or melting temperature of the polymer, allowing tremendous conductivity enhancement [12, 13]. The annealed material conductivity evolves as if the filler amount was increased, and this was called the dynamic percolation [14]. A large conductivity increase can be observed during this network modification process and as a result, the percolation law (**Equation 15**) parameters may be modified [15]. For instance, Combessis et al. observed a reduction of the percolation threshold φ_c of a very low-density polyethylene/CNT composite

from 1.9 vol % to 0.2 vol % over a 24 h annealing at 200°C [16]. Moreover, the filler content φ considered in **Equation 15** does not necessarily correspond to the total filler content but rather to an effective filler fraction φ_{eff} that is, electrically speaking, connected to the conductive network and may change with annealing time [17]:

$$\sigma = \sigma_0(\varphi_{eff}(t) - \varphi_c)^{\beta} \qquad \textbf{Equation 7}$$

The dynamic percolation through quiescent annealing treatments might be appealing for industrials to operate conductivity enhancements after processing steps that generally induce break up in fillers connections. Several models are proposed in the literature to describe the conductivity evolution during a quiescent treatment in the melt polymer [15, 17, 18], but the knowledge of the initial system is required for their use. The various percolation thresholds reported in the literature demonstrate that the ability of CNT to form a percolated pathway is extremely sensitive to the composition of the composite as well as processing conditions [8]. To determine the "percolation potential" of a system, a systematic study of the network modification by quiescent annealing seems required.

The present work aims to study the electrical behavior of CNT filled high density polyethylene composites prepared by a masterbatch dilution. An investigation on the network modification by quiescent treatments was conducted to determine the best ways for tuning the conductivity of the composite. The crystallization mechanism is not investigated here as it will be the topic of the next chapter.

II. Materials and Methods

1- Materials

Composites were realized by diluting a masterbatch containing multiwalled carbon nanotubes in various polyethylene matrices to obtain the desired filler's volume fraction. CNT (NC7000 from Nanocyl) are characterized by a volume resistivity of $10^{-4}\ \Omega.cm$, an average diameter of 9.5 nm and a mean length of 1.5 µm. Three industrial polyethylenes were used for the dilution in this study: HDPE XRT 70 (Total) (A), a HDPE Hostalen GF 7750 M2 (Lyondellbasel) (B) and a LLDPE M4040 (Total) (C) with respective MFI of 0.7 g/10 min (190°C - 5.0 kg); 3.3 g/10 min (190°C – 5 kg) and 4 g/10 min (190°C - 2.16 kg). Stearic acid from Sigma-Aldrich was used as an additive to facilitate the dispersion of CNTs. This material is characterized by a melt temperature of 69 °C and a density of 0.845 g/cm3.

Electrical measurements and annealing were performed on disk samples of 25 mm diameter and 2 mm thick prepared by compression molding at 200°C for 15 min.

2- Melt temperatures

The melting temperature was determined with a differential scanning calorimeter (Pyris Diamond DSC from Perkin Elmer). Samples followed heating cycles from 25 to 230°C with a scan speed of 5°C/min. The melting of PE crystals was found to happen between 100°C and 130°C.

3- Electrical characterization

Volume conductivity measurements were performed on a broadband dielectric spectrometer Novocontrol Alpha Analyzer over a frequency range from 1 Hz to 10^6 Hz. Samples are placed between two electrodes and pressed using a spring to optimize the reproducibility of the measurement by applying the same force on all samples. Electrical contacts were gold metalized to eliminate the influence of the contact resistance.

The dielectric spectrometer was coupled to a Quatro Cryosystem (Novocontrol) to perform electrical measurement at controlled temperature and in an inert atmosphere (Nitrogen). The frequency range was reduced to 10 Hz to 10^3 Hz to keep the period between measurements sufficiently short (around 10 s) compared to the entire duration of the variation. The heating and cooling rates were fixed at 5 °C/min. This set up allows conductivity measurements during quiescent annealing of samples above the melt temperature of the polymer.

III. Results and discussion

1- Influence of melt viscosity on the percolation threshold

The percolation threshold for merely pressed materials was first determined. Composites with various concentrations were prepared by diluting the same masterbatch with three different matrices (A, B and C). After compression molding, the electrical conductivity was directly measured. In accordance with the percolation theory, a transition from insulator to conductor is observed with increasing filler content once the critical volume fraction (percolation threshold) is reached as observed in **Figure 27**. For every matrix, the conductivity evolution as function of the CNT content was fitted using **Equation 15**. Fitting parameters are summarized in **Table 2** and clearly depict the influence of the polymer matrix on the percolation threshold. The percolation threshold was determined at a lower value for the matrix of highest MFI, that is the of lower melt viscosity (see **Figure 19** in chapter Materials and Methods). This critical value was determined as low as 0.4 vol % in the case of the M4040 (matrix C), while a more than three times higher CNT content was necessary for the most viscous matrix studied (matrix A).

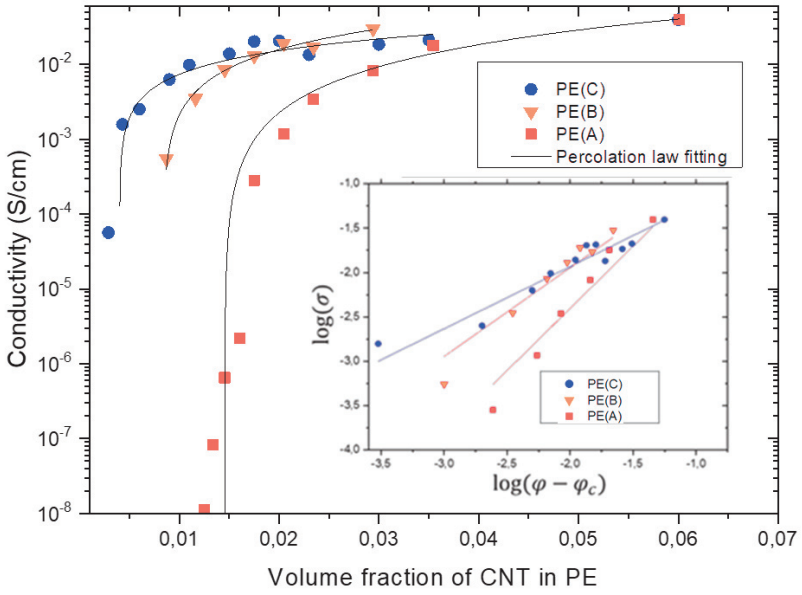

Figure 27: Electrical conductivity as function of the CNT volume fraction in different PE-CNT composites. Lines represent the percolation law obtained from fitting the experimental data. As inset is plotted the linearized expression of the conductivity

Table 2: parameters used in the percolation law (Equation 1) to fit the results presented on figure 1.

Polymer	σ_0 (S.cm^{-1})	φ_c (vol %)	β
M4040 (C)	0.33	0.4	0.7
GF7750 M2 (B)	1.5	0.8	1.0
XRT70 (A)	2.7	1.4	1.4

This observation is in accordance with previous studies on composites prepared by the masterbatch dilution with polypropylene of various viscosities [19]. They proposed that lower viscosities induced a better penetration inside the masterbatch leading to a better dispersion of the masterbatch particles. However, they highlighted the importance of the quality of the masterbatch as primary agglomerates existing in the highly filled compound are difficult to disperse [19].

The influence of the mixing time on the electrical properties was quickly studied for the most viscous matrix (A). Increasing the mixing time up to 20 minutes did not significantly modify the measured conductivity of hot-pressed samples. This result suggests that the used processing conditions allowed a sufficient dispersion of the masterbatch in the polymer matrix. In contrast, with increasing duration of compression molding, the measured conductivity of the sample increases. For instance, the conductivity of a HDPE (A)-CNT composite with a filler content of 1.15 vol% was measured in the range of 10^{-6} S.cm^{-1} when pressed 2 hours whereas it was found insulator after only 15 minutes.

2- Dynamic percolation of PE-CNT composites

a) Close to the percolation threshold

The conductivity evolution induced by the application of a thermal annealing on the composite attests from the ability of the conductive network to self-organize [16, 20]. The difference in mobility when using polymer of different viscosities could justify in part, the variation of conductivity at lower filler content (< 2 vol%) for those composites. Conductivity monitoring during quiescent treatment were then performed to investigate the extent of the conductivity improvement by the dynamic percolation phenomenon.

A quiescent annealing treatment was performed at 200°C on an initially insulating composite based on the more viscous PE (A). The CNT content was fixed at 0.9 vol %, a lower value than the percolation threshold determined for this matrix, but a higher value than this for the less viscous matrices. The AC conductivity (f= 1 kHz) evolution as function of the annealing time for this composite is presented in **Figure 28** with the temperature profile. The sample becomes progressively conductive up to a conductivity in the order of 10^{-5} S.cm^{-1} after an annealing of 8 hours. The creation of an infinite interconnected filler network in the matrix is noticed in **Figure 28** by the tremendous conductivity transition from insulating to conducting.

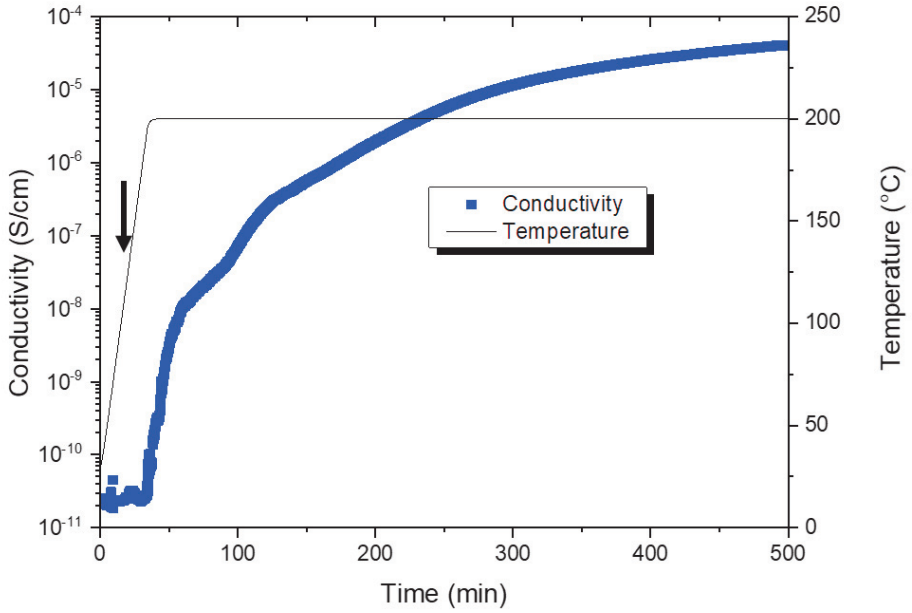

Figure 28: Conductivity change with annealing time at 200°C for PE (A) -CNT (0.9 vol % CNT). f= 1 kHz. The black arrow outlines the time when the temperature reaches the melting temperature of the PE.

The conductivity enhancement during annealing depicts the microstructural modification that strengthens the conductive filler network: the conductivity evolution attests from the intensification of nanotubes connections. The annealing triggers a conductivity increase analogous to the conductivity evolution with the total filler content as observed in

Figure 27. In Figure 28, the initial CNT content that are interconnected to take part of a conductive network is lower than the percolation threshold, but the annealing allows isolated CNTs to gradually connect and form an infinite network that becomes denser and denser. The effective concentration, corresponding to the CNT content taking part in the conductive network, thus increases with annealing time. The annealing for 8 hours of a 0.6 vol % CNT-PE (A) composite did not trigger an insulator to conductor transition, suggesting that the percolation threshold could not be reduced to that extent for this specific composite by the application of such treatment.

Percolation laws presented in Figure 27 and Table 2 are related to specific processing steps, namely merely pressed materials, and describe the evolution of conductivity as function of the CNT content in a non-equilibrium fixed state, as pointed out by the conductivity evolution during quiescent treatment. The difference between the total filler content and the interconnected content contributing to electrical conductivity is responsible, to a certain extent, for a difference in theoretical and practical percolation thresholds.

b) Above the percolation threshold

The impact of dynamic percolation on the conductivity of composite with an initially already conducting behavior was then studied by annealing PE - CNT with filler contents above the percolation threshold of the merely pressed materials. The conductivity evolution of a composite PE (A) – CNT (1.6 vol %) during an annealing treatment at 200°C for two hours is presented in Figure 29. A conductivity decrease first appears around the melting temperature of the polyethylene, outlined by the black arrow in Figure 27. As the available volume for the filler is increased when the crystalline phase melts, the network expands resulting first in the distancing of CNT-CNT connections hence a reduction of the global conductivity is observed. This phenomenon is analogous to the well-known Positive Temperature Coefficient of resistance (PTC) effect due to the depercolation of conductive fillers network when heating a composite of thermoplastic matrix [21]. This decrease is then followed by a conductivity increased up to a conductivity in the order of 10^{-3} $S.cm^{-1}$ representing the conductive network structuring. After around 40 min of annealing, the conductivity then reaches a steady level. Similar conductivity evolutions during annealing were observed by Deng on Polypropylene-CNT composites [22].

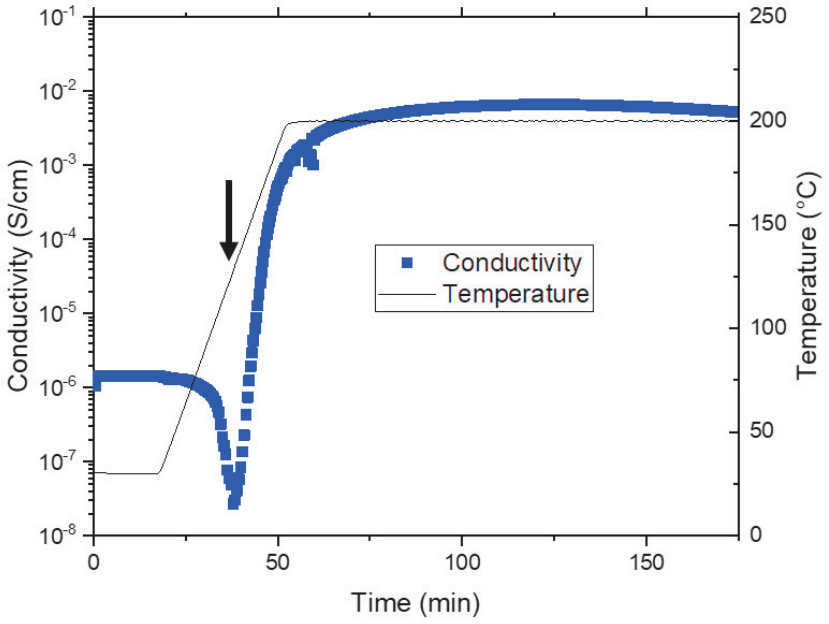

Figure 29: Conductivity change during annealing treatment (2 hours - 200°C) for PE (A) -CNT (1.6 vol % CNT). f = 1 kHz. The black arrow outlines the time when the temperature reaches the melting temperature of the PE.

From **Figure 29**, it is observed that an annealing treatment allows the nanotube network strengthening, even for higher CNT content, which means, even for an initially percolated network. To study the effect of annealing on the percolation law of the viscous matrix (A), samples with various CNT contents were annealed and the conductivity evolution was monitored. **Figure 30** compares the conductivity of PE(A) – CNT composites after an annealing of two hours with the conductivity of merely pressed solid PE (A) and (C) composites. It should be noted that the conductivity of the annealed samples did not necessarily reach a well-defined steady level in the case of low CNT contents (see **Figure 28**). However, conductivities gathered in **Figure 30** were taken after the same annealing duration as electrical properties of polymer-CNT composites are sensitive to the thermal history.

From **Figure 30**, a tremendous conductivity increase was made possible by the application of a quiescent annealing treatment on samples with CNT content close to the initially determined percolation threshold. For instance, an improvement of more than 4 orders of magnitude in conductivity was observed for PE (A) filled with 1.15 vol %. As a result, the percolation threshold for the viscous matrix A is obtained at lower concentrations (0.9 vol %). A percolation law was determined by fitting the experimental data using **Equation 15**. The percolation threshold, φ_c, was determined at 0.9 vol %, the pre-factor σ_0 at 20 S.cm^{-1} and the exponent β at 1.5.

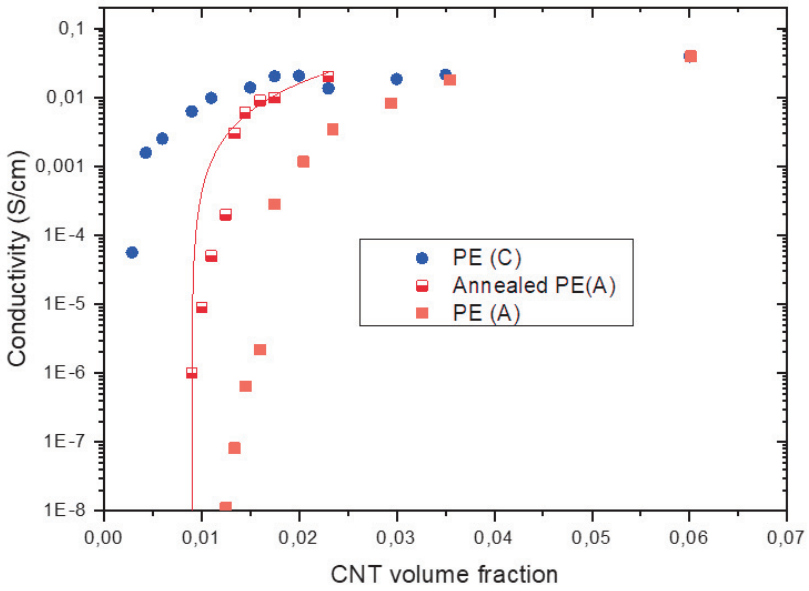

Figure 30: Impact of the annealing for two hours on the conductivity of PE-CNT composites as function of the CNT content. Red line is the percolation law obtained from the fitting of experimental data.

The conductivity of a polymer-CNT composite can indeed be enhanced by the application of a quiescent annealing treatment after processing steps. The most impressive conductivity evolution appears when the effective concentration goes from lower to higher than the effective percolation threshold since the conductivity then follows a power law.

3- Comparison with another polyethylene

The annealing treatment was then studied on a less viscous matrix to compare with previous results. The annealing of a 0.6 vol % CNT filled PE (C) composite for 2 hours is presented in **Figure 31**. The conductivity evolution of the sample is here compared to a PE(A)-CNT composite presenting a comparable conductivity. A similar behavior as in **Figure 29** is observed. Both composites first undergo a conductivity decrease caused by the matrix expansion causing a certain depercolation. Then an electrical recovery is observed. Although the total CNT content is three times lower, the measured conductivity is higher in the case of the polyethylene with the lowest viscosity. Moreover, it can be observed from **Figure 31** that the structuring speed is higher in the case of the PE(C). This could be explained by a lower polymer relaxation time that allows a quicker restructuration [17].

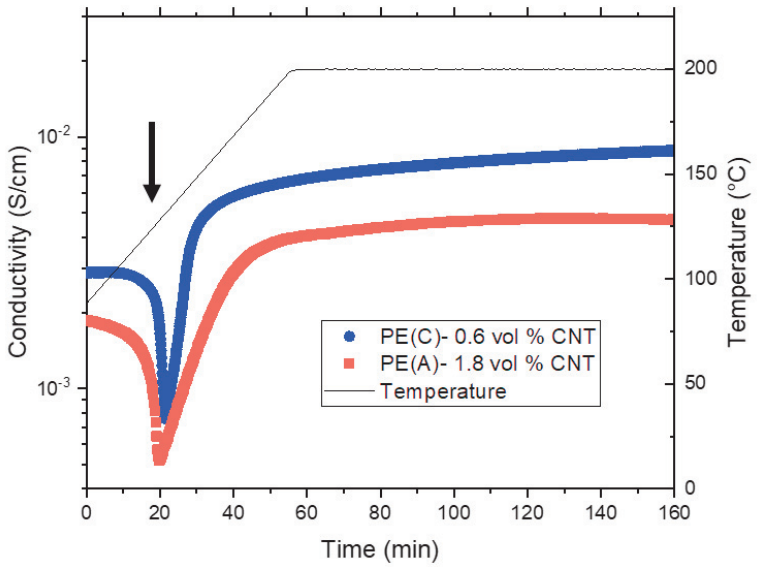

Figure 31: Annealing treatment of composites based on different polyethylene but with comparable conductivities. The black arrow outlines the time when the temperature reaches the melting temperature of the PE.

The potential percolation of the studied polyethylene with the lowest viscosity was evaluated by annealing a composite with CNT content lower than the percolation threshold initially determined on merely pressed samples. **Figure 32** shows the conductivity evolution during a two-hour thermal annealing of a PE (C) – CNT at a CNT content as low as 0.15 vol %. The initial conductivity of the sample is found around 10^{-9} S.cm^{-1} and is increased by more than 4 orders of magnitude after two hours of annealing at 160 °C.

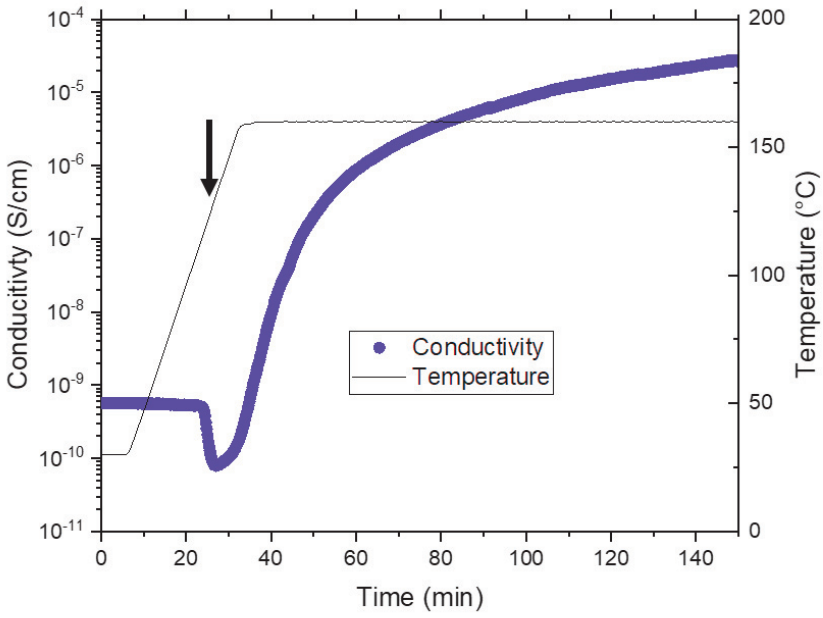

Figure 32: Conductivity change during annealing treatment (2 hours - 160°C) for PE (C) -CNT (0.15 vol % CNT). f = 1 kHz. The black arrow outlines the time when the temperature reaches the melting temperature of the PE.

As a result, the thermal treatment does not wipe out the variation in percolation thresholds for polymer of various viscosities and even allows composite with lower viscosity polymer to obtain electrical conductivity at very low CNT content (0.15 vol %). The observation with lowest viscosities seems in accordance with the assumption of Combessis that the existence of a percolation path is less dependent on the amount of conducting filler than on the annealing time [16]. The conductivity of PE-CNT composites with 0.6 vol % CNT using matrices (B) and (C) was measured at respectively $1 \cdot 10^{-3}$ S.cm^{-1} and $1 \cdot 10^{-2}$ S.cm^{-1} after only 2 hours of annealing. In contrast, an insulator to conductor transition was never observed during prolongated annealing (8 hours) of the more viscous matrix PE(A) filled with 0.6 vol % CNT composite. The higher percolation threshold might originate either from a CNT length shortening occurring during the masterbatch dilution, or an insufficient dispersion of the primary agglomerates remaining in the masterbatch.

4- Effect of surfactant addition on the conductivity recovery by dynamic percolation

Polymer-CNT interactions play a role in the electrical properties. Due to the low interactions between non-polar polymer (in our case polyethylene) and CNT, the dispersion of this filler can be difficult. Vasileiou suggested that the conductivity of polyolefin-CNT composites prepared by melt compounding might be inherently limited by the difficulty to obtain a suitable filler dispersion without damaging the integrity of the filler, especially in the case of viscous matrix [23].

To prevent the shortening of the filler caused by extended mixing time and faster mixing speed, the modification of the polymer-CNT interface was found effective to reduce the percolation threshold [24]. Various surface modification options are presented in the literature, yet the non-covalent functionalization of CNT presents the advantage of preserving the structural integrity of the filler [24, 25]. The addition of a surfactant is a simple and industrially applicable method to increase the conductivity of a polymer-CNT system [26, 27]. In the case of polyolefin, the use of non-ionic surfactants presented the best results of conductivity enhancement [28, 29]. An increase of conductivity from 10^{-14} to 10^{-4} S.cm^{-1} was observed by Müller et al. by the addition of 5 wt % of poly(ethylene glycol) during melt mixing of LLDPE-CNT (2 wt % CNT) composites. However, the origins of the positive effect of surfactant on the electrical properties are not very clear as the additive can modify different processing conditions.

Stearic acid (SA) is a fatty acid that has been used to ease the filler dispersion in various polymer-based composites, including polyolefins [30]. In this section, the impact of this surfactant on the electrical properties of viscous PE(A)-CNT composites was investigated.

a) Addition of stearic acid

Samples filled with 0.6 vol % CNT containing SA were prepared using the processing steps presented earlier. SA was directly incorporated during the masterbatch dilution step at a concentration of 1 vol %. Through initial conductivity measurement on solid sample the composite containing stearic acid was characterized as insulating ($\sigma \rightarrow 10^{-12}$ S.cm^{-1}). However, the application of an annealing treatment at 200 °C triggered a conductivity increase up to 10^{-7} S.cm^{-1} as displayed in **Figure 33**, while the composite PE(A)-CNT with the same CNT content remained insulator. The different behaviors observed during annealing treatment for PE(A)-CNT with and without SA highlights the reduction of the percolation threshold induced by the additive.

In **Figure 33**, the conductivity evolution for two hours annealing treatment for PE(A)-CNT with SA is represented by the orange squares. The sample was then cooled down to 30°C and a second annealing treatment was performed for two hours. The conductivity evolution during the second treatment is displayed in **Figure 33** by the green squares. The second treatment depicts more clearly the maximum level of conductivity reached by this specific system. It is generally accepted in the literature that the filler dispersion is the main factor influencing the conductivity of a polymer-CNT composite. The dispersion here seems modified by the addition of SA acting as a compatibilizer for the filler and the polymer.

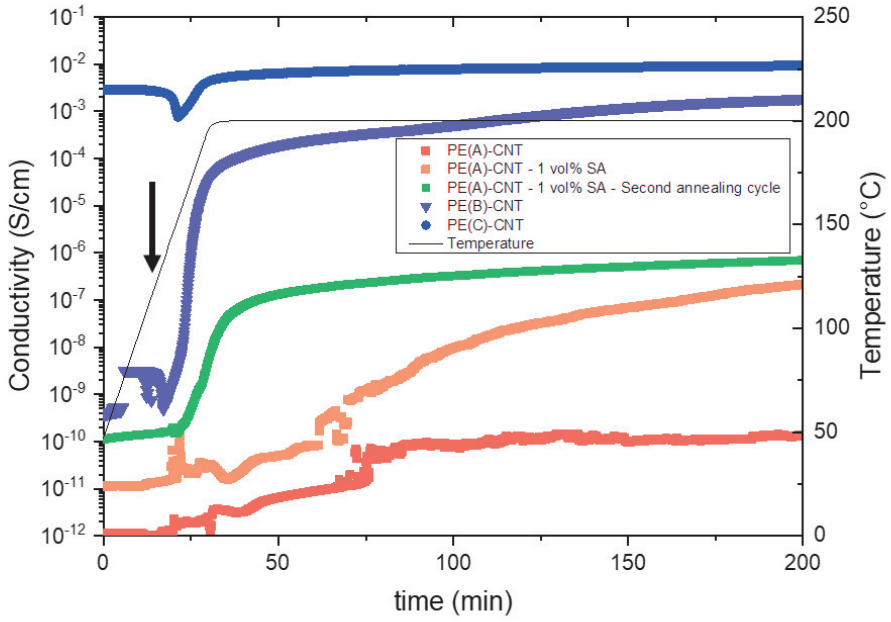

Figure 33: Conductivity evolution during annealing treatment for various PE-CNT (0.6 vol % CNT) systems. The black arrow outlines the time when the temperature reaches the melting temperature of the PE.

Figure 33 also displays the conductivity evolution during the annealing of PE(B) and PE(C)-CNT at the same CNT volume content to provide a comparison with systems presenting

a lower percolation threshold. It can be observed that the conductivity of PE(A)-CNT with SA remains around four orders of magnitude lower than the conductivity of PE(C)-CNT, even after thermal treatment.

Concerning PE(B)-CNT composites, the application of an annealing reduced the percolation threshold at CNT content lower than 0.6 vol % where it was determined at 0.8 vol % on merely pressed samples. Indeed, from **Figure 33** the conductivity of PE (B)-CNT composites with 0.6 vol % reaches a conductivity in the order of 10^{-3} S.cm^{-1} after annealing.

In comparison with HDPE(A)-CNT composites, while a greater difference in percolation thresholds is observed for LLDPE(C) composites, the use of HDPE(B) with a similar structure as the HDPE(A) with an intermediary viscosity ($\eta_0(A) \approx 10 \cdot \eta_0(B) \approx 50 \cdot \eta_0(C)$ at 200 °C) also led to a lower percolation threshold (φ_c<0.6 vol %). This result attests from the polymer viscosity effect on the achievable percolation threshold for a similar polymer structure.

b) Stearic acid content

The amount of SA introduced in the composite is crucial as an insufficient quantity would not allow any improvement while excessive quantities would induce processing problems [30] and without enhancing the dispersion anymore. For instance, Müller et al. observed a migration of PEG toward the surface of the composite when the additive is incorporated at high content [26].

PE(A)-CNT composite with various amount of SA were prepared to determine the ideal surfactant amount to obtain the highest conductivity. **Figure 34** presents the quiescent treatment of PE(A) filled with 0.6 vol % CNT for different SA contents. Samples with 0.5 vol % and higher SA content showed a conductivity improvement during the annealing. This observation suggests that the addition of 0.2 vol % is insufficient to enhance the filler dispersion. While similar behaviors are observed by the addition of 0.5 and 1 vol %, the conductivity evolution is slightly reduced for the composite with 5 vol % SA.

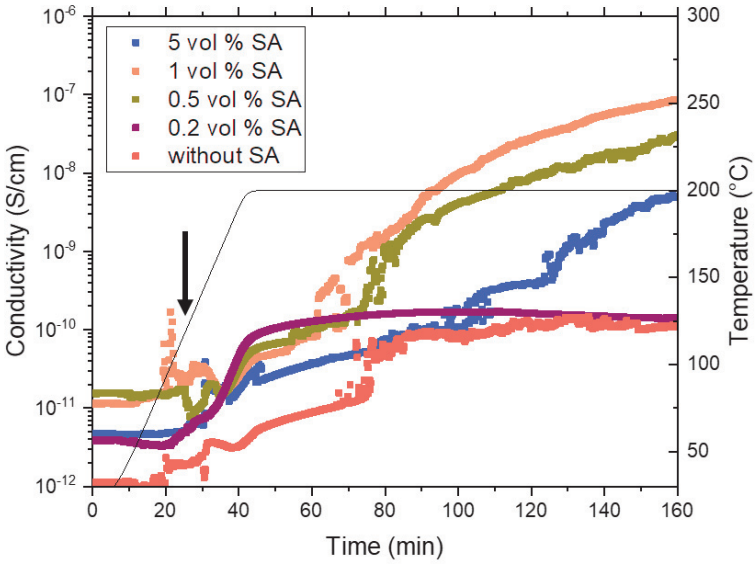

Figure 34: conductivity evolution during annealing treatment (200°C) of PE(A)- 0.6 vol % CNT with various SA content.

This variation might originate from a difference in the mechanical forces applied during the mixing step. Indeed, during the preparation of PE-CNT composites with the highest SA content, a reduction of the mixing force was noticed as presented in **Figure 35**.

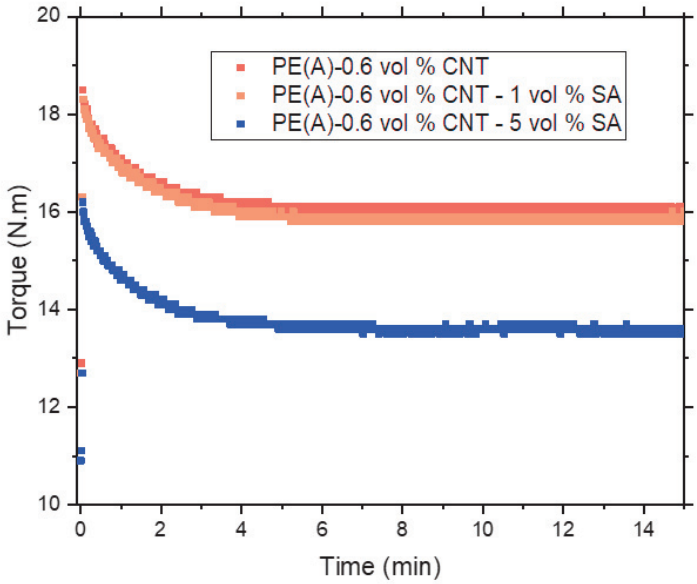

Figure 35: Mixing forces during the melt mixing at 200°C and 50 rpm for 15 min of PE(A)-CNT composites with various SA content.

A migration of the stearic acid on the surface of the sample was observed after melt mixing and compression molding steps. In **Figure 36** the sample with 5 vol % SA (**Figure 36 B**)

presents deposits at the surface that are not observed for lower SA contents pointing its migration toward the surface.

Figure 36: PE(A)-CNT (0.6 vol % CNT) samples with 1 vol % SA (A); 5 vol % SA (B). Picture C) is the sample B) half wiped.

These results suggest that for highest SA content (here 5 vol %), the additive induces a lubrication effect, resulting in slipping during the mixing step that are unfavorable for the CNT dispersion in the matrix. However, reduced mixing forces observed during the mixing step (**Figure 35**) could also be explained by a better dispersion of the filler in presence of SA.

As a result, the impact of SA on the electrical conductivity appears complex as this additive seems to ease the dispersion of the filler but also modifies the mixing forces that influence the electrical properties. The balance between these competing mechanisms varies depending on the additive content incorporated but can significantly improve the electrical conductivity of a viscous PE-CNT composite.

Conclusion

The percolation potential of a specific polymer-CNT combination is often evaluated by the conductivity as function of the filler content, but this characterization does not necessarily express the true potential of the network. The measured conductivity is representative for a frozen state, that may or may not be representative of the achievable conductivity.

A tremendous conductivity increase can be observed during a quiescent annealing treatment, corresponding to the dynamic percolation. Following the conductivity improvement induced by a thermal treatment appears as a convenient method to compare the percolation potential for various polymer-CNT systems since different nanotube network reorganizations are observed for various quiescent melt polymers. Using this characterization, the determined percolation threshold for a viscous PE-CNT system (η_0 = 10^5 Pa.s at 200 °C) was reduced from 1.4 vol % to 0.9 vol % over a 2-hour annealing at 200 °C. For a less viscous matrix (η_0 = $3 \cdot 10^3$ Pa.s at 200 °C), an initial percolation threshold of 0.4 vol % decreased to less than 0.15 vol % with annealing treatment.

The influence of the polymer viscosity on the achievable percolation threshold and the conductivity recovery speed was therefore observed. In the case of specific industrial applications, for instance when highly viscous polymers are required, composites present higher percolation thresholds, and greater amounts of filler are needed to obtain a conductive behavior. Short quiescent annealing treatments could be implemented in the industrial process to reduce the CNT amount introduced as it can trigger a conductivity enhancement. For instance, the annealing could be used as a surface treatment to recover a conducting behavior at the surface of the composite, that is sufficient for application such as electrical dissipation.

Reducing the percolation threshold using additives also appears as a good option when the polymer used is fixed by an application restriction. Small amounts of surfactant can effectively enhance the conductivity of a polymer-CNT composite. In this study the addition of around 1 vol % of stearic acid allowed observing an insulator to conductor transition that was not achievable in the case of this specific PE-CNT system. Since SA seems to play a role of surfactant as well as processing aid, the influence of this additive on the final properties remains however complex.

References

[1] M. Dresselhaus, G. Dresselhaus and P. Avouris, Carbon nanotubes: synthesis, structure, properties and applications., Springer Science & Business Media, 2003.

[2] S. Pande, A. Chaudhary, D. Patel, B. P. Singh and R. B. Mathur, "Mechanical and electrical properties of multiwall carbon nanotube/polycarbonate composites for electrostatic discharge and electromagnetic interference shielding applications.," *Rsc Advances,* vol. 4, no. 27, pp. 13839-13849, 2014.

[3] H. Pang, L. Xu, D. X. Yan and Z. M. Li, "Conductive polymer composites with segregated structures.," *Progress in Polymer Science,* vol. 39, no. 11, pp. 1908-1933, 2014.

[4] D. D. L. Chung, "Electromagnetic interference shielding effectiveness of carbon materials.," *Carbon,* vol. 39, no. 2, pp. 279-285, 2001.

[5] Z. Liu, G. Bai, Y. Huang, Y. Ma, F. Du, F. Li and Y. Chen, "Reflection and absorption contributions to the electromagnetic interference shielding of single-walled carbon nanotube/polyurethane composites.," *Carbon,* vol. 45, no. 4, pp. 821-827, 2007.

[6] I. Balberg, N. Binenbaum and N. Wagner, "Percolation thresholds in the three-dimensional sticks system.," *Physical Review Letters,* vol. 52, no. 17, p. 1465, 1984.

[7] S. Kirkpatrick, "Percolation and conduction.," *Reviews of modern physics,* vol. 45, no. 4, p. 574, 1973.

[8] W. Bauhofer and J. Z. Kovacs, "A review and analysis of electrical percolation in carbon nanotube polymer composites.," *Composites science and technology,* vol. 69, no. 10, pp. 1486-1498, 2009.

[9] T. McNally and P. Pötschke, Polymer-carbon nanotube composites: Preparation, properties and applications., Elsevier, 2011.

[10] D. Rousseaux, G. Vaes and C. Boukalidis, "Process for the Preparation of Composite Articles Having Enhanced Electrical Properties". U.S Patent 15/557,413, 2018.

[11] M. R. Watt and R. A. Gerhardt, "Factors that Affect Network Formation in Carbon Nanotube Composites and their Resultant Electrical Properties.," *Journal of Composites Science,* vol. 4, no. 3, p. 100, 2020.

[12] L. Moreira, R. Fulchiron, G. Seytre, P. Dubois and P. Cassagnau, "Aggregation of carbon nanotubes in semidilute suspension," *Macromolecules,* vol. 43, no. 3, pp. 1467-1472, 2010.

[13] T. Skipa, D. Lellinger, W. Böhm, M. Saphiannikova and I. Alig, " Influence of shear deformation on carbon nanotube networks in polycarbonate melts: Interplay between build-up and destruction of agglomerates.," *Polymer,* vol. 51, no. 1, pp. 201-210, 2010.

[14] C. Zhang, P. Wang, C. A. Ma, G. Wu and M. Sumita, "Temperature and time dependence of conductive network formation: dynamic percolation and percolation time.," *Polymer,* vol. 47, no. 1, pp. 466-473, 2006.

[15] M. Badard, A. Combessis, A. Allais and L. Flandin, "Modeling the dynamic percolation of carbon nanotubes and revisiting critical exponents.," *Materials Chemistry and Physics,* vol. 191, pp. 89-95, 2017.

[16] A. Combessis, N. Charvin, A. Allais, J. Fournier and L. Flandin, "Understanding dynamic percolation mechanisms in carbonaceous polymer nanocomposites through impedance spectroscopy: Experiments and modeling.," *Journal of Applied Physics,* vol. 116, no. 3, p. 034103, 2014.

[17] M. Marcourt, P. Cassagnau, R. Fulchiron, D. Rousseaux, O. Lhost and S. Karam, "A model for the electrical conductivity variation of molten polymer filled with carbon nanotubes under extensional deformation.," *Composites Science and Technology,* vol. 168, pp. 111-117, 2018.

[18] I. Alig, T. Skipa, M. Engel, D. Lellinger, S. Pegel and P. Pötschke, "Electrical conductivity recovery in carbon nanotube–polymer composites after transient shear.," *physica status solidi (b),* vol. 244, no. 11, pp. 4223-4226, 2007.

[19] M. Mičušík, M. Omastová, I. Krupa, J. Prokeš, P. Pissis, E. Logakis, P. Pötschke and J. Pionteck, "A comparative study on the electrical and mechanical behaviour of multi-walled carbon nanotube composites prepared by diluting a masterbatch with various types of polypropylenes.," *Journal of Applied Polymer Science,* vol. 113, no. 4, pp. 2536-2551, 2009.

[20] I. Alig, T. Skipa, M. Engel, D. Lellinger, S. Pegel and P. Pötschke, "Electrical conductivity recovery in carbon nanotube–polymer composites after transient shear.," *physica status solidi (b),* vol. 244, no. 11, pp. 4223-4226, 2007.

[21] G. Boiteux, C. Boullanger, P. Cassagnau, R. Fulchiron and G. Seytre, "Influence of Morphology on PTC in Conducting Polypropylene-Silver Composites.," *Macromolecular symposia,* vol. 233, no. 1, pp. 246-253, 2006.

[22] H. Deng, T. Skipa, R. Zhang, D. Lellinger, E. Bilotti, I. Alig and T. Peijs, "Effect of melting and crystallization on the conductive network in conductive polymer composites.," *Polymer,* vol. 50, no. 15, pp. 3747-3754, 2009.

[23] A. A. Vasileiou, A. Docoslis, M. Kontopoulou, P. Xiang and Z. Ye, "The role of non-covalent interactions and matrix viscosity on the dispersion and properties of LLDPE/MWCNT nanocomposites.," *Polymer,* vol. 54, no. 19, pp. 5230-5240, 2013.

[24] P. C. Ma, N. A. Siddiqui, G. Marom and J. K. Kim, "Dispersion and functionalization of carbon nanotubes for polymer-based nanocomposites: a review.," *Composites Part A: Applied Science and Manufacturing,* vol. 41, no. 10, pp. 1345-1367, 2010.

[25] Z. Ye and S. Li, "Hyperbranched Polyethylenes and Functionalized Polymers by Chain Walking Polymerization with Pd-Diimine Catalysis.," *Macromolecular Reaction Engineering,* vol. 4, no. 5, pp. 319-332, 2010.

[26] M. T. Müller, B. Krause and P. Pötschke, "A successful approach to disperse MWCNTs in polyethylene by melt mixing using polyethylene glycol as additive.," *Polymer,* vol. 53, no. 15, pp. 3079-3083, 2012.

[27] M. T. Mueller, P. Poetschke and B. Voit, "Dispersion of carbon nanotubes into polyethylene by an additive assisted one-step melt mixing approach.," *Polymer,* vol. 66, pp. 210-221, 66.

[28] L. Vaisman, H. D. Wagner and G. Marom, "The role of surfactants in dispersion of carbon nanotubes.," *Advances in colloid and interface science,* vol. 128, pp. 37-46, 2006.

[29] N. Grossiord, J. Loos, O. Regev and C. E. Koning, "Toolbox for dispersing carbon nanotubes into polymers to get conductive nanocomposites.," *Chemistry of materials,* vol. 18, no. 5, pp. 1089-1099, 2006.

[30] A. Patti, H. Lecocq, A. Serghei, D. Acierno and P. Cassagnau, "The universal usefulness of stearic acid as surface modifier: applications to the polymer formulations and composite processing.," *Journal of Industrial and Engineering Chemistry,* 2021.

Chapter 4.
Carbon nanotubes network modification induced by crystallization after quiescent annealing treatment of viscous Polyethylene-CNT composites

I. Introduction

The electrical properties of polymer filled composites rely on the interconnection of conductive fillers inside the polymer matrix [1, 2]. During processing steps, this continuous network is often modified as mixing forces can cause breaks up of filler-filler contacts leading to a reduction of the final electrical properties [3, 4]. The network state of an as processed polymer-CNT composite can therefore differ from an ideal situation, where all the CNTs are connected and present an optimal conductivity [5, 6]. The application of an annealing treatment at temperatures above the melting temperature (or the glass transition for amorphous matrix) was found effective to trigger the dynamic percolation [7, 8]. This self-organizing mechanism allows a conductivity recovery in the melt polymer and a reduction of the percolation threshold [9, 10].

The improvement of the conductivity through local quiescent annealing treatment could help to reduce the filler quantity required to obtain a specific conductivity level. However, a cooling to room temperature following this treatment is obviously unavoidable. During this temperature variation, the composite structure might be modified [11]. In the case of semi-crystalline polymers, the formation and growth of a crystalline phase in the heterogenous system is likely to disturb the filler network hence the conductivity of the material. A decent number of papers in the literature are focused on the morphology of CNT filled semi-crystalline polymer composites [12- 14]. It was observed for a wide range of systems that CNT is able to modify the crystallization kinetics as well as the crystalline morphology [12, 15- 18].

Concerning the impact of polymer crystallization on the conductivity of polymer-CNT composites, only some papers has tackled the subject [19- 26]. Various behaviors have been observed in the study of different semi-crystalline systems. The conductivity of semi-crystalline polymer-CNT composites could either increase [19, 23- 26] or diminish [19- 22] because of the crystallization process. From the plurality of observations, it therefore appears delicate to predict the conductivity evolution of a specific system induced by this mechanism.

Polyethylene is among the most used commodity polymer. The addition of carbon nanotubes in sufficient quantity in this inexpensive matrix is industrially valuable. However, the influence of PE crystallization on the conductive filler network must be studied to understand and determine the appropriate CNT quantity to add for a specific application. The study of the crystallization effect of a HDPE matrix in a CNT filled composite was therefore conducted in this chapter.

II. Materials & methods

1- Materials

Composites with the desired filler's volume fraction were obtained by diluting a PE filled with high CNT content in a polyethylene matrix. PE-CNT composites were prepared by direct melt mixing at 50 rpm for 15 minutes at 200°C. disk samples of 25 mm diameter and 2 mm thick were then prepared by compression molding at 200°C for 15 minutes before cooling down to room temperature.

Multiwalled Carbon nanotubes NC7000 (Nanocyl) were used in this study. They are characterized by a volume resistivity of 10^{-4} Ω.cm, an average diameter of 9.5 nm and a mean length of 1.5 µm. The polyethylene used for the preparation of the masterbatch is LLDPE M35160 (Total) with an MFI of 16 g/10 min (190°C – 2,16 kg). The masterbatch was diluted using three different industrial polyethylenes in this study. A viscous HDPE XRT70 (Total) (A) with a melt flow index (MFI) of 0.7 g/10 min (190°C - 5.0 kg); a HDPE Hostalen GF 7750 M2 (Lyondellbasel) (B) with a MFI of 3.3 g/10 min (190°C - 5.0 kg); a LLDPE M4040 (Total) (C) with a MFI of 4 g/10 min (190°C - 2.16 kg). At this step, it can be pointed out that, from this dilution technique, a non-negligible quantity of the polyethylene coming from the masterbatch is blended in the composite. For example, for a CNT content around 1.4 vol% which corresponds to the percolation threshold previously determined with the HDPE (A), the polymer matrix is finally composed of around 20% of LLDPE M35160.

A polystyrene (PS)-CNT composite was also used in this study for comparison with an amorphous matrix. This composite based on commercial amorphous polystyrene "crystal" PS 1160 (Total) was prepared by the masterbatch dilution technique following the protocol presented in patent WO2015014897 [27]. The PS is characterized by a MFI of 2.4 g/10 min (200°C - 5.0 kg).

2- Melt temperatures

Melting temperatures of studied polyethylenes were determined by differential scanning calorimetry (Perkin Elmer). Samples followed heating cycles from 30 to 230 °C with scan speeds of 5 and 20°C/min.

3- Polarized light microscopy

Polarized light microscopy were conducted using an optical microscope (LEICA DM2700 M) to monitor the spherulite structure of studied PE (A) and (C). Thin films were placed between glass slides, then melted above the melting temperature (to 180°C) and cooled to 70°C at speed of 5°C/min by means of a hot stage (FP82HT METTLER TOLEDO) to observe the polyethylene crystallization. Optical micrographs were taken using a digital camera (QICAM Fast1394 QIMAGING) along the cooling process.

4- Electrical characterization

Volume conductivity measurements were performed on a broadband dielectric spectrometer Novocontrol Alpha analyzer over a frequency range from 1 Hz to 10^6 Hz. Samples are placed between two electrodes and pressed using a spring to optimize the reproducibility of the measurement. Electrical contacts were gold metallized to eliminate the influence of the contact resistance.

The dielectric spectrometer was coupled to a Quatro Cryosystem (Novocontrol) to perform electrical measurement under controlled temperature and inert atmosphere (Nitrogen). The frequency range was reduced to 10 Hz to 10^3 Hz to keep acceptable period between time resolved measurements (a measurement around every 10 s). The heating and cooling rates were fixed at 5 °C/min. This set up allows conductivity measurements during quiescent annealing of samples above the melt temperature of the polymer.

III. Results and discussion

1- Influence of cooling and crystallization on the electrical conductivity

a) Crystallinity of the HDPE

The influence of CNT on the crystallization of PE was first studied by differential scanning calorimetry (DSC). Thermal properties of composites were characterized, and crystallization curves are shown in **Figure 37**. An isothermal annealing was performed well above their melting point (at 200°C) prior the temperature scan at 20°C/min. The crystallization temperatures as well as the crystallinities of the materials are summarized in **Table 3**. The dilution effect of the PE (A) by the masterbatch matrix is observable by a certain reduction of the crystallinity. Concerning the composite PE(A) containing CNT, the onset of crystallization is found at a slightly higher temperature (116°C instead of 113°C). This indicates that the CNTs have a noticeable nucleating effect on the PE crystallization mechanism. However, as expected, no effect on the final crystallinity is observed.

Regarding the PE(C) crystallization behavior in presence of CNT, the crystallization onset and peak are also shifted towards higher temperatures (5°C) revealing again a perceptible nucleating effect of CNTs on the PE(C) matrix crystallization.

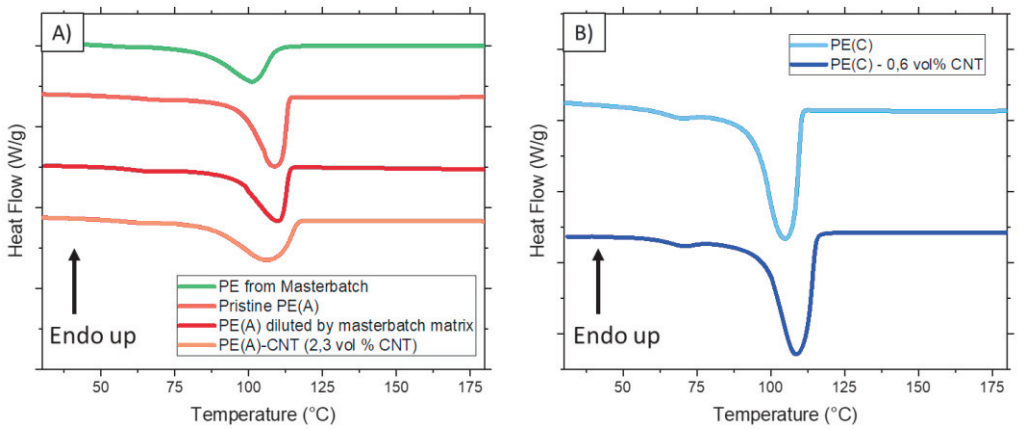

Figure 37: DSC curves for PE(A)-CNT (A) and PE(C)-CNT (B). Scan speed of 20 °C/min.

Table 3: DSC measurement of crystallization temperature and crystallinity of PE(A) and PE(C) composites.

Sample	T Onset (°C)	T peak (°C)	Crystallinity* (%)
Masterbatch matrix	109	101	44
PE(A)	114	109	59
PE(A) diluted in the masterbatch matrix	113	109	53
PE(A)-CNT	116	108	54
PE(C)	110	104	52
PE(C) – CNT (1 wt %)	115	108	51

* The crystallinity was calculated by dividing the crystallization enthalpy variation by the melting enthalpy variation of the perfect crystal (290 J/g [28, 29]).

Melting and crystallization temperatures were also determined by DSC measurements at a scan speed of 5°C/min to match the heating and cooling rates used during conductivity monitoring under controlled temperature. **Figure 38** presents DSC curves for PE(A) and PE(C) filled with respectively 1.45 vol% and 0.6 vol % CNT.

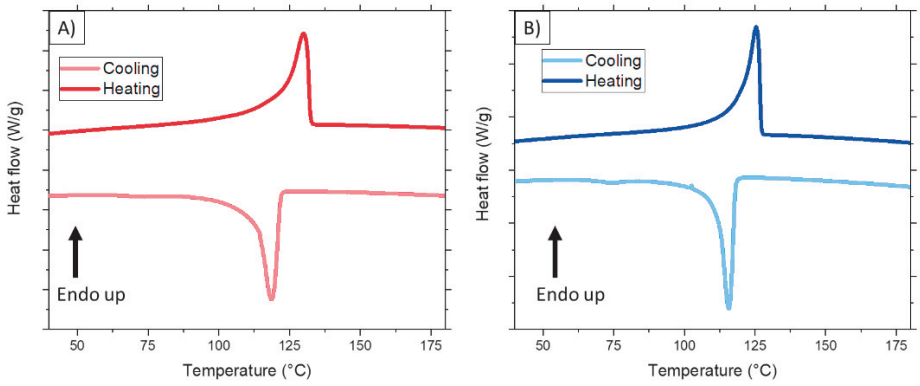

Figure 38: DSC cooling and heating curves for PE(A)-CNT (1.45 vol %) (A) and PE(C)-CNT (0.6vol %) (B) at a scan speed of 5°C/min.

For the PE(A)-CNT composite, the crystallization temperature is 120°C, while in the case of PE(C)-CNT it was determined at 118°C as observed in **Figure 38**.

The composites morphology is modified during the cooling down to room temperature with the apparition of the crystalline phase (around 50% of the polymer). This crystalline phase is likely to modify the CNT distribution and dispersion. Two opposite forecasts can be made with the apparition of an area where CNT can not be found in: conductivity can either increase of diminish.

Concerning the first option, CNT-CNT electrical contacts are responsible for the conductivity of the composite and, since the amorphous phase is reduced and the CNT are rejected from the crystalline phase, the effective concentration of CNTs in the amorphous phase is increased. A densification of CNT contacts in a smaller volume can induce an increase in conductivity [24]. This mechanism of phase exclusion inducing an enhancement in the composite conductivity was observed for various systems with the addition of a second filler or a second immiscible polymer in the composite [30- 32]. For instance, Marcourt et al. showed that the presence of polybutadiene nodules induced a confinement effect on CNT in a polystyrene matrix, resulting in a conductivity enhancement [32].

On the contrary, the apparition of the crystalline phase can be sources of conductivity reduction. In case of the crystal apparition in the vicinity of CNTs, the crystal growth could, for instance, create filler-filler disconnections breaking the conductive pathways [22]. Moreover, in case of nucleating effect, as it was noticed in the present work, it can be envisioned that some crystallites grow from the CNTs leading to their insulation from each other [24].

Conductivity measurements are useful to follow the state of dispersion and the structuring ability of polymer-CNT composites. The conductivity monitoring during temperature variation was here carried out to study the impact of the crystallization on the filler network efficiency.

b) Impact of cooling to room temperature on the conductivity with viscous HDPE

Conductivity monitoring of polymer-CNT composites during quiescent annealing treatment was previously found useful to follow the conductive network structuring (see chapter 3). Above the melting temperature of the polymer, the conductivity increase observed with the annealing time attests from the network strengthening also known as in the literature as the dynamic percolation. This phenomenon is responsible for a conductivity increase similar to the conductivity increase with the CNT content [33]. As a result, the application of 2 hours annealing of merely pressed PE(A)-CNT composites resulted in electrical conductivity enhancement as well as the reduction of the percolation threshold from 1.4 vol % CNT for solid samples to 0.9 vol % in the melt state (see **Figure 30**, chapiter 3). The cooling step following an annealing treatment is here focused.

Figure 39 presents the conductivity evolution during a 2-hour annealing at 200°C for a PE(A)-CNT (1.45 vol %) and the following cooling down to 30°C. Concerning the heating and annealing, the sample first experiences a conductivity decrease followed by the dynamic percolation mechanism triggering the conductivity enhancement as observed in the previous chapter. Firstly, around the melting temperature, the conductivity drops from an initial value of 10^{-4} S.cm^{-1} to around 10^{-6} S.cm^{-1}. This conductivity modification is a first hint of interaction

between the crystalline phase and CNTs. The conductivity evolution can be explained by the melting of the crystalline phase. As the amorphous phase expands, CNTs are distanced from others and a reduction of filler-filler connections is observed, resulting in a decrease of the measured conductivity. This behavior was observed for various PE-CNT systems and the effect is similar to the Positive Temperature Coefficient of resistance (PTC) effect observed during the heating of thermoplastic matrix composites [22, 34].

After this significant decrease in conductivity, the molecular mobility in the melt polymer allows a restructuring of the conductive network responsible for the conductivity increase. By means of an annealing treatment (200°C) for 2 hours, the conductivity of the composite increases up to a conductivity in the order of 10^{-2} S.cm^{-1} as presented in **Figure 39**. The sample is then cooled down to 30 °C at a cooling rate of 5°C/min. During this temperature variation, a sharp decrease in conductivity is observed around the crystallization temperature determined in **Figure 38**.

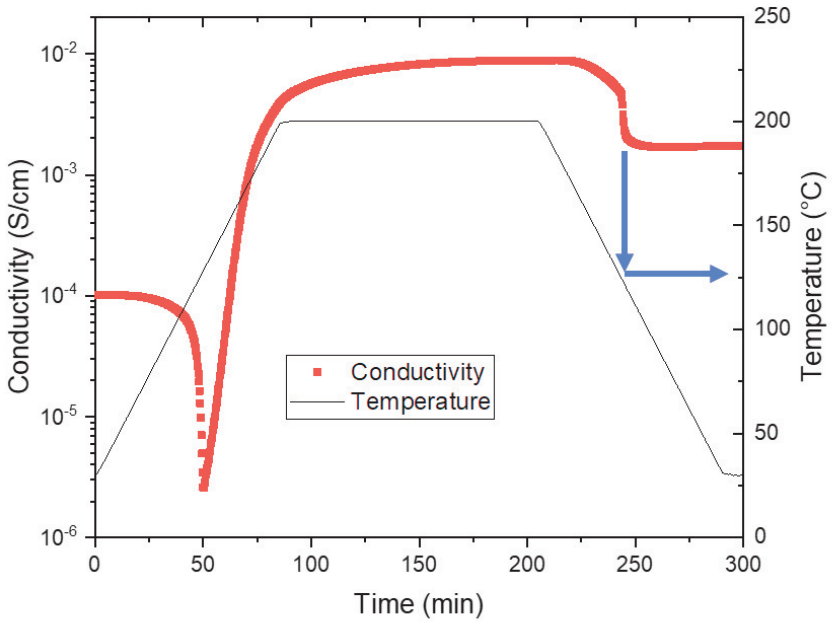

Figure 39: Conductivity evolution during annealing treatment (200°C) and the following cooling down to 30 °C for PE(A)-CNT (1.45 vol % CNT). f= 1kHz. Blue arrows outline the polymer crystallization.

A focus on the cooling step is proposed in **Figure 40**. From this close-up view, a small conductivity reduction is first observed with decreasing temperatures in molten state. This conductivity might result from a thermal contraction, inducing a network disruption. At around 120°C a sharp conductivity drop happens in around 2 minutes. Then the conductivity is stabilized at a level around $2 \cdot 10^{-3}$ S.cm^{-1}. The crystallization process was observed in DSC to start around this temperature, suggesting that this process is responsible for this noticeable conductivity modification. Once the crystallization process is over, the conductivity reaches a steady state.

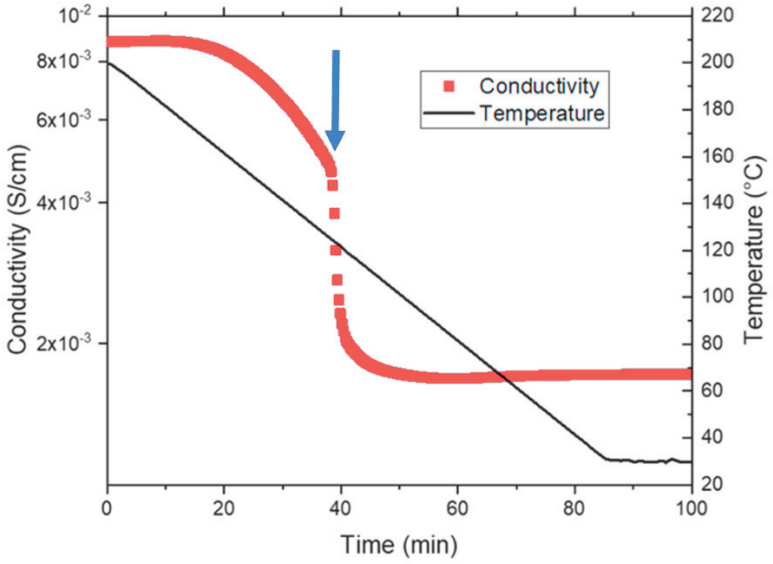

Figure 40: close-up view of the cooling step following the annealing treatment (200°C) for 120 minutes of a PE(A)-CNT (1.45 vol % CNT). The blue arrow outlines the crystallization temperature.

The maximum conductivity (around 10^{-2} S.cm^{-1}) is recorded when the sample is in the melt state, but a clear impact of PE crystallization on the conductivity is observed. While the conductivity is still enhanced after the sample is cooled down to room temperature from the initial value, the crystallization step turns out to disturb the conducting network in reducing the number of filler-filler connections. As a result of the 2 hours annealing treatment, the volume conductivity of the PE(A) filled with 1.45 vol % CNT increases from an order of magnitude from 10^{-4} S.cm^{-1} to 10^{-3} S.cm^{-1} for the solid composite.

c) Comparison with an amorphous polymer cooled down below the glass transition

To highlight the effect of crystallization on the CNT network the behavior of a polymer-CNT composite with an amorphous matrix was also studied. **Figure 41** presents the conductivity evolution during an annealing treatment of an amorphous polystyrene filled with 0.7 vol % CNT composite. The sample was heated above the glass transition temperature (100°C) for 1 hour at 160 °C and was then cooled down to 30 °C. From **Figure 41**, it is observed that the PS-CNT (0.7 vol % CNT) composite was characterized as initially insulator with a conductivity in the order of 10^{-10} S.cm^{-1}, but the application of an annealing treatment triggers the dynamic percolation.

Accordingly, a conductivity increase is observed because of the filler network structuring. After one hour at 160°C the conductivity reached a level of 10^{-6} S.cm^{-1} and is still increasing. Once the cooling to 30°C is initiated (t = 95 min in **Figure 41**) the conductivity slightly decreases, similarly to PE(A)-CNT composite in **Figure 39**. Once the temperature is below the glass transition temperature, the conductivity is stabilized at $2 \cdot 10^{-6}$ S.cm^{-1}, and no other modification is observed. In contrast to the cooling to room temperature of PE(A), no

sharp conductivity decrease is observed, supporting the idea that crystallization induced the modification observed in **Figure 39**.

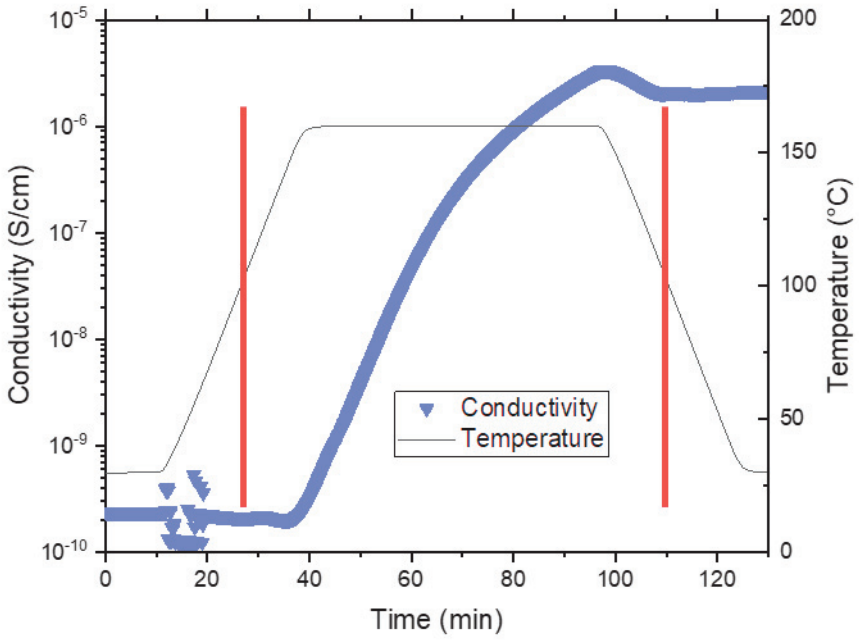

Figure 41: Conductivity (f= 1000Hz) evolution during annealing treatment (at 160°C for 60 minutes) and cooling down to room temperature for PS-CNT (0,7 vol %). red lines outline the transition above and below the glass transition of the PS.

d) Comparison with a LLDPE

The annealing effect on the conductivity evolution was studied for two PE of different structure in the previous chapter. The crystallization of the LLDPE(C) matrix in PE(C)-CNT composites was therefore also investigated and reported here in **Figure 42**. The application of an annealing treatment for 2 hours at 160°C allowed the modification from a conductivity of 10^{-9} S.cm^{-1} for merely pressed sample of PE(C)-CNT composites with 0.15 vol% to more than 10^{-5} S.cm^{-1}. During the cooling after the annealing, a significant conductivity loss around the crystallization temperature is observed in **Figure 42** for LLDPE-CNT composite. The behavior is similar to the one observed with HDPE(A)-CNT composites, also attesting from the disruption of the CNT network by the growing polymeric crystals.

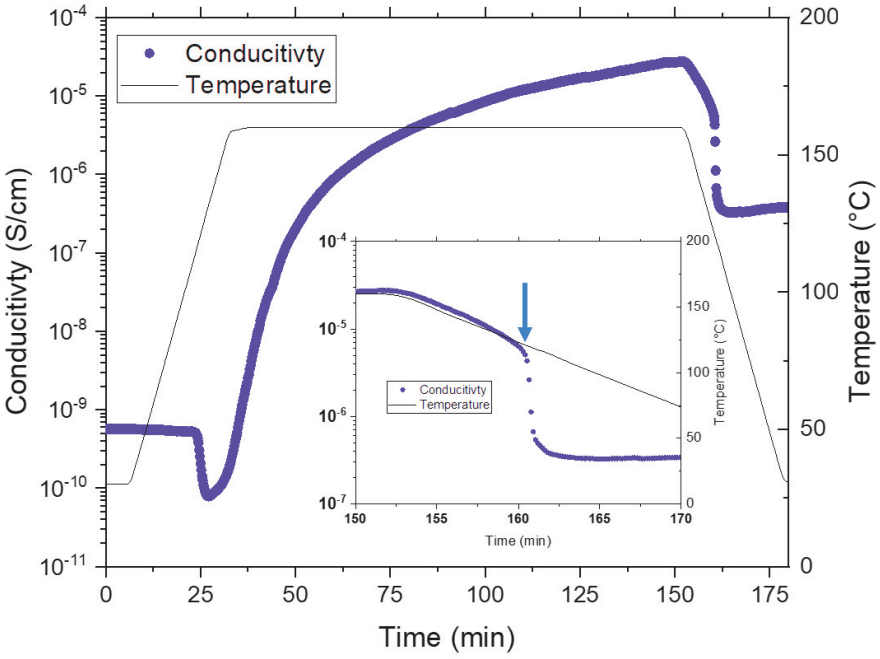

Figure 42: Conductivity (f= 1 kHz) evolution during an annealing treatment (at 160°C for 120 minutes) and the following cooling down to room temperature for LLDPE(C)-CNT (0,15 vol %). As inset is plotted a zoom of the cooling step. The blue arrow outlines the crystallization temperature.

In summary, during the cooling to room temperature of PE-CNT composites, for the two studied PE with different structure, a conductivity loss is observed around the crystallization temperature. This result is however not so surprising as a comparable crystalline morphology was observed by polarized optical microscopy for both pristine PE (A) and (C) matrices as presented in **Figure 43**.

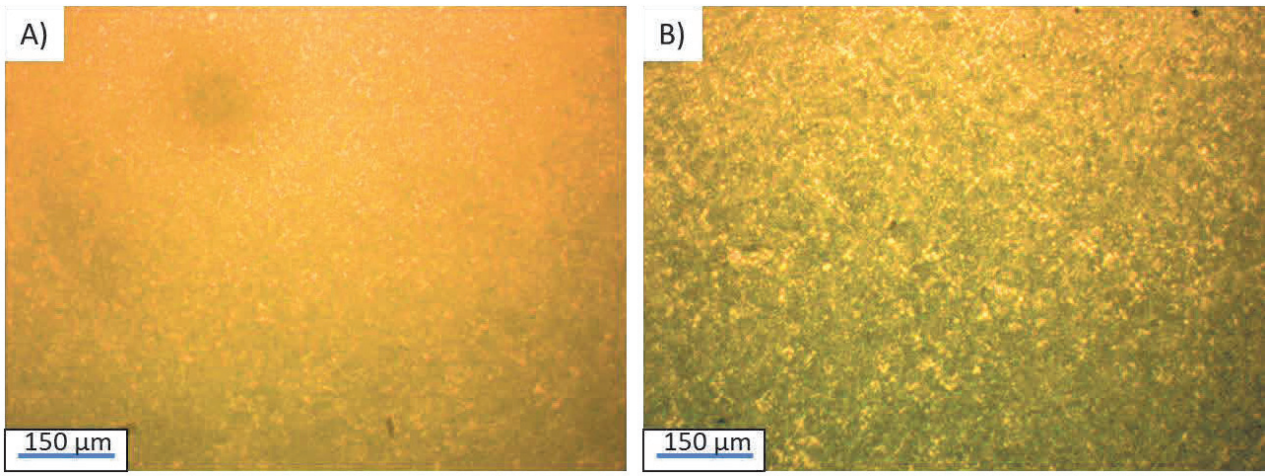

Figure 43: POM images of A) pristine HDPE (A) and B) LLDPE (C)

The apparition and growth of the crystalline phase seems responsible for filler-filler disconnections as conductivity loss is observed for these semi-crystalline matrices where it was not observed during the cooling of an amorphous PS-CNT composite.

2- Influence of the annealing time on the conductivity after crystallization

The dynamic percolation observed during annealing treatment clearly depicts the restructuring ability of the polymer-CNT composite. For a composite containing a fixed filler amount, the conductivity can be enhanced to a certain extent. This conductivity evolution can be explained by the densification of CNT connections with annealing time. In fact, the CNT amount that initially takes part in the conductive network, φ_{eff}, (i.e that are not isolated from other CNTs) is not necessarily equals to the total filler amount φ. The increase in conductivity observed during previously presented annealing treatments attests from the difference in effective and the total filler content. To observe the crystallization effect at different state of filler dispersion, PE-CNT composites were annealed up to different conductivity levels and then cooled down below the crystallization temperature.

Figure 44 presents the conductivity evolution of PE(A)-CNT composites (1.3 vol % CNT) for different annealing times at 200°C and the following cooling down. Merely pressed samples are characterized by a conductivity lower than 10^{-7} S.cm^{-1}. The variation observed in the initial conductivity is explained by its high sensitivity to the CNT network arrangement for filler content close to the percolation threshold. However, the annealing of the material at 200°C quickly rectifies the difference thanks to the dynamic percolation. Indeed, after 2 hours of annealing, both samples present a similar conductivity level in the order of 10^{-4} S.cm^{-1} as observed in **Figure 44**. The prolongation of the annealing for 1 hour allowed the enhancement of the conductivity above a level of 10^{-3} S.cm^{-1}. A focus on the cooling step is given in **Figure 45**. During the cooling to 30 °C of the composite, the PE crystallization induces a conductivity drop responsible for the loss of more than 2 orders of magnitude for the composite annealed for 2 hours. For the composite annealed for a longer period, the conductivity reduction is only of 1 order of magnitude from 10^{-3} to 10^{-4} S.cm^{-1}. In conclusion, the higher the conductivity is in the melt, the less the conductivity is reduced by the crystallization.

A second shorter annealing at 200°C was carried out following the 3 hours treatment. During this thermal treatment, the conductivity quickly recovers the level reached before the cooling step. This conductivity evolution clearly demonstrates the sensitivity of the CNT network on the thermal history. After one hour, the conductivity is comparable to the level reached during the previous annealing, and the cooling step to 30°C induces the same conductivity modification as observed in **Figure 44** and **45**.

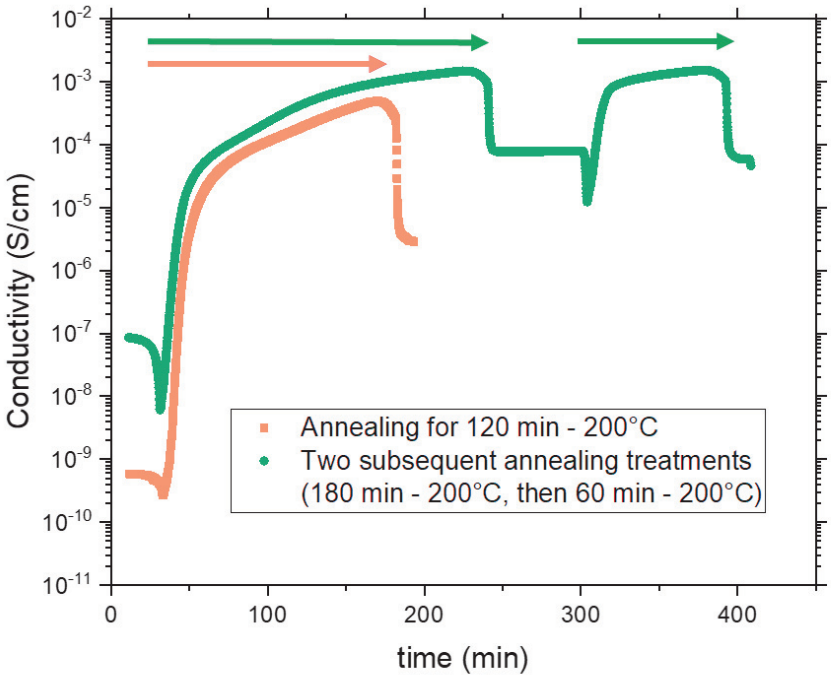

Figure 44: Conductivity evolution during annealing treatment at 200°C for different annealing and their following cooling down to room temperature for PE (A)- CNT (1.3 vol % CNT). Orange and green arrows delimit the annealing treatment.

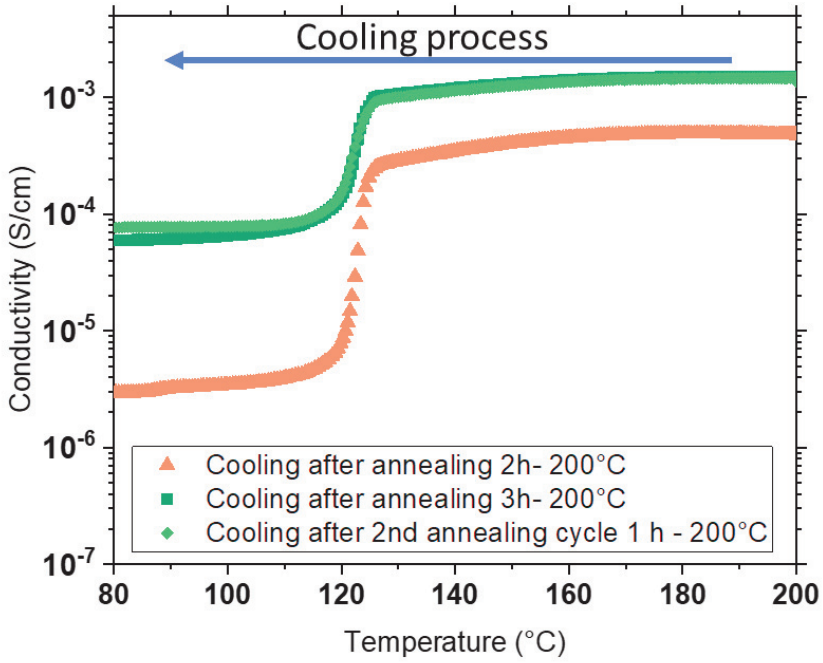

Figure 45: conductivity evolution as function of the temperature during the cooling process from 200°C to 30 °C of PE(A)-CNT composites (1.3 vol% CNT) following different annealing treatments (see Figure 8).

With annealing time, the effective CNT content increases toward the maximum value given by the total filler amount φ considered when the conductivity reaches a maximum conductivity. **Figure 46** presents the conductivity evolution of PE(C)-CNT (0.6 vol %) during annealing treatments of 1, 2 and 3 hours at 160°C. The PE(C) matrix was here chosen because the recovery kinetic is greater and therefore allows the obtention of a maximum conductivity at lower annealing times. From **Figure 46**, the maximum conductivity in the melt polymer is in the order of 10^{-2} S.cm^{-1} and is already observed after an annealing treatment of 1 hour and similar conductivities are measured for longer treatments.

During the three different experiments, the cooling to 30°C induced a conductivity drop from 10^{-2} S.cm^{-1} to a conductivity of $3 \cdot 10^{-3}$ S.cm^{-1}. Once the maximum conductivity is obtained in the melt polymer, the crystallization then induces the same conductivity loss.

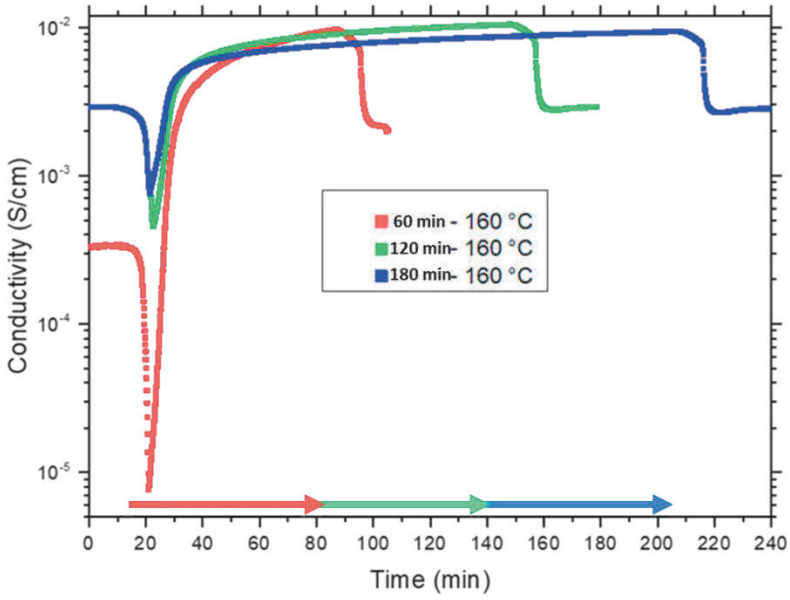

Figure 46: Conductivity evolution during the annealing for three duration (60, 120 and 180 hours) and the following cooling to room temperature for PE (C)-CNT (0.6 vol % CNT) composites. Arrows delimit the annealing treatments.

3- Impact of CNT content on the conductivity variation during crystallization

The influence of the cooling step on the conductivity for various CNT content was therefore investigated for the PE(A)-CNT system. Fernandez et al. observed for semicrystalline polyurethane (PUR)-CNT composites that the crystallization induced different conductivity modification depending on the CNT content. For composites with filler contents lower than the determined percolation threshold, the crystallization induced a conductivity decrease. For CNT content lower than the percolation threshold, the observed conductivity decrease can be explained by the reduction of the ionic conductivity as there is no filler conducting path. However, for CNT content well above the percolation threshold, the same cooling step led to a conductivity increase up to 2 orders of magnitude [19]. As a result, the PUR crystallization was found to enhance the conductivity of composites with an existing conducting filler

network. However, from the previously presented results, the conductivity of PE(A)-CNT system was found to be always decreased by the apparition of the crystalline phase. To compare both behaviors, it can be noted that the degree of crystallinity is lower for the PUR matrix, the crystallization seems to reduce the CNTs available volume and therefore induce a network densification. Whereas for the PE matrix, the nucleating effect of CNTs result in a disruption of the network.

Figure 47 presents the conductivity evolution during the annealing and the following cooling of a PE(A)-CNT composite close to the percolation threshold (0.9 vol % CNT). From the last chapter, the application of an annealing treatment for 8 hours allowed a tremendous increase of 6 orders of magnitude in the conductivity. However, the following cooling step induces an important drop in the conductivity. A loss of more than 3 orders of magnitude is observed in **Figure 47** during the cooling to 30°C of the sample. As a result, while an insulator to conductor transition was triggered during the annealing, the opposite change is observed during the cooling. The tremendous conductivity reduction observed in **Figure 47** attests from the network disruption by the crystallization: the effective filler content is reduced toward lower values.

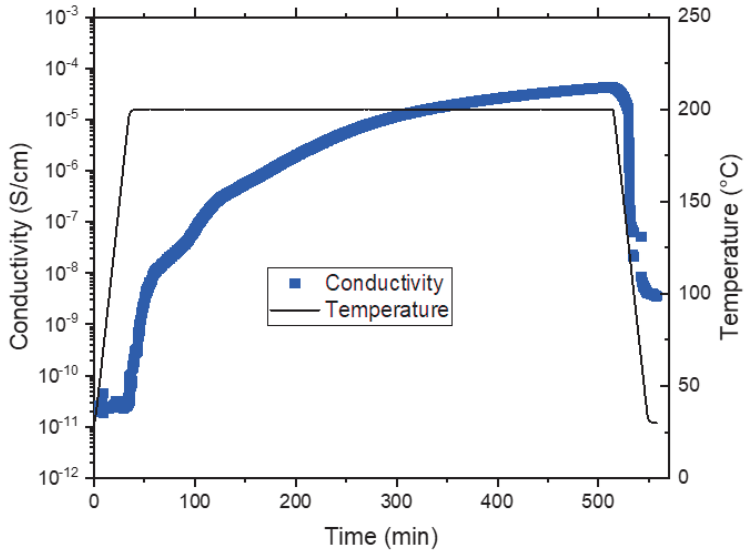

Figure 47: Conductivity evolution during annealing treatment at 200°C for 8 hours and the following cooling down to room temperature for PE (A)-CNT (0.9 vol % CNT).

Therefore, by comparing the conductivity loss observed in **Figure 39; 44 and 47**, the crystallization impact on the final conductivity of a composite seems more important for lower CNT contents.

It is generally well accepted that the correspondence between the measured conductivity and the effective CNT content is given by a percolation law. In the previous chapter, the percolation law was presented to describe the conductivity evolution as function of the CNT content for a PE(A)-CNT composite in the melt state after a 2-hour annealing. Using

this percolation law, the effect of crystallization on the CNT network efficiency was investigated. The effective CNT content of PE(A)-CNT composite in the melt state after 2-hour annealing was supposed to be equal to the total filler content.

By measuring the conductivity of PE(A)-CNT after the cooling step and using the percolation law for annealed composites in the melt state, the effective CNT content after crystallization was evaluated. **Figure 48** presents the evolution of the ratio of effective filler content φ_{eff} over the total filler fraction φ as function of the CNT content for merely pressed samples (before annealing) and after the annealing and crystallization.

From **Figure 48**, an interesting behavior is observed at CNT content well above the percolation threshold. The crystallization following the annealing induces a relative network modification becoming independent of the total CNT volume fraction at around 65 % of network efficiency. The crystallization of the PE matrix seems therefore responsible for the disconnection of around 35 % of the conductive network at the most. This result can be compared with the merely pressed samples where only 50 % of the CNT incorporated in the mix are taking part in the conducting network after crystallization for the same CNT content.

For lower CNT content, the crystallization step might trigger a transition from a conducting to an insulator composite as observed in **Figure 47** (from about 3.10^{-5} to 4.10^{-9} $S.cm^{-1}$). The benefit of an annealing treatment seems more reduced since the effective ratio for merely pressed and after annealing samples is close. However, as it was already stated, the conductivity variation is much more sensitive to the CNT content for CNT fractions close to the percolation threshold. Consequently, the small difference observed in **Figure 48** at lower CNT content still led to an enhancement of the conductivity of several orders of magnitude as observed in **Figure 44**.

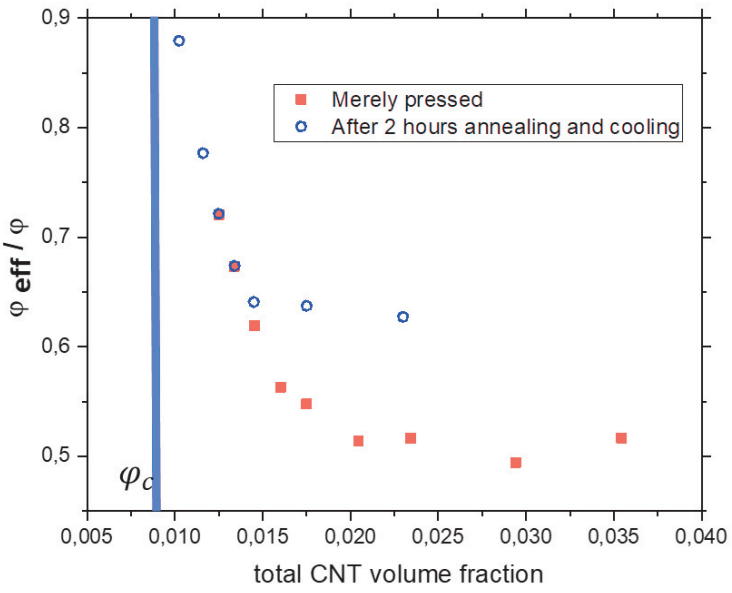

Figure 48: ratio of effective filler fraction over the total CNT content before and after 2 hours annealing treatment (200°C). Effective filler fraction is calculated using the percolation law determined from 2 hours annealing XRT 70 data.

The observations from **Figure 48** provide valuable information for the crystallization impact on the final electrical properties, especially for industrial applications. The crystallization impact on the CNT network structure can be predicted and the CNT content incorporated adapted for the aimed conductivity.

4- Impact of crystallization on the percolation law

In the last chapter, it was observed that the annealing treatment allowed the reduction of the percolation threshold of a PE-CNT composite after processing steps. However, the benefit of this treatment is reduced by the cooling step since the crystallization was found to always induce a conductivity reduction. The conductivity of PE(A)-CNT was measured after two hours annealing and the following cooling, for various CNT contents. **Figure 49** compares the conductivity evolution as function of the CNT content for PE(A)-CNT for merely pressed samples but also before and after the cooling following the annealing treatment. A percolation law is proposed to describe the conductivity evolution of the PE(A)-CNT composite after the cooling following the annealing process. The conductivity evolution with CNT content for other studied matrices are also presented in **Figure 49** and the impact of a 2-hour annealing with the following cooling down on few samples close to their percolation thresholds are also presented.

From **Figure 49** is observed the variation of the percolation depending on the different polyethylene matrices used. The percolation threshold is found at a higher CNT content for the PE(A), as presented in the previous chapter. **Table 4** summarizes the percolation laws proposed to describe the conductivity evolution for different systems used in this study. It should be noted that σ_0 and β parameters for annealed samples should be taken with caution because these values could be refined using a characterization of samples with higher CNT contents not available here. However, the percolation threshold values φ_c remain reliable differentiating the transition of the composite from an insulator to a conducting behavior and can be evaluated from **Figure 49**.

The application of an annealing treatment for 2 hours allows the reduction of the percolation threshold towards lower CNT content (0.9 vol % CNT compared to 1.4 vol % for merely pressed samples), but the cooling step reduces the conductivity enhancement induced by the annealing treatment. As a result, the percolation threshold of solid materials after an annealing treatment of 2 hours is found around 1.1 vol % of CNT. While the CNT network is disturbed by the crystallization of the matrix, the composite still benefits from the annealing in a conductivity enhancement.

Regarding composites based on PE(B) and (C) matrices, with shorter relaxation times, the application of an annealing treatment also allows conductivity enhancement in the vicinity of the percolation threshold. However, for CNT content more above the percolation threshold, this improvement is reduced. Indeed, the application of a 2-hour annealing allowed a conductivity improvement of more than 5 orders of magnitude for PE(C)-CNT (0.15 vol %) while the same treatment allowed a more moderate evolution for PE(C) filled with 0.6 vol % CNT (see **Figure 46**).

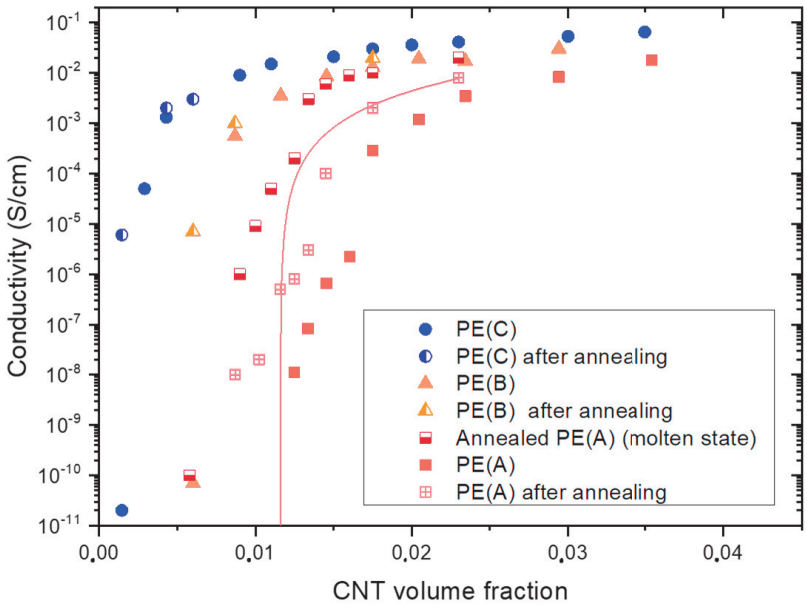

Figure 49: Conductivity as function of the CNT content. for PE-CNT nanocomposites cooled either just after pressing or after the annealing for two hours. The conductivity for the annealed composites in PE(A) before cooling is also shown. Red line is the percolation law

Table 4: fitting parameters for percolation law of PE-CNT presented in figure 4

Sample	σ_0 (S.cm^{-1})	φ_c (vol %)	β
M4040 (C)	0.33	0.4	0.7
XRT 70 (A)	2.7	1.4	1.4
Annealed XRT 70 (A)	20	0.9	1.5
After annealing XRT 70 (A)	30	1.1	1.8

Conclusion

The incorporation of a conductive filler in a polymer matrix is an attractive method to manufacture electrically dissipative materials. The theoretically low CNT content required to obtain suitable electrical conductivity positions this filler as a prime candidate. Depending on the properties of the polymer used but also the processing method, higher content may be needed to reach comparable conductivities.

The application of quiescent annealing treatment was found effective to improve to a certain extent the electrical conductivity of the polymer-CNT composite. The percolation threshold of PE(A)-CNT composites was reduced from 1.4 vol % CNT to 0.9 vol % in the melt polymer after an annealing treatment of 2 hours at 200°C. The structuring ability of the filler allows a densification of CNT-CNT connections in the melt polymer. However, in the case of semi-crystalline matrices, the cooling to room temperature following this thermal treatment can modify the conducting network. The efficiency of the annealing after cooling to room temperature for PE-CNT composites was here evaluated.

While various behaviors are reported in the literature, the apparition of the PE crystalline phase during the cooling step resulted here in a conductivity loss. For CNT content close to the percolation threshold (e.g. of PE(A) filled with 0.9 vol % CNT), a conductor to insulator transition could even be observed because of the polymer crystallization. The reduction of the global conductivity attests from the unavoidable network disruption during the cooling of the composite. Assuming that the conductivity follows the same percolation power law in the melt state and after crystallization, the cooling step is responsible for the disruption of the effective filler concentration up to a maximum of 35 %.

The conductivity of PE-CNT composite was still improved on solid samples by the application of the annealing (2 hours at 200°C) and the percolation threshold was determined around 1.1 vol % of CNT and the conductivity of composites with higher CNT content was enhanced.

References

[1] G. Mittal, V. Dhand, K. Y. Rhee, S. J. Park and W. R. Lee, "A review on carbon nanotubes and graphene as fillers in reinforced polymer nanocomposites.," *Journal of Industrial and Engineering Chemistry,* vol. 21, pp. 11-25, 2015.

[2] R. H. Baughman, A. A. Zakhidov and W. A. De Heer, "Carbon nanotubes--the route toward applications.," *science,* vol. 297, no. 5582, pp. 787-792, 2002.

[3] T. McNally and P. Pötschke, Polymer-carbon nanotube composites: Preparation, properties and applications., Elsevier, 2011.

[4] M. R. Watt and R. A. Gerhardt, "Factors that Affect Network Formation in Carbon Nanotube Composites and their Resultant Electrical Properties.," *Journal of Composites Science,* vol. 4, no. 3, p. 100, 2020.

[5] C. A. Martin, J. K. W. Sandler, M. S. P. Shaffer, M. K. Schwarz, W. Bauhofer, K. Schulte and A. H. Windle, "Formation of percolating networks in multi-wall carbon-nanotube–epoxy composites.," *Composites science and technology,* vol. 64, no. 15, pp. 2309-2316, 2004.

[6] I. Alig, D. Lellinger, M. Engel, T. Skipa and P. Pötschke, "Destruction and formation of a conductive carbon nanotube network in polymer melts: In-line experiments.," *Polymer,* vol. 49, no. 7, pp. 1902-1909, 2008.

[7] C. Zhang, L. Wang, J. Wang and C. A. Ma, "Self-assembly and conductive network formation of vapor-grown carbon fiber in a poly (vinylidene fluoride) melt.," *Carbon,* vol. 46, no. 15, pp. 2053-2058, 2008.

[8] C. Zhang, P. Wang, C. A. Ma, G. Wu and M. Sumita, "Temperature and time dependence of conductive network formation: dynamic percolation and percolation time.," *Polymer,* vol. 47, no. 1, pp. 466-473, 2006.

[9] A. Combessis, L. Bayon and L. Flandin, "Effect of filler auto-assembly on percolation transition in carbon nanotube/polymer composites.," *Applied Physics Letters,* vol. 102, no. 1, p. 011907, 2013.

[10] M. Badard, A. Combessis, A. Allais and L. Flandin, "Modeling the dynamic percolation of carbon nanotubes and revisiting critical exponents.," *Materials Chemistry and Physics,* vol. 191, pp. 89-95, 2017.

[11] I. Alig, P. Pötschke, D. Lellinger, T. Skipa, S. Pegel, G. R. Kasaliwal and T. Villmow, "Establishment, morphology and properties of carbon nanotube networks in polymer melts.," *Polymer,* vol. 53, no. 1, pp. 4-28, 2012.

[12] B. P. Grady, F. Pompeo, R. L. Shambaugh and D. E. Resasco, "Nucleation of polypropylene crystallization by single-walled carbon nanotubes.," *The Journal of Physical Chemistry B,* vol. 106, no. 23, pp. 5852-5858, 2002.

[13] S. Bose, A. R. Bhattacharyya, L. Häußler and P. Pötschke, " Influence of multiwall carbon nanotubes on the mechanical properties and unusual crystallization behavior in melt-mixed co-continuous blends of polyamide6 and acrylonitrile butadiene styrene.," *Polymer Engineering & Science,* vol. 49, no. 8, pp. 1533-1543, 2009.

[14] T. McNally, P. Pötschke, P. Halley, M. Murphy, D. Martin, S. E. Bell and J. P. Quinn, "Polyethylene multiwalled carbon nanotube composites.," *Polymer,* vol. 46, no. 19, pp. 8222-8232, 2005.

[15] A. R. Bhattacharyya, T. V. Sreekumar, T. Liu, S. Kumar, L. M. Ericson, R. H. Hauge and R. E. Smalley, "Crystallization and orientation studies in polypropylene/single wall carbon nanotube composite.," *Polymer,* vol. 44, no. 8, pp. 2373-2377, 2003.

[16] R. Haggenmueller, J. E. Fischer and K. I. Winey, "Single wall carbon nanotube/polyethylene nanocomposites: nucleating and templating polyethylene crystallites.," *Macromolecules,* vol. 39, no. 8, pp. 2964-2971, 2006.

[17] L. Li, C. Y. Li and C. Ni, "Polymer crystallization-driven, periodic patterning on carbon nanotubes.," *Journal of the American Chemical Society,* vol. 128, no. 5, pp. 1692-1699, 2006.

[18] J. Yang, C. Wang, K. Wang, Q. Zhang, F. Chen, R. Du and Q. Fu, "Direct formation of nanohybrid shish-kebab in the injection molded bar of polyethylene/multiwalled carbon nanotubes composite.," *Macromolecules,* vol. 42, no. 18, pp. 7016-7023, 2009.

[19] M. Fernández, M. Landa, M. E. Muñoz and A. Santamaría, "Electrical conductivity of PUR/MWCNT nanocomposites in the molten state, during crystallization and in the solid state.," *European polymer journal,* vol. 47, no. 11, pp. 2078-2086, 2011.

[20] I. Alig, D. Lellinger, S. M. Dudkin and P. Pötschke, "Conductivity spectroscopy on melt processed polypropylene–multiwalled carbon nanotube composites: recovery after shear and crystallization.," *Polymer,* vol. 48, no. 4, pp. 1020-1029, 2007.

[21] H. Deng, T. Skipa, R. Zhang, D. Lellinger, E. Bilotti, I. Alig and T. Peijs, " Effect of melting and crystallization on the conductive network in conductive polymer composites.," *Polymer,* vol. 50, no. 15, pp. 3747-3754, 2009.

[22] H. Pang, Y. C. Zhang, T. Chen, B. Q. Zeng and Z. M. Li, "Tunable positive temperature coefficient of resistivity in an electrically conducting polymer/graphene composite.," *Applied Physics Letters,* vol. 96, no. 25, p. 251907, 2010.

[23] G. O. Lim, K. T. Min and G. H. Kim, "Effect of cooling rate on the surface resistivity of polymer/multi-walled carbon nanotube nanocomposites.," *Polymer Engineering & Science,* vol. 50, no. 2, pp. 290-294, 2010.

[24] B. Li, Y. C. Zhang, Z. M. Li, S. N. Li and X. N. Zhang, "Easy fabrication and resistivity-temperature behavior of an anisotropically conductive carbon nanotube− polymer composite.," *The Journal of Physical Chemistry B,* vol. 114, no. 2, pp. 689-696, 2010.

[25] K. Jeon, S. Warnock, C. Ruiz-Orta, A. Kismarahardja, J. Brooks and R. G. Alamo, "Role of matrix crystallinity in carbon nanotube dispersion and electrical conductivity of iPP-based nanocomposites.," *Journal of Polymer Science Part B: Polymer Physics,* vol. 48, no. 19, pp. 2084-2096, 2010.

[26] M. Zhang, W. Jia and X. Chen, " Influences of crystallization histories on PTC/NTC effects of PVDF/CB composites.," *Journal of applied polymer science,* vol. 62, no. 5, pp. 743-747, 1996.

[27] D. Rousseaux, O. Lhost, P. Lodefier and E. Scandino, "Masterbatches for preparing a composite materials with enhanced conductivity properties, process and composite materials produced". US Patent 10,431,347, 2019.

[28] B. Wunderlich, Macromolecular Phys. Vol. 3: Crystal Melting, New York: Academic Press, 1980.

[29] J. D. &. M. R. L. Hoffman, "Kinetic of crystallization from the melt and chain folding in polyethylene fractions revisited: theory and experiment.," *Polymer,* vol. 38, no. 13, pp. 3151-3212, 1997.

[30] H. D. Bao, Z. X. Guo and J. Yu, "Effect of electrically inert particulate filler on electrical resistivity of polymer/multi-walled carbon nanotube composites.," *Polymer,* vol. 49, no. 17, pp. 3826-3831, 2008.

[31] P. Pötschke, A. R. Bhattacharyya and A. Janke, "Morphology and electrical resistivity of melt mixed blends of polyethylene and carbon nanotube filled polycarbonate.," *Polymer,* vol. 44, no. 26, pp. 8061-8069, 2003.

[32] M. Marcourt, P. Cassagnau, R. Fulchiron, D. Rousseaux, O. Lhost and S. Karam, "High Impact Polystyrene/CNT nanocomposites: Application of volume segregation strategy and behavior under extensional deformation.," *Polymer,* vol. 157, pp. 156-165, 2018.

[33] A. Combessis, N. Charvin, A. Allais, J. Fournier and L. Flandin, "Understanding dynamic percolation mechanisms in carbonaceous polymer nanocomposites through impedance spectroscopy: Experiments and modeling.," *Journal of Applied Physics,* vol. 116, no. 3, p. 034103, 2014.

[34] G. Boiteux, C. Boullanger, P. Cassagnau, R. Fulchiron and G. Seytre, "Influence of Morphology on PTC in Conducting Polypropylene-Silver Composites.," *Macromolecular symposia ,* vol. 233, no. 1, pp. 246-253, 2006.

Chapter 5.
Electrical conductivity under shear flow of molten Polyethylene filled with carbon nanotubes: experimental and Modeling

Reformatted version of paper originally published in:

Polymer engineering and science, April 2021, Volume 61 N°4 pp 1129-1138

Electrical conductivity under shear flow of molten Polyethylene filled with carbon nanotubes: experimental and Modeling

Anatole Collet[1], Anatoli Serghei[1], Olivier Lhost[2], Yves Trolez[2], Philippe Cassagnau[1], René Fulchiron[1]*

[1] *Univ Lyon- Université Lyon 1, CNRS, Ingénierie des Matériaux Polymères (IMP-UMR 5223), 15 Boulevard Latarjet, 69622 Villeurbanne Cedex (France)*
[2] *Total Research and Technology Feluy, Zone Industrielle Feluy C, 7181 Feluy, Belgique*

Abstract

This work aims to describe the conductivity evolution of polymer composites (polyethylene filled with carbon nanotubes) during a shearing deformation. Rheo-electric measurements were carried out to observe the shear-induced fillers network modification. Extended steady shear forces the conductivity to evolve asymptotically to a steady level attesting to an equilibrium between structuring and break up mechanisms in the melted polymer. Numerous experiments were conducted to cover a wide range of shear rate from 0.05 s^{-1} to 10 s^{-1} and for carbon nanotubes concentrations between 1.3 vol% and 2.9 vol%. A model is proposed to predict the conductivity evolution under shear deformation using a simple kinetic equation inserted in a percolation law. Structuring parameter was found to be solely dependent on the temperature whereas shear induced modification terms were found to be mostly driven by the shear rate and the fillers content.

Keywords:

Nanocomposites; melt; polyethylene (PE); shear; conducting polymers; modeling

I. Introduction

During last decades, carbon nanotubes (CNT) have proven their value as filler in polymer nanocomposites and find their place in numerous industrial applications [1-3]. This material can be used whether to improve mechanical properties [4] or to implement new features to a polymer matrix such as electrical conductivity [5]. Concerning the latter, the high aspect ratio of this material enables the improvement of a matrix with a theoretically low CNT content, less than one percent [6, 7].

In practice, the percolation threshold occurs at higher concentration [8, 9]. Nanotubes are characterized by a high aspect ratio with a contorted shape. They are generally aggregated and the structure of the network resulting from the aggregates interconnections can vary significantly with the polymer matrix, the processing method and nanotube type [10]. Electrical properties rely on a continuous network composed by contacts between small aggregates and individual CNTs [11-14]. A contact here is considered as an electrical contact, which means an electrical charge transfers between CNT by any mechanism (including tunnel effect) [15-17]. This complex grid can be modified during processing steps (Thermoforming, mould injection, extrusion…) by the applied mechanical deformation [14, 18-20]. For cost reasons but also in-

use mechanical properties, a very low CNT content is desired but this leads to electrical properties very dependent on processing steps and turns the manufacturing of conductive polymer composites into an industrial challenge [21].

To develop the comprehension of physical mechanisms responsible for the CNT network modification in melt polymer, rheological analysis coupled with conductivity measurement is valuable. A convenient way to monitor the CNT network in a polymer matrix is to measure the electrical response. This specific measurement allows full characterization of the conductivity characterization during quiescent treatment as well as during shear deformation.

In 2007, Obzrut used a rheoelectric set up and managed to monitor the destruction of the conductive network for polypropylene/CNT composites under steady shear [22]. The shear induced conductor to insulator transition [23] as well as the dynamic percolation [24] have now been observed under various condition and for different matrices. These phenomena depict the ability of the filler's network to evolve in a polymer melt whether to decrease or increase the number of CNT-CNT connections in the sample.

To describe the competition between structuring and destruction mechanisms in shear flow, a first model was proposed by Skipa et al. [25]. The evolution of the agglomerates fraction contributing to the electrical conductivity was expressed by the following kinetic **Equation 10**:

$$\frac{d\varphi_{eff}}{dt} = k_0\left(\varphi - \varphi_{eff}\right)^n + k_1\left(\varphi - \varphi_{eff}\right) - k_2\varphi_{eff} \qquad \text{Equation 10}$$

Where φ_{eff} is the effective volume fraction of conductive agglomerates, φ the filler volume fraction of agglomerates at the equilibrium ($t \to \infty$) and k_0, k_1 and k_2 the kinetic parameters relating to the process of quiescent agglomeration, shear-induced agglomeration and shear induced destruction, respectively. In **Equation 10**, a simple first order kinetics (n=1) was taken for the quiescent agglomeration phenomenon. Moreover, it was postulated that the last two kinetic parameters depend on the shear rate $\dot{\gamma}$ but also on the CNT species in the sample (large and small agglomerates and separated nanotubes). This equation introduced in a percolation law well describes the measured conductivity evolution of polycarbonate-CNT composites under shearing. However, in this model, each of these CNT species is governed by its specific kinetic law, so that many fitting parameters are introduced with difficult decoupling due to the rather imprecise definition of the boundaries between the three species [25].

Recently Marcourt et al. [26] developed a model describing the conductivity evolution of a CNT filled composite under extensional deformation. They assumed that CNTs, whether they are regrouped as agglomerates or just individual, take part in the sample's electrical conductivity as long as they are connected to the interconnected network [14]. In other words, more than counting CNTs that are connected to each other by contacts, the model was developed by considering an efficient part of the volume fraction of CNTs and a non-efficient part. The efficient part contains the CNTs incorporated in the percolation network (providing

an electrical path from one surface of the material to the other). Conversely, aggregates that may possibly be connected to each other but without any contact with this percolation network are considered in the non-efficient part. It follows that the kinetic laws simply govern the exchanges between both parts.

Using this approach, a kinetic equation was proposed to describe the response to an elongational deformation:

$$\frac{d\varphi_{eff}}{dt} = k_{build}(\varphi - \varphi_{eff}) - 2k_{break}\dot{\varepsilon}^2\varphi_{eff}t \qquad \text{Equation 11}$$

where φ_{eff} is the filler volume fraction that belongs to the percolated network, φ the total filler volume fraction, k_{build} and k_{break} are respectively the structuring and break-up kinetic constants. The first one has the dimension of the inverse of time, and the second one is adimensional. $\dot{\varepsilon}$ is the extensional rate. In the case of extensional stress, they observed that only the structuring mechanism was dependent on temperature following the same dependence as the matrix viscoelastic behavior. Thus, it was concluded that the structuring mechanism was due to the molecular mobility around CNTs. As regards the network breaking, it was shown to be solely relative to the deformation, following a negative exponential law of the squared deformation. In this case, it was concluded that the elongation contributes only to the network destruction systematically leading to a conductivity loss for moderate and high elongation rates [26]. This model allowed the prediction of the electrical conductivity under extensional deformation but also the conductivity recovery after cessation of the deformation.

For shear flow, the impact of the deformation on the conductive network is still unclear. Contrary to what has been observed for elongation, the effect of deformation is not only the total destruction of the conductor network and a part of the fillers fraction remains efficient. In this work, based on the conductivity monitoring during shear deformation, the mechanisms of the CNTs network modification are described. A simple model is proposed to predict the conductivity variation for HDPE/CNT melted composites under shear deformation.

II. Materials & methods

1- Samples

Polyethylene filled with carbon nanotubes composites were prepared by melt blending using the masterbatch dilution method in a dynamic mixer HAAKE™ Rheomix QC. Multiwalled carbon nanotubes (MWCNT), NC7000 from Nanocyl, were used. They are characterized by an average diameter of 9.5 nm, a mean length of 1.5 µm and a volume resistivity of $10^{-4}\ \Omega.cm$. A masterbatch containing Carbon nanotubes was diluted in a polyethylene matrix by direct mixing at 50 rpm for 15 minutes at 200°C to obtain desired filler's volume fraction. The used high-density polyethylene (HDPE), XRT70 from Total (PE(A), has a melt flow index (5 kg, 190°C) of 0.7 g/10min. Then, the material was compression molded at 200°C as disks of 25 mm diameter and 2 mm thick. The compression cycle in the press was of around 15 minutes at 200°C before the cooling down to room temperature.

2- Rheo-electrical set up

Electrical and viscoelastic measurements were carried out on an ARES G2 rheometer (TA Instruments). To enable the simultaneous characterization, ring-plate geometry electrodes were used and connected to a B2987A Electrometer (Keysight technologies). This set-up was already used by Moreira et al. [13] at ambient temperature. The conductivity is measured perpendicularly to the shear plane. It allows the electrical resistance measurement owing to a constant thickness of the sample while applying a quasi-homogeneous shear rate throughout the sheared material. The higher and smaller diameters of the cell are respectively 25 and 22 mm, inducing only 14% of strain difference in the analyzed sample. A picture of the rheological configuration can be seen in **Figure 50**. As the lower ring/electrode is rotating, the electrical signal is collected using a connector whereas the stationary upper electrode is directly connected to the electrometer.

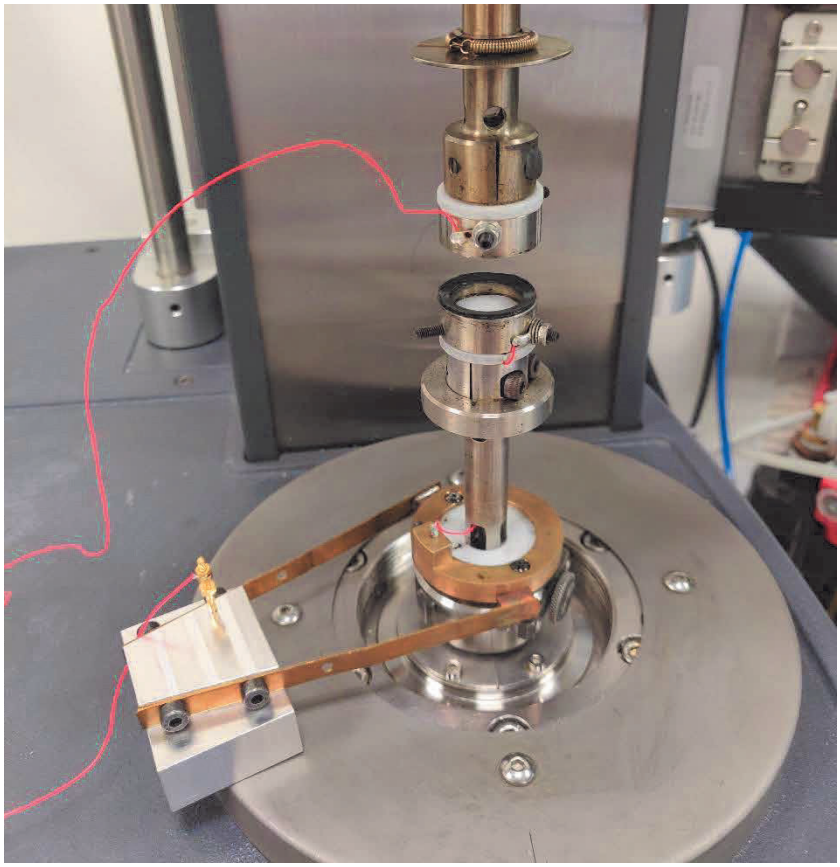

Figure 50: Picture of the rheological cell used for simultaneous conductivity measurement

A 1 V direct current (DC) was applied to the system and the resistance is measured every 0.1 s. The volume conductivity σ (S/cm) is obtained using the geometry of the sample:

$$\sigma = \frac{h}{S.R} \qquad \text{Equation 12}$$

where h is the thickness, S the surface of the ring (in our case equal to 2 cm^2) and R the measured resistance of the sample. The resistance of the short-circuited set-up was first

measured, and the obtained value was around 1 Ω, which is negligible compared to the measured resistance of the studied materials.

The samples were cut from pressed disks and placed between the ring cells. To ensure a good contact with both electrodes, temperature was set at 200°C to melt the polyethylene and the upper ring was brought in contact with the sample. The edge was removed to eliminate squeezed out material.

A quiescent treatment of around 15 minutes at 200°C was set until the sample conductivity regains a quasi-equilibrium state. Then a constant shear rate was applied to study the destruction and structuring process of the CNT network in the melt polymer.

As a preliminary analysis, the percolation law (**Equation 6)** linking the measured conductivity to the effective CNT content was determined for annealed samples:

$$\sigma = \sigma_0(\varphi_{eff} - \varphi_c)^{\beta} \qquad \textbf{Equation 6}$$

where φ_{eff} is the effective CNTs volume fraction, defined as the filler concentration contributing to the conductivity of the sample. For these quiescent treatments, φ_{eff} value was assumed to correspond to the total filler volume fraction φ of the sample once the conductivity has reached a steady level. Experiments were carried out on specimens with a CNT content varying from 1.3 to 2.9 vol%. Scilab software was used to fit the parameters by means of a non-linear least square regression subroutine. From these experiments fitting, the obtained value of the percolation threshold φ_c is 1.15 vol%, the exponent β is 2, and the pre-factor σ_0 is 0.9 S.cm^{-1}.

III. Description of the proposed model

1- Structuring induced by quiescent annealing

The conductivity of a polymer-CNT composite is determined by the fraction of fillers that are interconnected but above all that are linked to the percolated network which offers an electrical pathway through the material. In molten polymer, annealing allows isolated CNTs to reconnect with the conductive network. In the case of samples that are not in the equilibrium (initial effective volume fraction, $\varphi_{eff}^{initial} \neq \varphi$), thermal diffusion of the polymer surrounding the CNTs enables the conductivity recovery [26].

In **Equation 6**, it is assumed that only the carbon nanotubes fraction that contributes to this network is accountable for the electrical conductivity. Isolated disentangled CNT and agglomerates detached from the network are inactive for the electrons transport.

Previous works presented models describing well the asymptotical behavior of conductivity in polymer-CNT composite during quiescent treatment. According to Marcourt et al. [26], the evolution of the effective fraction of CNTs in the sample is given by the following kinetic equation:

$$\left.\frac{d\varphi_{eff}}{dt}\right|_{structuring} = k_{build}(\varphi - \varphi_{eff}) \qquad \textbf{Equation 8}$$

where φ is the total filler fraction; φ_{eff} is the filler fraction connected in the conductive network, necessarily limited to φ. For a given matrix the parameter k_{build} is only dependent on the annealing temperature and is directly linked to the relaxation time of the polymer matrix.

The analytical solution of this equation allows a direct correspondence between effective concentration and annealing time:

$$\varphi_{eff} = \varphi + (\varphi_0 - \varphi)e^{-k_{build}.t} \qquad \textbf{Equation 9}$$

where φ_0 corresponds to the initial effective filler fraction (which differs from φ when the material is not at the equilibrium).

In this study the k_{build} parameter was determined experimentally around the value of 1.3×10^{-2} s^{-1} by fitting **Equation 9** combined with **Equation 6** on conductivity measured curves during the annealing of previously sheared samples. This value turned out to be suitable for all experiments carried out at 200°C with all the tested filler concentrations, independently of the deformation history. The impact of temperature on the structuring parameter has been verified by analyzing the conductivity recovery at 180 and 160°C of pre-sheared samples. The parameter k_{build} was deduced to be 1×10^{-2} and 7×10^{-3} s^{-1} respectively. **Figure 51** shows a comparison of the model and the experiments after various pre-shear for the three tested temperatures. These results are in accordance with the assumption that the molecular mobility inside the polymer has a prevailing role in the structuring mechanism. These parameter values will therefore be fixed in the following for modeling the results with the same matrix at these three temperatures of experiments.

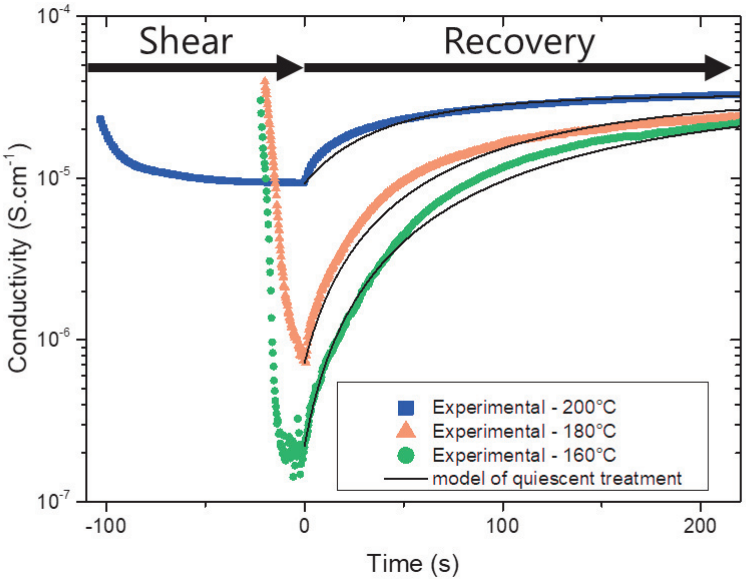

*Figure 51: Conductivity evolution of a HDPE/CNT (1.75 vol% MWCNT) under shear deformation (time <0 s) and during following quiescent treatment (time ≥0 s) for various temperature. black lines are calculated curves using **Equation 9**.*

2- Network modification under shear stress

Deformation can alter the conductivity of a sample by modifying the conductive filler network structure, orientation, or dispersion [25]. For example, in elongation, the CNTs are strained apart from each other, destructing fillers connections hence triggering a conductor to insulator transition [14]. Conversely, in the case of shear deformation, both increase and decrease in conductivity can be achieved. During a shear experiment, the effective concentration evolves monotonically depending on the initial network structure and the applied deformation. Alig showed on insulating specimens that steady shear can induce a dynamic percolation up to a stationary conductivity value [25]. On the other side, a shear deformation can also trigger a reduction in the conductivity of a sample with an initially well-connected CNT network [25]. In any case, the steady conductivity level reached during a shear deformation is found lower than in the quiescent melt. This stationary state is resulting from mechanisms of connection-disconnection of CNT contact under a shear deformation.

In this work, for experiments under shear leading to a steady conductivity, this steady level was always lower than this obtained for quiescent treatments (regardless of the shear rate, the temperature, or the CNT content). Moreover, for samples taken directly from the pressing operation i.e. which are out of equilibrium ($\varphi_{eff}^{initial} < \varphi$), the recovery was slower when a shear was applied. For these reasons, rather than introducing a shear induced structuring parameter, the shear is considered here only as causing breakup. However, at long times, and contrary to what was obtained for elongation, a finite effective fraction (φ_∞) is achieved. In the material, this fraction can be considered as the result of continuous removals and collisions of CNT aggregates leading to a kind of equilibrium under shear. Thus, the impact of a shear flow on the effective filler fraction is considered according to the following kinetic equation:

$$\left.\frac{d\varphi_{eff}}{dt}\right|_{shearing} = -k_{break}(\varphi_{eff} - \varphi_\infty) \qquad \textbf{Equation 16}$$

where k_{break} is the breaking parameter with a dimension of an inverse time; φ_∞ the equilibrium filler efficient fraction. Both parameters evolution with the shear rate will be discussed in the next section. Overall, the time derivative evolution of the effective CNT concentration can be simply expressed as the sum of both structuring and shearing equations:

$$\frac{d\varphi_{eff}}{dt} = k_{build}(\varphi - \varphi_{eff}) - k_{break}(\varphi_{eff} - \varphi_\infty) \qquad \textbf{Equation 17}$$

This differential equation has the following analytical solution:

$$\varphi_{eff} = \frac{k_{build}.\varphi + k_{break}\varphi_\infty}{k_{build} + k_{break}} + \frac{(\varphi_0 - \varphi_\infty)k_{break} + (\varphi_0 - \varphi)k_{build}}{k_{build} + k_{break}} e^{-(k_{build} + k_{break})\cdot t} \qquad \textbf{Equation 18}$$

From the coupling of this equation and the previous percolation equation (**Equation 6**), the conductivity evolution as a function of time can be calculated and compared to the measured curves. The value of the initial effective filler fraction φ_0 was determined using the measured initial conductivity. The parameters k_{break} and φ_∞ were then fitted to experimental

data with the use of a nonlinear least square regression algorithm (the parameter k_{build} was already determined from quiescent measurements).

For $k_{break} \ll k_{build}$, the effective filler concentration follows the same evolution as a quiescent treatment, but for sufficient shearing forces, both structuring and destruction parameters will contribute to the network modification.

IV. Results and discussion

1- Fitting the evolution of conductivity during shear stress

The rheo-electrical set-up was configured to measure the sample resistance every 0.1 s, allowing an accurate direct monitoring of the conductivity evolution during shear. To observe the destruction mechanism, the samples were first subjected to an annealing, so that the initial conductivity tended to the total filler concentration.

As a first illustration of the shear rate impact on the competition between structuring and destruction mechanisms, deformations up to five were applied to a HDPE/CNT (2 vol% MWCNT) sample at different shear rates. **Figure 52** shows the measured and calculated electrical conductivities as a function of time for start-up shearing experiments at different shear rates varying from 0.1 s^{-1} to 1 s^{-1}. For these experiments, the shear was started when the sample has reached approximately the same conductivity (9×10^{-5} S/cm) after annealing. The obtained conductivity decrease is explained by the destruction of CNT-CNT connections induced by the flow removing aggregates from the conductive network leading to the reduction of the effective filler fraction.

Figure 52 also shows that faster shear rates correspond to a lower steady conductivity level during shear. This result, in accordance with previous observation [25], shows the presence of destructive mechanisms during shear and their intensification with increasing $\dot{\gamma}$. The resulting conductivity loss is more abrupt, and the destruction mechanisms are stronger.

It can be mentioned that the calculated results well predict the limiting conductivity under shear when adjusting only the k_{break} and φ_∞ parameters. The fitted parameter values are summarized in **Table 5**. These values clearly indicate that k_{break} increases with the shear rate while φ_∞ decreases in the range of experiments. The following section discusses the possible rationalization of these two parameters variations.

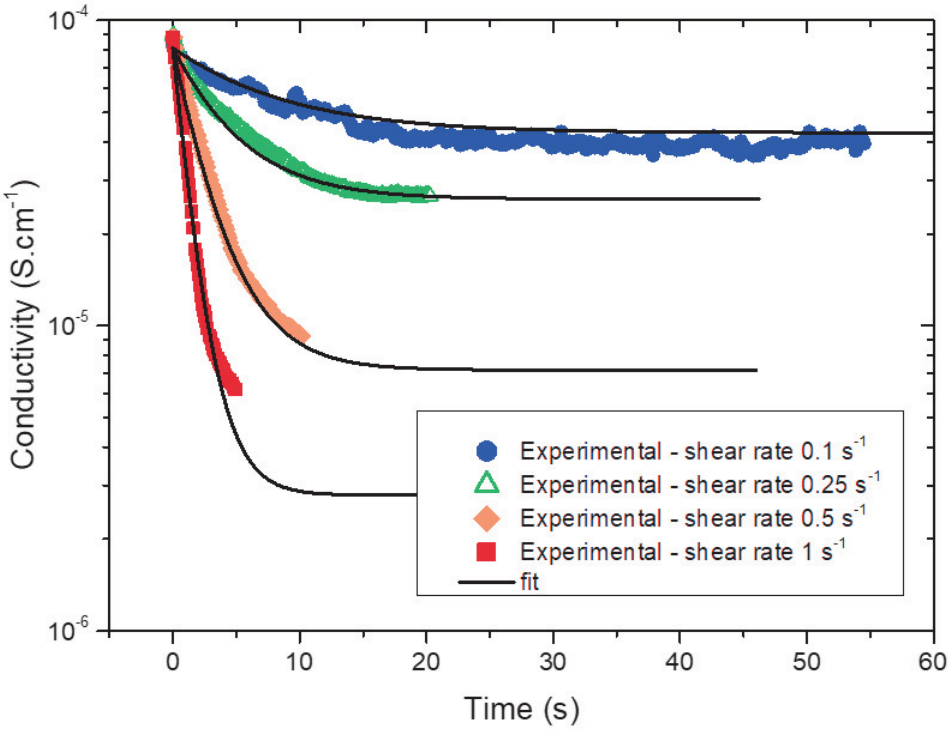

Figure 52: Conductivity variation during shear at 200°C as a function of time for HDPE/CNT (2.0 vol%) at various shear rates for a total strain of 5. Symbols: experimental data; lines: calculated curves with ***Equation 17*** *and parameters shown in* ***Table 5***

Table 5: fitting parameters of different shear experiment of a HDPE-CNT (2.0 vol% MWCNT) at 200°C. The parameter k_{build} *was fixed to* 2.0×10^{-2} s^{-1}.

Shear rate (s^{-1})	k_{break} (s^{-1})	φ_∞
0.1	0.10	1.8×10^{-2}
0.25	0.19	1.7×10^{-2}
0.5	0.29	1.4×10^{-2}
1	0.55	1.3×10^{-2}

2- Shear rate dependence of the breaking parameter

To understand the impact of shear rate on the breaking parameter k_{break}, various shear rates were applied and the conductivity response resulting from the shear was fitted with **Equation 17**. Shear rates from 0.05 s^{-1} to 10 s^{-1} were applied to samples with different CNT contents. In this respect, it can be mentioned that the choice of applied shear rates was related to the CNT contents because, for high contents (far above the percolation threshold), the applied shear rate must be high to give a significant conductivity decrease, whereas for CNT contents close to the threshold, a lower shear rate is sufficient. The resulting values of k_{break} are shown in **Figure 53** and clearly indicate a dependence on the shear rate. The error bars correspond to the standard deviation calculated for experiments that were reproduced up to seven times. This correlation indicates that the breaking parameter is controlled by the deformation rate and this dependence appears linear in the studied range (on a bi-logarithmic scale such as in **Figure 53**, this is shown by a slope equal to 1). Moreover, it can be seen in

Figure 53 that the variations of k_{break} with the shear rate merge for all the studied CNTs amounts.

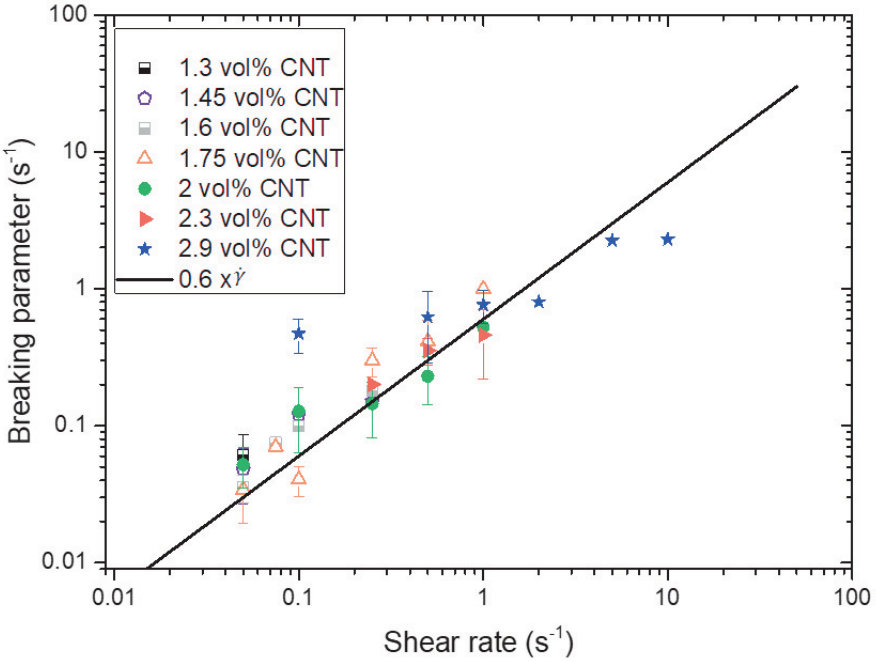

Figure 53: Adjusted break up parameter versus applied shear rate. Error bars are standard deviation obtained for repeated experiments.

The temperature of experiments was also varied to investigate its possible influence on the breaking parameter. As mentioned in a previous section, the temperature influences the building parameter k_{build} and this parameter was fixed to the pre-evaluated values (according to the temperature). Then, the values of k_{break} were adjusted. **Figure 54** exhibits the calculated breaking parameter for HDPE/CNT (1.75 and 2.9 vol% MWCNT) at 3 temperatures. In this graph, the adjusted k_{break} evolves in the same way as a function of the shear rate, whether the experiments were carried out at 160, 180 or 200°C.

Nevertheless, it should be added that the conductivity final equilibrium value for a given shear rate is different from a temperature to another because the building process increases with the matrix mobility. Conversely, with increasing the shear rate, the conductive filler network undergoes faster partial destruction, and the equilibrium will occur at a lower conductivity due to a lower effective concentration. Therefore, from these results it can be concluded that the breaking mechanism is largely related to the shear rate, but it is independent of both temperature and filler amount. Therefore, for the following of this work, the breaking parameter is linked to the shear rate by a simple linear relation:

$$k_{break} = \alpha\, \dot{\gamma} \qquad \textbf{Equation 19}$$

with α being an adimensional coefficient that was evaluated to 0.6 in this study.

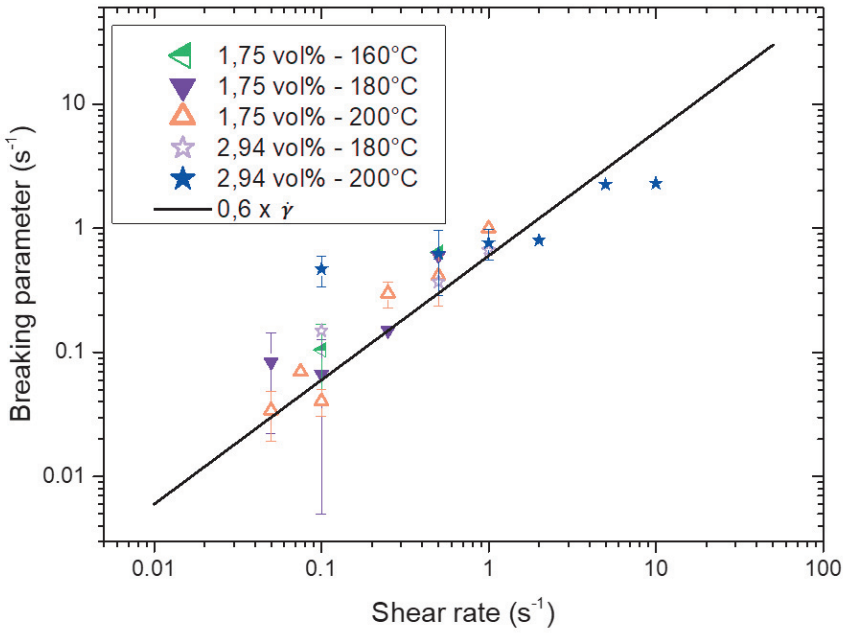

Figure 54: Adjusted break up parameter versus applied shear rate for experiments at different temperatures. Error bars are standard deviation obtained for repeated experiments.

It can be noticed that while k_{build} parameter was found to be governed by the molecular mobility of the polymer matrix as already observed for polystyrene-CNT composites [26], the k_{break} parameter seems highly linked to the nanotubes network. Here, only an unique polymer-filler system was studied (same CNT length, matrix, composite preparation…) but this breaking parameter will likely be modified for a different system.

3- Variations of φ_∞

The value of both k_{build} and k_{break} parameters were thus determined and experimental data were fitted by adjusting again the φ_∞ parameter. Suitable fittings were still obtained for the conductivity evolution during steady shear deformation. The obtained equilibrium filler fraction φ_∞ is plotted versus the shear rate in **Figure 55** for various CNT contents. The first obviousness from this plot is the clear dependence of this parameter on the sample total CNT content: for increasing filler fractions higher φ_∞ values were determined.

The influence of the shear rate on φ_∞ is mostly noticeable in **Figure 55** for samples with a filler content of 2 vol% (green filled circles). A decrease of the equilibrium efficient fraction from 1.8 vol% to 1.15 vol% was obtained over the entire applied shear rate range. The same trend is observed for other CNT contents, but with variable intensities. Taking the example of composites with a CNT concentration of 1.75 vol%, φ_∞ only shifts from 1.4 vol% at 0.05 s^{-1} to 1.15 vol% for highest shear rates. However, at high shear rates (>1 s^{-1}), only a few experiments with the highest concentration (2.9 vol%) were reliable in determining φ_∞ so that a definitive interpretation of its variation for high shear rates would be impossible.

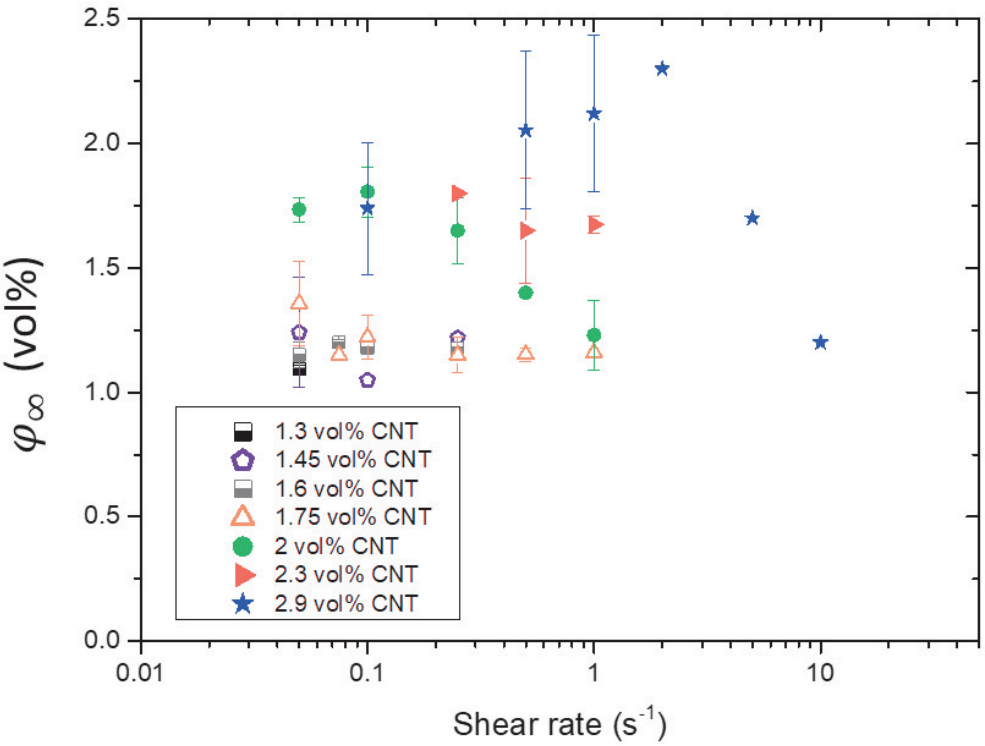

*Figure 55: Equilibrium effective fraction versus shear rate for HDPE-CNT composites at various CNT content. The φ_∞ parameter was adjusted from **Equation 17** with fixed break up and building parameters. Error bars are standard deviation obtained for repeated experiments.*

In the model proposed by Skipa et al. [20] (**Equation 10**) a shear induced agglomeration term was used to describe the ability of CNT to agglomerate to the network. In this work, in **Equation 17**, the equilibrium effective filler fraction φ_∞, is considered as a parameter that characterizes the shear induced destruction, balanced by a structuring, that occurs at long times of shear deformation. Under a shearing flow, the fillers are conveyed by the flowing matrix and this action mainly disconnects CNT-CNT contacts when the effective filler fraction is close to the total filler fraction ($\varphi_{eff} \approx \varphi$). If there is a non-negligible quantity of carbon nanotubes that are isolated from the conductive network ($\varphi_{eff} < \varphi$), the induced movement can help the reconnection to this network. The equilibrium effective fraction here testifies to the competition between shear induced creation and destruction of CNT contacts. The lower the φ_∞ is, the more predominant is the break-up mechanism over the shear induced structuring.

The Temperature influence on the equilibrium efficient fraction was also investigated similarly to the previous section. The measured conductivity evolution with the shear rate at different temperatures has been fitted adjusting only φ_∞. The determined values are plotted in **Figure 56** showing that φ_∞ appears independent of the temperature (but still dependent on the total CNT amount). In fact, this conclusion is consistent with the description of φ_∞ which results from simultaneous removals and re-integrations of CNT aggregates in the conductive network due to the shear. If the re-integrations were due to the molecular mobility in the surrounding matrix, φ_∞ would certainly be temperature dependent.

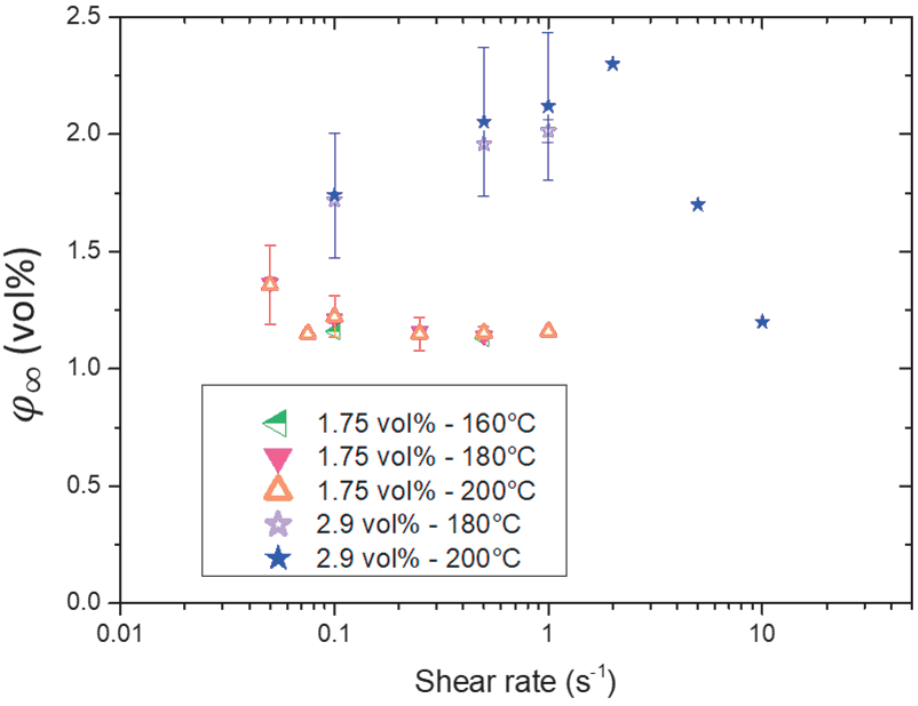

Figure 56: Equilibrium effective fraction versus applied shear rate for experiments at different temperatures. Error bars are standard deviation obtained for repeated experiments.

Thus, the equilibrium effective fraction was shown to be independent of the temperature, but it was observed in **Figure 56** that this parameter is dependent on the total CNT amount (φ). It remains difficult to determine a clear and strong variation of φ_∞ with the shear rate. Nonetheless, when φ_∞ presented in **Figures 55** and **56** are normalized by the filler total fraction φ, a unique pattern, presented in **Figure 57**, seems to emerge.

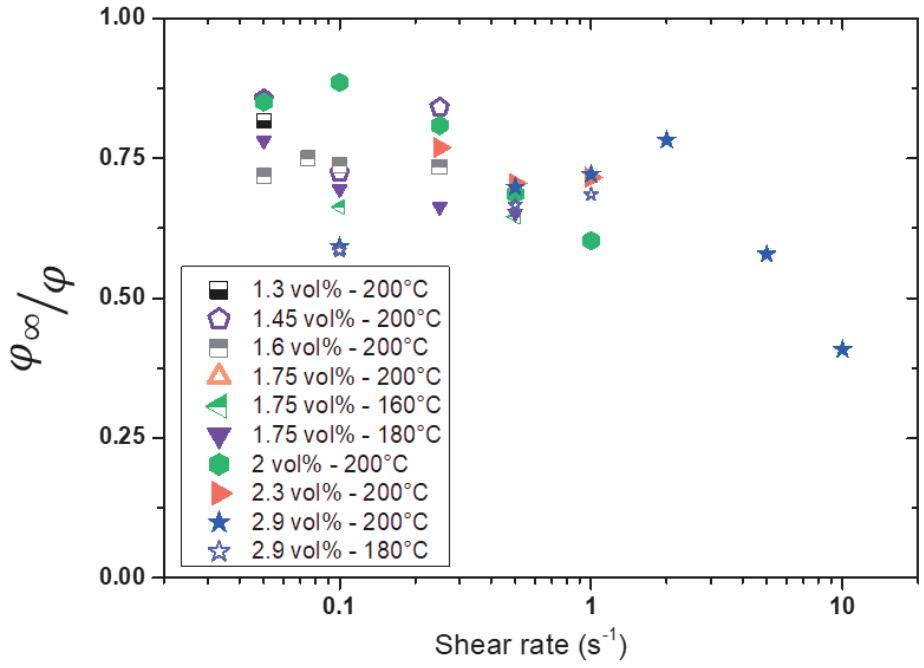

Figure 57: φ_∞ parameter normalized by the total filler fraction φ as a function of the shear rate for HDPE/CNT composites at various CNT contents.

Nevertheless, at this stage, it would be pointless to attempt to establish a more precise direct quantitative relation between φ_∞ and φ. Therefore, the individual φ_∞ values obtained for given conditions of shear rate, temperature and CNT fraction will be used in the following section to further evaluate the proposed model.

4- Modeling the electrical conductivity under shear flow

As an illustrating example of the model validity, in **Figure 58**, the conductivity evolution measured at 200°C for a CNT fraction of 2 vol% is compared to the data calculated with the model, and the parameters displayed in **Table 6** (i.e. the breaking parameter k_{break} is calculated with **Equation 19**. Even though small differences appear between measured and the calculated results, the model well predicts the shear induced conductivity evolution over a range from 0.1 to 1 s^{-1} for a composite with a 2 vol% of CNT content.

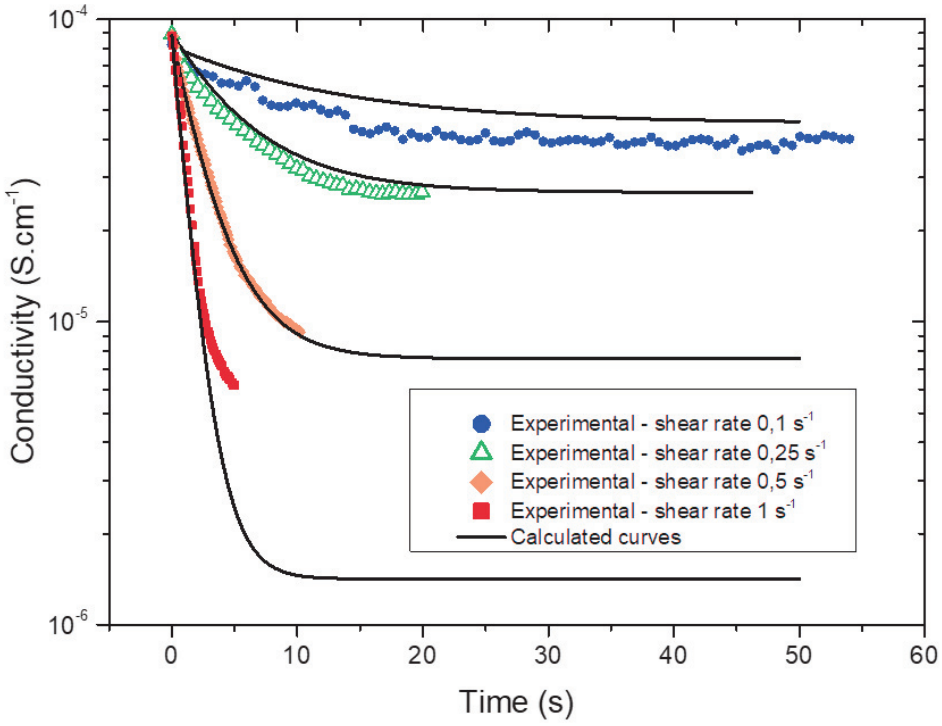

Figure 58: Conductivity as a function of time during shear deformation to 5 of HDPE/MWCNT (2 vol%) at 200°C for different shear rates

Table 6 : Parameters value for the modeling of conductivity evolution during deformation of a HDPE/CNT (2 vol% MWCNT) at 200°C for different shear rates. The parameter k_{build} was fixed to 2.0×10^{-2} s^{-1}

Shear rate (s^{-1})	k_{break} (s^{-1})	φ_∞
0.1	6×10^{-2}	1.8×10^{-2}
0.25	0.15	1.7×10^{-2}
0.5	0.3	1.4×10^{-2}
1	0.6	1.2×10^{-2}

The reliability of the model was also tested for a more complex shear history. A HDPE/CNT (1.75 vol% of MWCNT) was first annealed for 10 minutes. Then, a shear deformation was applied with successive lower and lower shear rates (0.25; 0.1 and 0.05 s^{-1}) for around

50 seconds each and the electrical response was measured. The measured conductivity evolution is compared with the calculated data with the proposed model in **Figure 59**. The good accordance between both curves shows the ability of the model to well predict the conductivity evolution even for complex shearing histories.

During such an experiment, the initial effective concentrations (φ_0 in **Equation 18**) for the second and the third shear rate steps are different from this of the first step which is equal to the total fraction φ, considering the sample previously annealed. In fact, the initial effective fraction for one step is the ending effective fraction φ_{eff} calculated for the previous step. Moreover, an increase of the electrical conductivity during both these steps was observed. The first shear step (shear rates of 0.25 s^{-1} for 46 s) mainly causes CNT-CNT connections break-up, until the conductivity reaches a steady level corresponding to the equilibrium between structuring and destruction mechanisms. When the shear rate is then reduced (to 0.1 s^{-1} for 42 s and then to 0.05 s^{-1} for 58 s), the conductivity evolves monotonically toward higher values. The breaking mechanism is reduced, and the network state is stabilized at a higher effective fraction. Consequently, the conductivity asymptotically increases. Once the shear is stopped, the breaking parameter equals to zero and the conductivity follows a quiescent recovery. Therefore, it is shown that, depending on the initial effective filler fraction an applied shear rate can either induce an increase or a decrease of the conductivity as it was already pointed out by Skipa et al. [25].

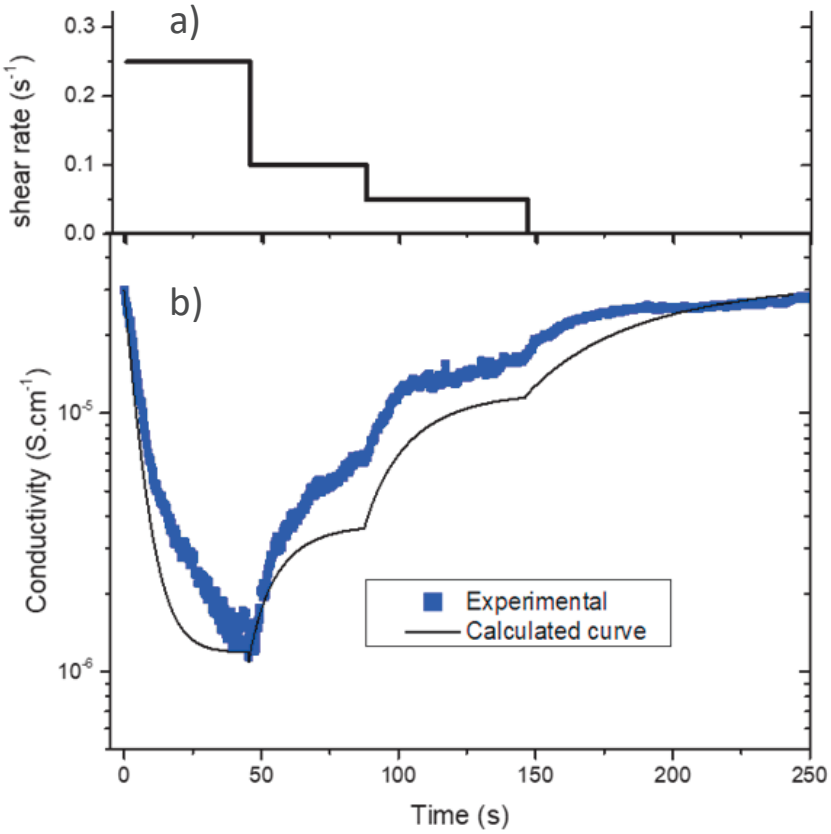

Figure 59: (a) Shear rate as a function of time. (b) Conductivity as a function of time of HDPE/MWCNT (1.75 vol%) during deformation at successive lower and lower shear rates followed by a quiescent recovery at 200°C. Symbols are experimental data and solid lines are model.

Conclusion

The monitoring of the electrical conductivity was used in this work to study the building and breaking mechanisms of the carbon nanotubes network in a molten polymer under shear flow. The observations led to the proposition of a model describing the conductivity variation under shear flow for composites of polyethylene filled with carbon nanotubes. This model has been tested for materials with CNT contents nearby and above the percolation threshold (1.15 vol% here) for a large range of shear rates and different temperatures. First, the structuring parameter, responsible for the conductivity enhancement under a quiescent annealing treatment, was determined. Then, the impact of the shear strain on the effective filler fraction for the HDPE/CNT composite was identified. It was observed that the breaking parameter was linearly dependent solely on the shear rate. An equilibrium effective fraction was introduced to report on the ability of the conductivity to stabilize at a certain level during the shear deformation. This factor was found to be related to the material total filler fraction and, to a lesser extent, to the applied shear rate. However, quantitative explanations of these tendencies are not entirely clear yet.

Finally, the proposed model gives the possibility to predict the conductivity evolution during shear deformation over a wide range of shear rate and filler concentrations regardless the initial state of the sample (possibly out of equilibrium). Considering that the parameters may be linked, for instance, to the quality of the dispersion as well as the type of CNT, the model might be adapted to other polymer-CNT composites.

Acknowledgements

This work was funded by the French National Association for Research and Technology (ANRT) and the company Total (CIFRE convention N°2017/1593)

References

1 R. H. Baughman, A. A. Zakhidov and W. A. de Heer, "Carbon Nanotubes--the Route Toward Applications." *Science,* vol. 297, no. 5582, p. 787-792, 2002.

2 G. Mittal, V. Dhand, K. Y. Rhee, S. J. Park and W. R. Lee, "A review on carbon nanotubes and graphene as fillers in reinforced polymer nanocomposites." *Journal of Industrial and Engineering Chemistry,* vol. 21, p. 11-25, 2015

3 R. F. Gibson, "A review of recent research on mechanics of multifunctional composite materials and structures." *Composite structures,* vol. 92, no. 12, p. 2793-2810, 2010.

4 J. N. Coleman, U. Khan, W. J. Blau and Y. K. Gun'ko, "Small but strong: a review of the mechanical properties of carbon nanotube–polymer composites." *Carbon,* vol. 44, no. 9, p. 1624-1652, 2006.

5 H. Pang, L. Xu, D. X. Yan and Z. M. Li, "Conductive polymer composites with segregated structures." *Progress in Polymer Science,* vol. 39, no. 11, p. 1908-1933, 2014.

6 E. J. Garboczi, K. A. Snyder, J. F. Douglas and M. F. Thorpe, "Geometrical percolation threshold of overlapping ellipsoids." *Physical Review E,* vol. 52, no. 1, p. 819-828, 1995

7 I. Balberg, N. Binenbaum and N. Wagner, "Percolation Thresholds in the Three-Dimensional Sticks System." *Physical Review letters,* vol. 52, no. 17, p. 1465, 1984.

8 J. Chen, B. Liu, X. Gao and D. Xu, "A review of the interfacial characteristics of polymer nanocomposites containing carbon nanotubes." *RSC advances,* vol. 8, no. 49, p. 28048-28085, 2018.

9 W. Bauhofer and J. Z. Kovacs, "A review and analysis of electrical percolation in carbon nanotube polymer composites." *Composites Science and Technology,* vol. 69, no. 10, p. 1486-1498, 2009.

10 Z. Spitalsky, D. Tasis, K. Papagelis and C. Galiotis, "Carbon nanotube–polymer composites: Chemistry, processing, mechanical and electrical properties." *Progress in Polymer Science,* vol. 35, no. 3, p. 357-401, 2020.

11 I. Alig, P. Pötschke, D. Lellinger, T. Skipa, S. Pegel, G. R. Kasaliwal and T. Villmow, "Establishment, morphology and properties of carbon nanotube networks in polymer melts." *Polymer,* vol. 53, no. 1, p. 4-28, 2012.

12 S. Pegel, P. Pötschke, G. Petzold, I. Alig, S. M. Dudkin and D. Lellinger, "Dispersion, agglomeration, and network formation of multiwalled carbon nanotubes in polycarbonate melts." *Polymer,* vol. 49, no. 4, p. 974-984, 2008.

13 L. Moreira, R. Fulchiron, G. Seytre, P. Dubois and P. Cassagnau, "Aggregation of Carbon Nanotubes in Semidilute Suspension." *Macromolecules,* vol. 43, no. 3, p. 1467-1472, 2010.

14 M. Marcourt, P. Cassagnau, R. Fulchiron, D. Rousseaux, O. Lhost and S. Karam, "An original combined method for electrical conductivity measurement of polymer composites under extensional deformation." *Journal of Rheology,* vol. 61, no. 5, p. 845-857, 2017.

15 T. Takeda, Y. Shindo, Y. Kuronuma and F. Narita, "Modeling and characterization of the electrical conductivity of carbon nanotube-based polymer composites." *Polymer,* vol. 52, no. 17, p. 3852-3856, 2011.

16 C. Feng and L. Jiang, "Micromechanics modeling of the electrical conductivity of carbon nanotube (CNT)–polymer nanocomposites." *Composites Part A: Applied Science and Manufacturing,* vol. 47, p. 143-149, 2013.

17 Y. Zare and K. Y. Rhee, "A power model to predict the electrical conductivity of CNT reinforced nanocomposites by considering interphase, networks and tunneling condition." *Composites Part B: Engineering,* vol. 155, p. 11-18, 2018.

18 S. Li, J. G. Park, Z. Liang, T. Siegrist, T. Liu, M. Zhang, Q. Cheng, B. Wang and C. Zhang, "In situ characterization of structural changes and the fraction of aligned carbon nanotube networks produced by stretching." *Carbon,* vol. 50, no. 10, p. 3859-3867, 2012.

19 D. Lellinger, D. Xu, A. Ohneiser, T. Skipa and I. Alig, "nfluence of the injection moulding conditions on the in-line measured electrical conductivity of polymer–carbon nanotube composites." *physica status solidi (b),* vol. 245, no. 10, p. 2268-2271, 2008.

20 I. Alig, D. Lellinger, M. Engel, T. Skipa and P. Pötschke, "Destruction and formation of a conductive carbon nanotube network in polymer melts: In-line experiments." *Polymer,* vol. 49, no. 7, p. 1902-1909, 2008.

21 P. C. Ma, N. A. Siddiqui, G. Marom and J. K. Kim, "Dispersion and functionalization of carbon nanotubes for polymer-based nanocomposites: a review." *Composites Part A: Applied Science and Manufacturing,* vol. 41, no. 10, p. 1345-1367, 2010.

22 J. Obrzut, J. F. Douglas, S. B. Kharchenko and K. B. Migler, "Shear-induced conductor-insulator transition in melt-mixed polypropylene-carbon nanotube dispersions." *Physical Review B,* vol. 76, no. 19, p. 195420/1-9, 2007.

23 W. Bauhofer, S. Schulz, A. Eken, T. Skipa, D. Lellinger, I. Alig, E. Tozzi and D. Klingenberg, "Shear-controlled electrical conductivity of carbon nanotubes networks suspended in low and high molecular weight liquids." *Polymer,* vol. 51, no. 22, p. 5024-5027, 2010.

24 A. Combessis, Charvin, A. N., F. J. A. and L. Flandin, "Understanding dynamic percolation mechanisms in carbonaceous polymer nanocomposites through impedance spectroscopy: Experiments and modeling." *Journal of Applied Physics,* vol. 116, p. 034103-1-10, 2014.

25 T. Skipa, D. Lellinger, W. Böhm, M. Saphiannikova and I. Alig, "Influence of shear deformation on carbon nanotube networks in polycarbonate melts: Interplay between build-up and destruction of agglomerates." *Polymer,* vol. 51, no. 1, p. 201-210, 2010.

26 M. Marcourt, P. Cassagnau, R. Fulchiron, D. Rousseaux, O. Lhost and S. Karam, "A model for the electrical conductivity variation of molten polymer filled with carbon nanotubes under extensional deformation." *Composites Science and Technology,* vol. 168, p. 111-117, 2018.

Conclusion and perspectives

Polymer-carbon nanotubes composites was found useful for many applications. The use of this material is particularly attractive for electrical charge dissipation since a sufficient conductivity can be obtained at low fillers content. Nevertheless, the sensitivity of the filler network on processing conditions remains a challenge to produce composites with suitable conductivity at acceptable CNT contents.

The present study investigated the evolution of the carbon nanotubes conducting network in a polyethylene filled composites in the melt state and during the cooling down to room temperature. Conductivity measurements were extensively used here to detect and understand the network structuring and destructing mechanisms that may occur in the melt polymer during processing steps. The conductivity behavior of a polyethylene-CNT composite was studied in quiescent melt as well as during shear deformation experiments.

The structuring mechanism of the CNT network in the melt polymer was first investigated to evaluate the extent of the conductivity recovery for a specific PE-CNT system. The quiescent annealing treatment was studied with the aim to increase the conductivity for different PE matrices and various CNT contents up to their maximum possibility. This treatment allowed a noticeable reduction of the percolation threshold for a HDPE-CNT composite.

During extrusion, a shear rate gradient appears in the thickness of the composite, a heterogeneous network modification will therefore occur, and a conductivity gradient is likely to appear in the thickness of the final part. As shear rates are greater at the surface of the product, this area should present the lowest conductivity. An annealing treatment could be imagined at this localized area to trigger the conductivity recovery while maintaining the integrity of the manufactured part.

The addition of a surfactant, here the stearic acid, was also considered to reduce the percolation threshold of the PE matrix with the highest studied viscosity. Stearic acid acting as a surfactant as well as a processing aid, a clear influence of this additive on the final properties of the composite is yet to be determined. Additional studies could be conducted to determine the precise role of this additive and the optimized

The effect of the PE crystallization on the CNT network was then examined because the composite structure is modified by the apparition of the crystalline phase. The network breakup by the PE crystalline phase was observed by means of conductivity monitoring during the composite cooling to room temperature. A conductivity drop was indeed observed for PE-CNT composites at the crystallization temperature, suggesting that PE crystals growing in the vicinity of the filler damage the conducting network. As a result, the benefit of the annealing on the conductivity is reduced by the crystallization. In order to reduce the conductivity loss induced by crystallization, the effect of different experimental conditions (cooling rate, after a shear deformation…) or the addition of an additional component (a second filler, an additive…) could be investigated.

Finally, the influence of a shear deformation on the network structure was studied by means of rheological and electrical coupled analysis. This deformation encountered, for instance during the extrusion process is also modifying the CNTs arrangement in the melt polymer. The experimental set up allowed to investigate the effect of various experimental conditions on the conductivity modification. A model was then proposed to describe the conductivity evolution of PE-CNT composites during shear deformation. The evolution of the effective filler content with deformation is described by a kinetic equation, based on the simultaneous network structuring and destructing mechanisms. This model allows a prediction of the conductivity of the composite for various CNT contents, temperature and on a large range of shear rates.

To go further, the model could be tested with processing conditions encountered during extrusion (temperature, flow, …) to evaluate the conductivity evolution during the processing of composite sheets or pipes. Other studies can also be considered to deepen the comprehension of the processing conditions influence on the conductivity of polymer filled with electrically conductive fillers. For instance, the impact of CNT type, polymer properties or the quality of the dispersion could be investigated by the assessment of the model parameters on other polymer-CNT systems. It could also be interesting to extend this study with other conductive fillers, to compare the strength of various percolated networks.

Moreover, in this study rheological measurements were not exploited on combined rheo-electrical experiments. The recovery of the percolated network after a transient shear could be observed with the monitoring of viscoelastic properties to clearly differentiate the apparition of the rheological and the electrical percolated network.